TAMPEREEN TEKNILLINEN YLIOPISTO
TAMPERE UNIVERSITY OF TECHNOLOGY

VIKTOR RIKKONEN

EVALUATION AND PARAMETERIZATION OF A CONTROL SOFTWARE DEVELOPMENT-ORIENTED REAL-TIME ENGINE MODEL FOR MEDIUM SPEED DUAL-FUEL ENGINE

Master's Thesis Work

Examiners: Senior Research Fellow Jani Jokinen, Professor Jose Martinez Lastra
Examiner and topic approved by Academic Board on 1st February 2017

ABSTRACT

VIKTOR RIKKONEN: Evaluation and parametrization of a control software development-oriented real-time engine model for medium speed dual-fuel engine
Tampere University of Technology
Master of Science Thesis, 71 pages, 6 Appendix pages
March 2017
Master's Degree Programme in Automation Engineering
Major: Factory Automation and Industrial Informatics
Examiners: Senior Research Fellow Jani Jokinen, Professor Jose Martinez Lastra

Keywords: dual-fuel engine, zero-dimensional model, mean value engine model, model-in-the-loop simulation, Matlab, Simulink

Increasing engine performance requirements and demanding markets pose challenges for engine manufacturers, which has led to more complex control systems. Engine control software development is expensive and time consuming process especially in marine industry. Engine modeling and rapid prototyping are proposed to shorten control system development cycles. Model in the loop simulation can be used to test control system functionality. For this purpose, a zero dimensional mean value engine model is parameterized for a Wärtsilä 6 cylinder medium speed four stroke dual fuel engine.

Before parameterization, dual fuel engine operating cycle and combustion process are reviewed in order to model the processes based on physical phenomena. The Combustion Model is the most complex of all the modeled systems. Other systems of the mean value engine model are Engine Model that covers air flow through the engine, Gas System that models fuel gas admission, Fuel System that is in charge of diesel fuel injection, Lube Oil System that simulates heat transfer to lubricating oil and Cooling Water Circuit that handles engine and charge air cooling. These systems are modeled to a varying degree of accuracy. The equations used to model the components of each system are presented. Instrument and start air systems of the engine are not modeled.

The engine model is made with Matlab/Simulink. In order to test the control system against the model and ensure their compatibility, control inputs used to influence the plant model and measurement outputs for control system feedback are processed. Test run on the actual engine is made to collect reference data of the engine's performance. Measured data is used to parameterize the engine model via simulation on development computer. The model is then discretized for real time simulation. During real time simulation on target computer, engine controllers are parameterized to get realistic response.

Engine model accuracy is validated by comparing steady-state performance and transient response of the model against measured engine data. Analysis of the results confirms that engine model accuracy is sufficient for control system functionality testing. However, the accuracy is not enough for control system calibration. Due to adequate accuracy, realistic cause and effect relationships between different engine systems and real time simulation capabilities, the engine model can be used for rapid prototyping based control system development.

TIIVISTELMÄ

VIKTOR RIKKONEN: Ohjausjärjestelmäkehitykseen soveltuvan reaaliajassa ajettavan moottorimallin evaluointi ja parametrisointi keskinopealle monipolttoainemoottorille
Tampereen teknillinen yliopisto
Diplomityö, 71 sivua, 6 liitesivua
Maaliskuu 2017
Automaatiotekniikan diplomi-insinöörin tutkinto-ohjelma
Pääaine: Factory Automation and Industrial Informatics
Tarkastaja: yliopistotutkija Jani Jokinen, professori Jose Martinez Lastra

Avainsanat: monipolttoainemoottori, nollaulotteinen malli, moottorin keskiarvomalli, model-in-the-loop-simulointi, Matlab, Simulink

Jatkuvasti kovenevat polttomoottoreiden suorituskyvyn vaatimukset ja haastavat markkinat ovat asettaneet haasteita moottorien valmistajille. Tämä on johtanut yhä monimutkaisempien ohjausjärjestelmien kehitykseen ja käyttöön. Moottorien ohjausjärjestelmäkehitys on kallis ja aikaa vievä prosessi erityisesti meriteollisuudessa. Moottorin mallinnus ja nopea mallipohjainen kehittäminen voivat lyhentää järjestelmien kehityksen syklejä. Model in the loop simulointia voidaan käyttää ohjausjärjestelmien toiminnallisuuden testaukseen. Tämän työn tarkoitus on parametrisoida nollaulotteinen moottorimalli kuvaamaan Wärtsilän 6 sylinterisen keskinopean nelitahtisen monipolttoainemoottorin toimintaa.

Ennen parametrisointia moottorin toimintaperiaate ja paloprosessi käydään läpi, jotta mallia voidaan kehittää fysikaalisten ilmiöiden pohjalta. Palomalli onkin moottorimallin monimutkaisin osa. Muiden mallinnettavien moottorin järjestelmien tehtävät ovat: moottorin ilmavirtausten säätely, maakaasun annostelu, diesel polttoaineen ruiskutus, voiteluöljyn lämmönsiirto sekä moottorin ja ahtoilman jäähdytys. Nämä eri järjestelmät on mallinnettu vaihtelevalla tarkkuudella. Jokaisen järjestelmän komponenttien mallinnukseen käytetyt yhtälöt on esitelty työssä. Käyttöilman sekä startti-ilman järjestelmiä ei ole mallinnettu.

Moottorimalli on tehty Matlab/Simulink ohjelmistolla. Jotta ohjausjärjestelmän toimintaa voitaisiin testata mallia vasten, niiden yhteensopivuus on varmistettava. Siksi moottorimallin sisäänmenojen ja ulostulojen signaalit käsitellään ennen käyttöä. Oikealla laivamoottorilla ajetaan testejä, jotta saadaan kerättyä viitedataa moottorin toiminnasta. Näitä mittauksia käytetään mallin parametrisoinnissa kun moottoria simuloidaan mallinnustietokoneella. Sitten malli diskretoidaan, jotta simulointeja voidaan tehdä reaaliajassa tehokkaammalla kohdetietokoneella. Myös säätimet parametrisoidaan, jotta mallin vaste saadaan realistiseksi.

Moottorimallin tarkkuus validoidaan vertaamalla simuloituja arvoja oikean moottorin mittausdataan. Moottorin vakaiden toimintapisteiden ja siirtymätilojen analysointi vahvistaa, että mallin tarkkuus on riittävä ohjausjärjestelmien toiminnallisuuden testaukseen. Malli ei kuitenkaan ole riittävän tarkka järjestelmien kalibrointiin. Mallin hyväksyttävä tarkkuus, kyky kuvata realistisesti eri järjestelmien vaikutusta toisiinsa ja reaaliaikainen simuloitavuus mahdollistavat moottorimallin käytön nopeassa mallipohjaisessa ohjausjärjestelmäkehityksessä.

PREFACE

This master's thesis was sponsored by Wärtsilä, the greatest engine manufacturer in the world. I want to thank Matias Palmujoki for supervising this thesis. I also want to thank Jari Hyvönen for giving me this opportunity and his team at EPPF for supporting me with their expertise.

I want to thank Jani Jokinen for the administrative help he provided on behalf of Tampere University of Technology. This work ends my studies with, hopefully, a glorious graduation. I want to thank all my friends that I made during the years of my studies. May they all finish their theses and drink their bottles of "Diplomi-Insinööri", brewed by engineers.

I want to give warm thanks to all my fellow trainees and externals for the great company they were at work and all the good times we shared during the year in Vaasa. I also wish to thank all my friends from Tampere who provided remote "assistance" via Whatsapp. Annala squad will always stick together.

I thank my family for the solace and support they gave me whenever I needed it, or even if I didn't. Most of all, I thank my fiancée for waiting for me. This piece of work is dedicated to you Jocelyn. Studying was fun while it lasted. Now it's time to get to business. Allekirjoittanut kiittää ja kuittaa.

Tampere, 22.3.2017

Viktor Rikkonen

CONTENTS

LIST OF SYMBOLS AND ABBREVIATIONS

0-D	zero-dimensional
1-D	one-dimensional
2-D	two-dimensional
ABP	air bypass
AFR_s	stoichiometric air-fuel ratio
BDC	bottom dead center
BMEP	brake mean effective pressure
CEA	Chemical Equilibrium with Applications
EOI	end of injection
EVC	exhaust valve closing
EVO	exhaust valve opening
EWG	exhaust wastegate
FMEP	friction mean effective pressure
GVU	gas valve unit
HIL	hardware-in-the-loop
HT	high temperature
IMEP	indicated mean effective pressure
IVC	inlet valve closing
IVO	inlet valve opening
LNG	liquefied natural gas
LT	low temperature
MEP	mean effective pressure
MIL	model-in-the-loop
MVEM	mean value engine model
NO_x	nitrogen oxide emissions
ODE	ordinary differential equation
PC	personal computer
PID	proportional-integral-derivative
PMEP	pumping mean effective pressure
RAM	random access memory
SAE	Society of Automotive Engineers
SOI	start of injection
TCP/IP	transmission control protocol / internet protocol
TDC	top dead center
W6L34DF	Wärtsilä 6-cylinder dual-fuel engine with 34 cm bore diameter

a	crank radius
A	area
α	angular acceleration
B	bore diameter
σ	Stefan-Boltzmann constant
c_p	specific heat at constant pressure
c_v	specific heat at constant volume
η	efficiency
γ	ratio of specific heats
h	enthalpy
h_c	heat transfer coefficient

H	coefficient describing restriction flow properties
I	inertia
l	piston rod length
L	stroke length
λ	air-fuel equivalence ratio
m	mass
$\dot{m}$	mass flow
M	molar mass, torque
n	number of moles, rotational speed
N_{cyl}	number of cylinders
ω	angular speed
p	pressure
ϕ	fuel-air equivalence ratio
ψ	molar nitrogen/oxygen ratio
Q	heat energy
$\dot{Q}$	heat transfer rate
Q_{LHV}	lower heating value
r_c	compression ratio
R_s	specific gas constant
R_u	universal gas constant
T	temperature
θ	crank angle
u_p	mean piston speed
U	internal energy
V	volume
V_c	clearance volume
V_d	cylinder volume displaced by piston
W	work
x_b	burned gas fraction
y	molar hydrogen/carbon ratio
z	molar oxygen/carbon ratio

1. INTRODUCTION

1.1 Engine design and control system development

Increasing requirements for internal combustion engines on power demand, reduced fuel consumption, lower emissions and better drivability create the need for continuous engine development. The mechanical aspects of combustion engine are well established so the focus has been on increasing engine efficiency with structural improvements based on computational fluid dynamics analyses and better management of engine processes achieved with new control methods. Control system development is an iterative process of defining requirements, developing control functions, testing and calibration. As control systems become more complex, the number of sensors, actuators and control parameters increases. Therefore, control software verification has become very time-consuming. In addition, testing on real engines is highly expensive due to engine size and fuel consumption. Not only have markets grown to be more demanding, but also the delivery times have become shorter. These factors have led to the concepts of engine simulation and rapid prototyping.

Simulation can be used to support control software development. Instead of running tests on actual engine, control functions can be tested and validated on an engine model. In the first development phases the control system can be run together with an engine model, which is called model-in-the-loop (MIL) simulation. When the control system testing is moved to an actual engine, instead of taking the time to implement the control functions in machine code for control modules, the system can be run on a real-time simulation platform using high-level language to directly operate the engine. This is called rapid (control) prototyping. The real engine can also be replaced with an accurate model running in real-time on a target computer. MIL simulation and rapid prototyping can greatly shorten control software development cycles. [12 p. 406]

1.2 Problem description

Engine can be modeled with varying degrees of accuracy. Modeling can make major contributions to control software development depending on the detail of the model. In the beginning of the development process, already a simple engine model that has only the core functionality can help to identify key variables and rational control methods. Modeling actual engine processes enables the developers to test how different control concepts influence system behavior. Including the key processes of multiple engine systems allows testing the control software functionality on a larger scale by running the engine systems together. If the model describes all required engine processes accurately

enough, it can be used in rapid prototyping-based simulation to optimize control system design and control functions as well as to perform initial system calibration.

Wärtsilä has long utilized engine test rig simulation in control software development. However, there was no existing accurate engine plant model for MIL type simulation. Simple engine models had been made to give indicative results of some engine process values. Those models were sufficient for testing the basic operating principle of controllers. Wärtsilä had seen the need to create a detailed engine specific model in order to get more accurate results. A model was made to correspond to W6L34DF engine in the test laboratory. However, the model was very complex and at the time too heavy for real-time simulation. It was put aside until an opportunity came along with rapid control prototyping project to find out if the model can be used for control software development. However, the W6L34DF laboratory engine had undergone modifications that had changed its characteristics to the extent that the model was not corresponding to the real engine anymore. In addition, the model needed to be compatible with the new control system under development. Therefore, the engine model was to be evaluated and parameterized to provide as good accuracy as possible.

1.3 Objectives and research methods

The main objective of this master's thesis is to parameterize the W6L34DF engine model. In the process, the answers to the following research questions will be sought. First one is to evaluate the accuracy of the model after the completion of parameterization work. The engine model accuracy will be analyzed both in steady-states and during transient operation. Another important research question is, if the accuracy of the model will be sufficient for rapid prototyping-based control system development. In addition, methods to improve the accuracy will be discussed and flexibility of the model will be evaluated. For rapid prototyping purposes it is also important to know, if the engine model can be used for real-time simulation. The last objective is to determine whether model-in-the-loop simulation has the potential to bring added value to control software development.

Matlab/Simulink provides a high-level language simulation platform for modeling dynamic systems. In order to evaluate the W6L34DF engine model performance, an integrated system model will be created in Simulink. This model will be used to analyze engine processes and to evaluate if the applied assumptions and equations represent the necessary engine features. The parameterization approach will be to preserve the component-based engine model structure and use MIL simulation to verify model accuracy. In this thesis the focus will be on gas operation of the engine meaning that simulation will be done mostly in gas mode.

1.4 Thesis outline

The core topics of this thesis are modeling and simulation of a marine medium-speed dual-fuel engine. The text is organized into 6 chapters. Chapter 1 provides introduction to the thesis and outlines the purpose of the research. Chapter 2 gives an overview of the operation, thermodynamics and working cycles of internal combustion engines. In Chapter 2.1 the Wärtsilä W6L34DF engine is introduced together with a brief explanation of its operating principle. Chapter 2.2 explains the 4-stroke cycle of dual-fuel engines. The theory behind engine combustion process which takes place inside the cylinders is then covered in Chapter 2.3 including all the equations that will be used to model the process.

Chapter 3 considers mean value engine modeling and examines the W6L34DF model. The methodologies adopted when building the model are introduced in Chapter 3.1. The structure of the mean value engine model is then presented in Chapter 3.2. The chapter describes the purpose, components and operating principles of the systems that the engine is divided into. The systems are modeled to a varying degree of detail, and the applied physical equations are provided for each modeled component. Chapter 3.3 introduces the combustion model and presents the solutions used to capture the effects of complicated thermodynamic processes and relate them to engine power. The combustion model uses a separate crank-angle-degree-based solver when the rest of the engine model execution is time-based.

Chapter 4 discusses the parameterization and simulation of the engine model. Chapter 4.1 introduces the simulation environment and model set up. Test run of the real engine is described in Chapter 4.2. Chapter 4.3 considers the main steps of the parameterization process and some problems that were encountered during simulation with development PC. Real-time simulation is then discussed in chapter 4.4.

Chapter 5 reports simulation results for steady-state and dynamic operation. The results are analyzed and compared to measurements from the actual engine in Chapter 5.1. Model accuracy is reviewed as well. Chapter 5.2 presents some alternative modeling methods to consider. Chapter 5.3 regards overall engine model performance and evaluates if thesis objectives are met. Future development suggestions are also brought up. Finally, Chapter 6 gives the overview and conclusions of the thesis.

2. COMBUSTION ENGINE OPERATION THEORY

2.1 W6L34DF engine introduction and operating principle

The Wärtsilä W6L34DF engine is a four-stroke medium speed dual-fuel internal combustion engine. An image of the engine is shown in Figure 1. The engine has 6 in-line cylinders with a bore of 34 cm. Dual-fuel means that it can use two different fuels as the main fuel: diesel or gas. During diesel operation, diesel fuel is injected directly into combustion chamber of each cylinder with mechanical jerk pumps. In gas mode, gas is used as the main fuel and is introduced into the combustion chamber as a mixture with air. As a contrast to traditional gas engines, W6L34DF does not have spark plugs. Instead, diesel is used as pilot fuel to ignite the air-gas mixture under high cylinder pressure. This method is called compression ignition which is used for both diesel and gas operation. W6L34DF is a single-stage turbocharged engine.

Figure 1. *W6L34DF engine. [21]*

The basic operation principle of an internal combustion engine is that chemical energy of the fuel is released through combustion process, during which fuel is burned with the presence of oxidizer. Internal combustion engines typically use hydrocarbon fuels that are composed of carbon and hydrogen. Most often the fuel is a mixture of different hydrocarbons. The most common fuels are methane, propane, hexane, isooctane, methanol, ethanol, gasoline and diesel. Internal combustion engines used in marine vessels almost exclusively use different diesels and natural gas which primarily consists

of methane. Sometimes, other fuels are also used in maritime, for example, the world's first ethane-powered marine vessel made its first voyage in March 2016 [8]. The other essential component of combustion process is the oxidizer. Air is used for that purpose as it is composed of 20.95 % oxygen, 78.09 % nitrogen and 0.93 % other gases [11 p. 64]. Together, fuel and air form the working fluids of internal combustion engines.

Combustion of the air-fuel mixture causes an accelerated expansion of high pressure product gases inside the cylinder chamber. As a result, the gases apply direct force to the piston of the engine. This force starts moving the piston downward from top dead center (TDC) position. After piston has moved over the distance of stroke length, it reaches the bottom dead center (BDC). Linear movement of the piston is transferred to rotational movement of the engine crankshaft via connecting rod, which makes the engine flywheel rotate as well. Geometry of the cylinder, piston, connecting rod and crankshaft is shown in Figure 2. The flywheel of the engine is attached directly to the crankshaft so they have the same rotational speed. This is called the engine speed. The nominal speed of W6L34DF engine is 750 rpm. The same mechanism is used for each cylinder of the engine to transfer the mechanical energy of all pistons to the crankshaft. The phases of a combustion process taking place in the cylinder are divided over two crankshaft revolutions, which makes one engine cycle. The four-stroke engine cycle will be discussed more in-depth in the next chapter.

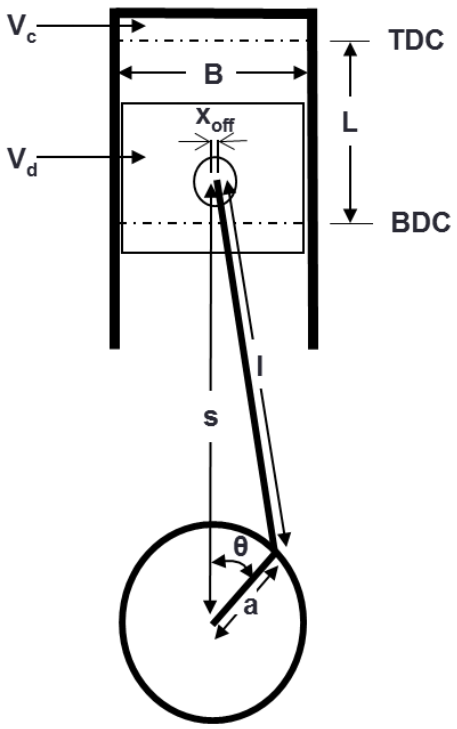

Figure 2. *Geometry of cylinder, piston, connecting rod and crankshaft. [2]*

The power of the engine depends on the number of cylinders and their size. Cylinder volume displaced by the piston V_d depends on bore diameter B and stroke length L. The space between piston crown and cylinder head forms the combustion chamber, also referred to as the cylinder chamber. Some of the chamber volume is not swept by the piston even at top dead center. That is called clearance volume V_c. The ratio of total cylinder volume and clearance volume is defined as compression ratio $r_c = \frac{V_d+V_c}{V_c}$, which is an important parameter when considering engine performance. The compression ratio of the modeled W6L34DF engine is 12.6. Possible piston pin offset is defined as x_{off}. The connecting rod length is marked with l, and a is crank radius. The crank angle is denoted with θ. Those can be used to calculate the distance between crank axis and piston pin axis as $s = a \cdot \cos\left(\theta + \sqrt{l^2 - (x_{off} + a \cdot sin\theta)^2}\right)$. The output of each W6L34DF cylinder is 500 kW. Thus, rated mechanical power of the engine is 3000 kW. Rated power is the highest power the engine is allowed to develop in continuous operation [5 p. 74]. Another way to measure engine's performance is the mean effective pressure (MEP), which is obtained by dividing the work produced per cycle by the cylinder volume displaced per cycle [5 p. 50]. It can be also thought as the average pressure exerted on the piston during each power stroke. There are different types of mean effective pressures used to represent engine's capacity to do work during different portions of its cycle.

2.2 Four-stroke engine cycle

As the name suggests, the four-stroke internal combustion engine cycle consists of four phases: intake stroke, compression stroke, expansion stroke which is also called power stroke and exhaust stroke. These four piston movements take place over two crankshaft revolutions comprising one engine cycle. The phase of the engine is usually measured in crank angle degrees (°ca). The duration of each phase is 180 °ca meaning that one engine cycle covers 720 °ca. During the intake stroke piston moves downward from TDC to BDC and fresh air-fuel charge is drawn into the combustion chamber. Then comes the compression stroke and piston moves upward from BDC toward TDC compressing the air-fuel mixture. Before the piston reaches TDC, diesel fuel is injected into cylinder chamber initiating combustion. After TDC piston starts moving down pushed by expanding gases. Therefore, the movement between TDC and BDC is now called the expansion/power stroke. The exhaust stroke is the last phase of engine cycle as piston moves back up from BDC to TDC and pushes the exhaust gases out of the cylinder. [5 p. 81–83]

The four-stroke cycle can also be broken down into five separate processes: intake, compression, combustion, expansion and exhaust. These processes take place in the combustion chamber of the cylinder. In short, reactants (fuel and air) flow into the cylinder, their chemical energy is released and products (exhaust gases) flow out. A

simulation of a complete engine cycle can be built with models for each of these processes. All process models require some degree of approximation in order to apply gas laws and thermodynamic equations. [11 p. 161–162]

The four phases defined above are divided equally over 720 crank angle degrees as they are tied to top dead center and bottom dead center of the piston. However, the beginning and end of each of the five processes varies according to intake and exhaust valve opening and closing times as well as fuel injection. The engine cycle will now be explained in detail based on the valve events. As the cycle begins, piston is at TDC and inlet valve is open. Intake stroke begins, piston moves down and cylinder chamber is filled with fresh charge from the intake manifold. Even though intake stroke lasts until BDC, inlet valve can be closed before that. If inlet valve closing (IVC) happens at BDC, combustion chamber will be fully filled with fresh gases. [5 p. 84] If intake valve closes before BDC, air intake ceases and the compressed air charge will expand due to cylinder chamber volume increase until piston reaches BDC. The latter IVC method is called Miller timing. The goal of Miller timing is to reach a lower cylinder temperature at a desired cylinder pressure at the start of compression. [22] As the piston continues to move downwards after IVC, expansion cooling of the cylinder gas causes its temperature at BDC to drop to values below what the temperature would otherwise be after intercooler when intake valve closes later. Miller timing reduces the work required to compress the gases and lowers NO_x emissions. However, as the temperature goes down, charge air pressure decreases as well. Therefore, turbocharger has to take this into account by delivering air with higher pressure than the initial compression pressure so that desired cylinder pressure is attained. [15 p. 53] Common Miller timing is about 40 °ca.

After BDC the piston starts moving upward and compression stroke begins. Due to mechanical work exerted by the piston, air-fuel mixture is compressed to a higher temperature and pressure [5 p. 81]. Near the end of the compression stroke diesel fuel is injected directly into combustion chamber depending on operation mode. Main fuel is injected about 12 °ca and pilot fuel about 30 °ca before TDC. The injector nozzle structure forces high pressure diesel spray to atomize into drops that evaporate and mix with fresh charge. Because the temperature inside cylinder chamber is above diesel fuel’s ignition point, it ignites spontaneously initiating the combustion process. [11 p. 27] The burning air-fuel mixture releases heat and increases cylinder pressure. Combustion continues over TDC into expansion phase for as long as there is unburned fuel and air left. Maximum cylinder pressure is reached around 17° after TDC, at which point the combustion is 50 % complete. During expansion stroke the piston is pushed downwards as fuel energy is released and work is delivered to the piston. During this work transfer the fuel’s chemical energy is converted to mechanical energy of crankshaft and flywheel. Combustion ends around 30 °ca after TDC. The timing of the combustion event significantly affects the maximum power of the engine. With the right

ignition timing the work transfer from cylinder gases to piston can be maximized resulting in maximum torque. Exhaust valve opening (EVO) happens about 50 °ca before BDC soon after combustion has ended. [5 p. 84]

As piston starts moving upward after BDC, exhaust phase begins. Exhaust gases expand out of the high pressure combustion chamber into the lower pressure exhaust manifold causing cylinder pressure to decrease rapidly. Near the end of exhaust stroke, about 10 °ca before TDC, inlet valve opening (IVO) takes place. When piston reaches TDC, the engine cycle is complete and next cycle begins. The valve event not mentioned yet is the exhaust valve closing (EVC). EVC occurs around 10 °ca after TDC, which is in the beginning of the cycle. This means that intake and exhaust valves are open at the same time for the duration of approximately 20 °ca. [5 p. 85] The time of valve overlap is called scavenging period. As intake manifold pressure is higher than exhaust manifold pressure due to turbocharging, fresh intake gases push the remaining exhaust gases out when entering cylinder. Blowing the cylinder clean of residual gases is called scavenging. [5 p. 353]

Intake and exhaust valves play an important role during engine operation. The valves control gas exchange and thus affect the combustion and power generation of an engine. The valves are driven with camshaft which rotates at half the crankshaft speed. [11 p. 15] The camshaft contains cams that are shaped according to the desired valve lift profile. As the camshaft rotates, the cams connect to the valves through a rocker arm mechanism and push on the valve stem, forcing the valve open by lifting it from its seat. W6L34DF is a fixed cam engine, meaning that the valve opening and closing times are fixed to the camshaft. Therefore, changing valve timings requires modifying the actual camshaft. Different valve timings are briefly analyzed to highlight the impact on engine performance. Exhaust valve opening influences the work transfer that the gases produce on the piston. Too early EVO reduces cylinder pressure causing a loss in expansion work, while too late opening gives higher pressure increasing pumping work done by piston during exhaust stroke. IVO affects pumping work as well. During the part of intake stroke when inlet valve is open, the high pressure charge air coming from intake manifold produces work on the piston. Whether the overall pumping work is positive or negative depends on engine speed and load as well as turbocharger efficiency. Inlet valve closing greatly influences volumetric efficiency of the engine as it directly determines the time that fresh air has to enter the cylinder. Volumetric efficiency is used to describe the effectiveness of the engine’s ability to induct new air into the cylinders. Valve overlap and scavenging can have a positive effect on volumetric efficiency of the engine as cleaning the cylinder of exhaust gases leaves more space for fresh charge. Valve overlap can also improve the turbocharger response. In addition to camshaft-based valve systems, there are advanced methods to freely control the opening and closing profiles of the valves called variable valve actuation. However, they require new actuation system design, which is not available for W6L34DF. [5 p. 350–353]

As the engine is a dual-fuel engine, it can operate on gas or diesel as its main fuel. There are slight differences in gas exchange during different phases of the engine cycle depending on the used fuel used. Figure 3 visualizes the differences during intake, compression and ignition. During gas operation, natural gas is premixed with air in the intake manifold right before cylinder. In diesel mode only air is drawn during intake process. Compression phase is identical in both cases. Combustion is then initiated with compression ignition method regardless of the main fuel. The differences between gas and diesel modes are injection timing, amount of injected fuel and the injector being used. During gas operation diesel serves as the pilot fuel with the only purpose of igniting the air-fuel mixture. The injected diesel is only 1–5 % of the total combustion energy requirement. In order to provide reliable short injection periods smaller injector has to be used. The time of pilot injection is also earlier than main diesel injection due to longer ignition delay. In diesel mode diesel is the only fuel to run the engine, and larger injector with bigger nozzle holes is used. There are also differences regarding the combustion process. When pilot diesel ignites the gas mixture, flame starts to propagate through the combustion chamber releasing heat and increasing cylinder pressure. During diesel operation a large portion of the fuel ignites immediately after injection and burning continues throughout the injection period for as long as there is fuel.

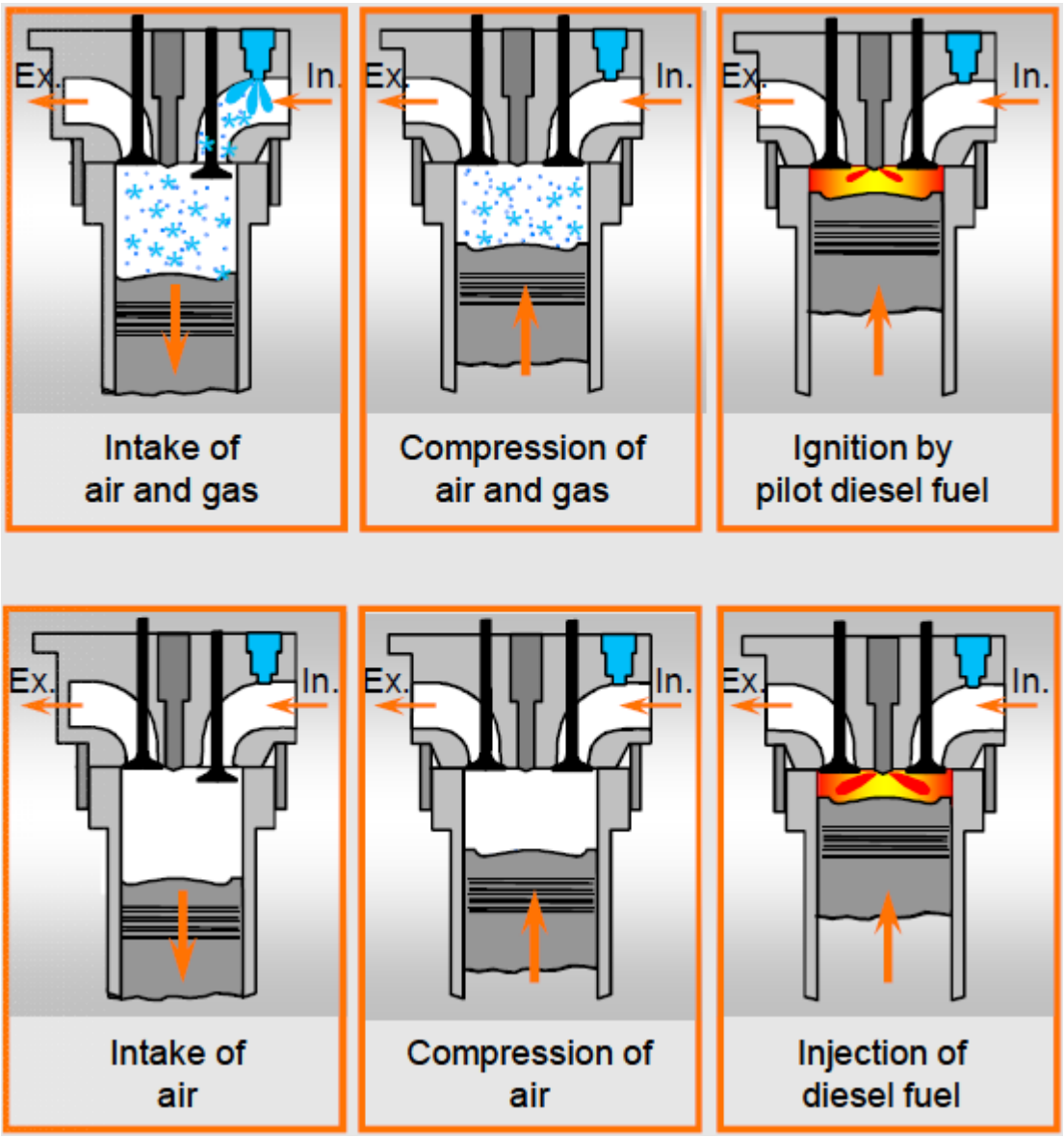

Figure 3. *Differences between diesel and gas modes during engine cycle. Gas operation above and diesel below. [20]*

A p-V diagram can be used to visualize the dependence between cylinder pressure and volume during the five processes introduced in this chapter. The work transfer from gas to the piston over the four-stroke engine cycle can be obtained from the diagram by integrating around the curve, thus, calculating the area enclosed by the diagram. Gross indicated work is defined as the work delivered to the piston over compression and expansion strokes only. The work transfer between the piston and the cylinder gases during intake and exhaust strokes is called the pumping work. [11 p. 46–47]

2.3 Combustion process

Combustion of air-fuel mixture inside the engine cylinder is one of the key processes that control engine power. Therefore, it is important to understand the relevant combustion phenomena and basic thermochemistry in order to model the process. The combustion process is a fast exothermic gas-phase reaction. [11 p. 62–63] Combustion is initiated with pilot fuel injection, followed by an inflammation and flame propagation through premixed fuel, air and burned gas mixture until it reaches combustion chamber walls and extinguishes. As the flame grows and propagates across the combustion chamber, the pressure rises and reaches its maximum after TDC but before the reactants are fully burned. Pressure then decreases as the cylinder volume continues to increase during the remainder of the expansion stroke. [11 p. 371–372]

Fuel and oxidizer react during the combustion process to produce products of different composition. Oxygen is the reactive component of air serving as the oxidizer. When there is just enough oxygen to completely burn the fuel, the combustion is called stoichiometric. The W6L34DF engine operates according to lean combustion principle, meaning that there is more oxygen than what is required to completely burn the fuel. This can be expressed with two different ratios: air-fuel equivalence ratio λ (lambda) and fuel-air equivalence ratio ϕ. Lambda can also be called the relative air-fuel ratio, and it is defined as the actual air-fuel ratio divided by the stoichiometric air-fuel ratio. The fuel-air equivalence ratio is the actual fuel-air ratio divided by the stoichiometric fuel-air ratio. These two ratios are inverse of each other and it can be written that $\lambda = \phi^{-1}$. Fuel-lean mixtures have $\lambda > 1$ and $\phi < 1$, and with fuel-rich mixtures it is the opposite. For stoichiometric mixtures both ratios equal one. [11 p. 71]

The cylinder chamber of internal combustion engine can be analyzed as an open system which exchanges heat and work with its surrounding environment [11 p. 83]. During the process individual species in the reactant and product gas mixtures can be modeled as ideal gases with sufficient accuracy allowing the use of ideal gas law [11 p. 107]. The first law of thermodynamics describes conservation of energy by relating changes in the internal energy (or enthalpy) of the working fluids to heat and work transfer [11 p. 73]. The second law of thermodynamics can be used to derive an expression for the maximum useful work that the engine can deliver [11 p. 83]. These are the basic laws that govern the engine combustion process. In the equations that will be presented in this thesis, parameters such as volume V, pressure p, temperature T and mass m define the state of a system. Differentials marked as dV and dp or $\dot{T}$ and $\dot{m}$ define the rate of change of the system state.

Each of the working fluid species has their own thermodynamic properties. In order to quantify these properties, it is necessary to know the chemical composition of the reactants and products of the combustion process. The combustion formula common to all hydrocarbon fuels is introduced below as formula 2.1

$$\varepsilon\phi\mathrm{C} + 2(1-\varepsilon)\phi\mathrm{H_2} + \mathrm{O_2} + \psi\mathrm{N_2}$$

$$\rightarrow n_{CO_2}\mathrm{CO_2} + n_{H_2O}\mathrm{H_2O} + n_{CO}\mathrm{CO} + n_{H_2}\mathrm{H_2} + n_{O_2}\mathrm{O_2} + n_{N_2}\mathrm{N_2}, \qquad (2.1)$$

where $\varepsilon = \frac{4}{4+y}$, y is the molar $\mathrm{H/C}$ ratio of the fuel, ϕ denotes fuel-air equivalence ratio, ψ means molar $\mathrm{N/O}$ ratio and n_i denotes moles of species i per mole of $\mathrm{O_2}$ reactant. In other words, the number of moles of both reactant and product species is given as per mole of $\mathrm{O_2}$ in the original mixture. As the focus in this thesis is on lean operated combustion engines, CO and $\mathrm{H_2}$ concentration levels of products are close to zero and can be ignored. [11 p. 103] Formula 2.1 can further be modified for fuels containing oxygen, such as alcohols and alcohol-hydrogen blends, by replacing ϕ with ϕ^*, and ψ with ψ^* that are explained in equations 2.2 and 2.3 [11 p. 105]

$$\phi^* = \zeta\phi, \qquad (2.2)$$

and

$$\psi^* = \left(1 - \frac{\varepsilon \cdot z}{2}\right)\zeta\psi, \qquad (2.3)$$

where $\zeta = \frac{2}{2-\varepsilon \cdot z(1-\phi)}$ and z is the molar $\mathrm{O/C}$ ratio.

The composition of the working fluids changes during the engine operating cycle. The details of the actual paths by which these transformations take place are not completely understood, especially regarding fuels with complicated structure. [11 p. 72] However, during intake and compression the composition of unburned reactant gases does not change significantly. It is therefore sufficiently accurate to assume that the composition is frozen. [11 p. 101] During combustion process and much of the expansion phase the burned product gases are close to chemical equilibrium. This means that chemical reactions produce and remove each species at equal rates so no net change in composition occurs. [11 p. 86] A temperature dependent equilibrium constant can be defined for each chemical reaction [2]. As the burned gases in combustion chamber cool during expansion phase, the chemical reactions become extremely slow and working fluid composition eventually becomes fixed. This is usually assumed to occur at temperatures under 1700 K. Therefore, during the exhaust process the composition can be considered frozen again. [11 p. 116] As a result, the burned gas composition can be solved when combustion is over and temperature decreases enough. The relative number of moles of each species $\mathrm{n_i}$ in the product mixture of formula 2.1 can be obtained per mole of $\mathrm{O_2}$ reactant from an element balance, the results of which are shown in Table 1.

Table 1. *Burned gas composition under 1700 K for lean combustion. [11 p. 104]*

Species	**n_i, moles of gas / moles of O_2 reactant**
CO_2	$\varepsilon\phi$
H_2O	$2(1-\varepsilon)\phi$
CO	0
H_2	0
O_2	$1-\phi$
N_2	ψ

The total amount of burned gas moles in the product mixture per mole of O_2 is given by equation 2.4

$$n_b = \sum n_i = (1-\varepsilon)\phi + 1 + \psi. \tag{2.4}$$

During actual exhaust and intake phases, as gases are exchanged between engine manifolds and cylinder chamber, it is not possible to completely replace all of the exhaust gases with fresh unburned mixture. After the exhaust valve closes, there will always be some burnt products from previous cycle left inside the combustion chamber. These are called residual gases, and residual fraction x_r can be defined as the ratio of residual mass and the total gas mass in the cylinder chamber after intake valve closure. The W6L34DF engine does not utilize exhaust gas recirculation so the burned gas fraction x_b in the reactant mixture equals the residual fraction. Thus, there will be a fraction of the burned product gases in the combustion chamber among with inducted fresh air and fuel forming the contents of the next cycle unburned mixture. When burned gas fraction is taken into account, and fuel composition is expressed as a function of its own molar mass, the reactant side of formula 2.1 can be written in the following form

$$(1-x_b)\left[\frac{4}{M_f}(1+2\varepsilon)\phi\left(CH_y\right)_\alpha + O_2 + \psi N_2\right] + x_b\left(n_{CO_2} + n_{H_2O} + n_{CO} + n_{H_2} + n_{O_2} + n_{N_2}\right),$$

where x_b is the burned gas fraction, $\left(CH_y\right)_\alpha$ is the chemical formula of the fuel and M_f the molecular weight of the fuel. As can be seen from the expression above, there is now less fuel per mole of O_2 reactant as the presence of residual gases is taken into account. Table 2 shows the relative number of moles of the unburned species n_i in this reactant mixture.

Table 2. *Unburned mixture composition under 1700 K for lean combustion. [11 p. 106]*

Species	n_i, moles of gas / moles of O_2 reactant
CO_2	$x_b \varepsilon \phi$
H_2O	$2x_b(1-\varepsilon)\phi$
CO	0
H_2	0
O_2	$1 - x_b\phi$
N_2	ψ

The total number of moles of the unburned mixture n_u can be obtained from equation 2.7

$$n_u = (1 - x_b)\left[\frac{4(1+2\varepsilon)\phi}{M_f} + 1 + \psi\right] + x_b n_b, \tag{2.7}$$

and the number of fuel moles n_f per mole of O_2 is given by equation 2.8

$$n_f = \frac{4(1-x_b)(1+2\varepsilon)\phi}{M_f}. \tag{2.8}$$

In both Tables 1 and 2 CO and H_2 concentrations are zero, which is due to lean combustion process that always has excess O_2 present to oxidize hydrocarbons. The tables are independent of each other meaning that the composition given by one does not influence the other. Table 1 gives the composition of the burned mixture (products of combustion process), and Table 2 gives the composition of the unburned mixture (gas species on reactants side). The residual gases can be considered inert because they will not react during combustion anymore. They will however, affect the values of specific heats c_p (specific heat at constant pressure) and c_v (specific heat at constant volume).

According to the law of conservation of mass, the mass of the products in a chemical reaction must equal the mass of the reactants. Thus, the masses of burned and unburned mixture of the same reaction equal to the sum of fuel mass and original mass of air. The mass m_{RP} per mole of O_2 is given by equation 2.9 [11 p.106]

$$m_{RP} = 4\phi(1 + 2\varepsilon) + 32 + 28.16\psi. \tag{2.9}$$

The molecular weights of the burned (M_b) and unburned (M_u) mixtures can now be determined using equations 2.10 and 2.11, where

$$M_b = \frac{m_{RP}}{n_b} \tag{2.10}$$

and

$$M_u = \frac{m_{RP}}{n_u}. \tag{2.11}$$

With the equations defined in the first part of this chapter, the composition model for working fluids of the engine has been created. In order to simulate combustion process, a model for thermodynamic properties of those fluids is also required. There are multiple methods for predicting the properties of unburned and burned mixtures. The most important property related to engine heat release and cylinder pressure modeling is the ratio of specific heats $\gamma = c_p/c_v$ [14]. While some of the most basic models assume constant state enthalpies and specific heats for the full engine operation temperature range, they are useful for illustrative purposes only. In reality, the enthalpies and specific heats change as a function of temperature. The engine temperature range of interest can also be divided into segments with constant or linear properties in their respective ranges. This approach results in models with moderate accuracy. The previously mentioned assumptions of having frozen mixture compositions and equilibrium states can be applied again to generate more complete thermodynamic models that are based on polynomial curve fits to actual data gathered about each species in the mixture. [11 p. 101] This kind of data has been generated by NASA Lewis Research Center (now the Glenn Research Center). Their computer program CEA (Chemical Equilibrium with Applications) was published in 1994. It can be used to calculate chemical equilibrium product concentrations from a set of reactants, and to determine thermodynamic properties of the product mixture. [16] The polynomial approximations for specific heat and enthalpy as functions of temperature are given in equations 2.12 and 2.13 [11 p. 130]

$$\frac{c_{p_i}}{R_u} = a_{i1} + a_{i2}T + a_{i3}T^2 + a_{i4}T^3 + a_{i5}T^4 \tag{2.12}$$

and

$$\frac{h_i}{R_u T} = a_{i1} + \frac{a_{i2}}{2}T + \frac{a_{i3}}{3}T^2 + \frac{a_{i4}}{4}T^3 + \frac{a_{i5}}{5}T^4 + \frac{a_{i6}}{T}, \tag{2.13}$$

where R_u is the universal gas constant, T is gas temperature and a_{ij} are coefficients for gas species i. Enthalpy is needed in order to calculate combustion product dissociation [2]. The coefficients are obtained by least-squares method matching with thermodynamic property data from NIST-JANAF Thermochemical Tables. Usually there are two sets of coefficients and two different temperature intervals. In the NASA program these are 300 to 1000 K, which is appropriate for unburned mixture thermodynamic property calculation, and 1000 to 5000 K, which is applicable for burned mixture property calculation. [11 p. 92] Coefficients are given for gas species of CO_2, H_2O, CO, H_2, O_2, N_2, OH, NO, O and H, and are presented in Table 3.

Table 3. *Coefficients a_{ij} for thermodynamic properties of gas species. [11 p. 131]*

Species	T range, K	a_{i1}	a_{i2}	a_{i3}	a_{i4}	a_{i5}	a_{i6}	a_{i7}
CO_2	1000–5000	0.44608(+1)	0.30982(−2)	−0.12393(−5)	0.22741(−9)	−0.15526(−13)	−0.48961(+5)	−0.98636(0)
	300–1000	0.24008(+1)	0.87351(−2)	−0.66071(−5)	0.20022(−8)	0.63274(−15)	−0.48378(+5)	0.96951(+1)
H_2O	1000–5000	0.27168(+1)	0.29451(−2)	−0.80224(−6)	0.10227(−9)	−0.48472(−14)	−0.29906(+5)	0.66306(+1)
	300–1000	0.40701(+1)	−0.11084(−2)	0.41521(−5)	−0.29637(−8)	0.80702(−12)	−0.30280(+5)	−0.32270(0)
CO	1000–5000	0.29841(+1)	0.14891(−2)	−0.57900(−6)	0.10365(−9)	−0.69354(−14)	−0.14245(+5)	0.63479(+1)
	300–1000	0.37101(+1)	−0.16191(−2)	0.36924(−5)	−0.20320(−8)	0.23953(−12)	−0.14356(+5)	0.29555(+1)
H_2	1000–5000	0.31002(+1)	0.51119(−3)	0.52644(−7)	−0.34910(−10)	0.36945(−14)	−0.87738(+3)	−0.19629(+1)
	300–1000	0.30574(+1)	0.26765(−2)	−0.58099(−5)	0.55210(−8)	−0.18123(−11)	−0.98890(+3)	−0.22997(+1)
O_2	1000–5000	0.36220(+1)	0.73618(−3)	−0.19652(−6)	0.36202(−10)	−0.28946(−14)	−0.12020(+4)	0.36151(+1)
	300–1000	0.36256(+1)	−0.18782(−2)	0.70555(−5)	−0.67635(−8)	0.21556(−11)	−0.10475(+4)	0.43053(+1)
N_2	1000–5000	0.28963(+1)	0.15155(−2)	−0.57235(−6)	0.99807(−10)	−0.65224(−14)	−0.90586(+3)	0.61615(+1)
	300–1000	0.36748(+1)	−0.12082(−2)	0.23240(−5)	−0.63218(−9)	−0.22577(−12)	−0.10612(+4)	0.23580(+1)
OH	1000–5000	0.29106(+1)	0.95932(−3)	−0.19442(−6)	0.13757(−10)	0.14225(−15)	0.39354(+4)	0.54423(+1)
NO	1000–5000	0.31890(+1)	0.13382(−2)	−0.52899(−6)	0.95919(−10)	−0.64848(−14)	0.98283(+4)	0.67458(+1)
O	1000–5000	0.25421(+1)	−0.27551(−4)	−0.31028(−8)	0.45511(−11)	−0.43681(−15)	0.29231(+5)	0.49203(+1)
H	1000–5000	0.25(+1)	0.0	0.0	0.0	0.0	0.25472(+5)	−0.46012(0)

An approximation for the specific heat of fuel (in the vapor phase) has also been fitted to the polynomial function form shown in equation 2.14 [11 p. 130]

$$c_{p_f} = A_{f1} + A_{f2}t + A_{f3}t^2 + A_{f4}t^3 + \frac{A_{f5}}{t^2}, \tag{2.14}$$

where A_{fi} are coefficients for different fuels f, and $t = T(\mathrm{K})/1000$. Coefficients for methane, propane, hexane, isooctane, methanol, ethanol, two types of gasoline and diesel are given in Table 4. The coefficients for pure hydrocarbon fuels are from thermodynamic tables. Gasoline and diesel fuel coefficients are obtained from chemical analysis. [11 p. 132] The table also shows stoichiometric air-fuel ratios $(\mathrm{A/F})_\mathrm{s}$ for those fuels.

Table 4. *Coefficients A_{fi} for thermodynamic properties of fuels. [11 p.133]*

Fuel	Formula	Molecular weight	$(A/F)_s$	$(F/A)_s$	A_{f1}	A_{f2}	A_{f3}	A_{f4}	A_{f5}	A_{f6}	A_{f8}
Methane	CH_4	16.04	17.23	0.0580	−0.29149	26.327	−10.610	1.5656	0.16573	−18.331	4.3000
Propane	C_3H_8	44.10	15.67	0.0638	−1.4867	74.339	−39.065	8.0543	0.01219	−27.313	8.852
Hexane	C_6H_{14}	86.18	15.24	0.0656	−20.777	210.48	−164.125	52.832	0.56635	−39.836	15.611
Isooctane	C_8H_{18}	114.2	15.14	0.0661	−0.55313	181.62	−97.787	20.402	−0.03095	−60.751	20.232
Methanol	CH_3OH	32.04	6.47	0.1546	−2.7059	44.168	−27.501	7.2193	0.20299	−48.288	5.3375
Ethanol	C_2H_5OH	46.07	9.00	0.1111	6.990	39.741	−11.926	0	0	−60.214	7.6135
Gasoline	$C_{8.26}H_{15.5}$	114.8	14.64	0.0683	−24.078	256.63	−201.68	64.750	0.5808	−27.562	17.792
	$C_{7.76}H_{13.1}$	106.4	14.37	0.0696	−22.501	227.99	−177.26	56.048	0.4845	−17.578	15.235
Diesel	$C_{10.8}H_{18.7}$	148.6	14.4	0.0694	−9.1063	246.97	−143.74	32.329	0.0518	−50.128	23.514

The total specific heats of reactant and product mixtures can then be determined by inserting moles n_i and specific heats c_{p_i} of each species per mole of O_2 into equation 2.15

$$c_p = \frac{1}{m_{RP}} \sum n_i \, c_{p_i}. \tag{2.15}$$

For the unburned mixture we get equation 2.16

$$c_{p_u} = \frac{1}{m_{RP}}\left(n_u \sum c_{p_i} + n_f c_{p_f}\right), \tag{2.16}$$

and for the burned mixture equation 2.17

$$c_{p_b} = \frac{1}{m_{RP}} n_b \sum c_{p_i}. \tag{2.17}$$

These are constant pressure specific heats that can be used to calculate the specific heat ratios γ (gamma). Gamma is defined as the ratio of specific heat at constant pressure to specific heat at constant volume $\gamma = c_p/c_v$. There is also another relation between c_p and c_v that has the expression $c_p - c_v = R_s$, where R_s is the specific gas constant. Thus, c_v can be written $c_v = c_p - R_s = c_p - \frac{R_u}{M}$, and the ratio of specific heats can be expressed as in equation 2.18

$$\gamma = \frac{c_p}{c_v} = \frac{c_p}{c_p - \frac{R_u}{M}}. \tag{2.18}$$

With the theory presented up to this point, the composition and thermodynamic properties of reactants and products of the combustion process can be determined. As gamma varies according to the used fuel, amount of air, reactant and product composition, burned gas fraction as well as temperature inside combustion chamber, the presented equations provide a good basis for accurate combustion modeling. This will be followed by the analysis of thermodynamic quantities of combustion process such as energy, pressure and temperature. Variable specific heat ratio can be used to create combustion models that react realistically to changing composition of unburned and burned gases. As gas temperature increases during compression and combustion and then decreases during expansion and exhaust, the value of gamma will also behave accordingly. [11 p. 387]

As mentioned before, the combustion chamber can be modeled as an open system shown in Figure 4. The system boundary is marked with dashed line. During combustion process the chemical energy of the fuel is released. The amount of energy which can be released into the system by combustion can be expressed with equation 2.19

$$Q_{complete} = m_f Q_{LHV}, \tag{2.19}$$

where m_f is fuel mass in the system and Q_{LHV} is lower heating value of the fuel [11 p. 81]. Most of this energy is converted into work done on the piston by the expanding gases. The rest can be considered as losses. A portion of the produced energy is transferred to the cylinder walls (cylinder liner) through convection. Work and heat transfer consume the largest portions of fuel energy, which is indicated by their arrow sizes in Figure 4. The small arrow in the bottom right corner of the figure describes crevice losses. [11 p. 383] They are caused by charge flow into and out of crevice

regions between piston, rings and the liner. The loss mainly comes from temperature loss as the crevice gases will be close to the wall temperature. [2] The top arrow pointing into the system indicates diesel fuel injection into the combustion chamber which takes a small amount of energy to vaporize fuel droplets.

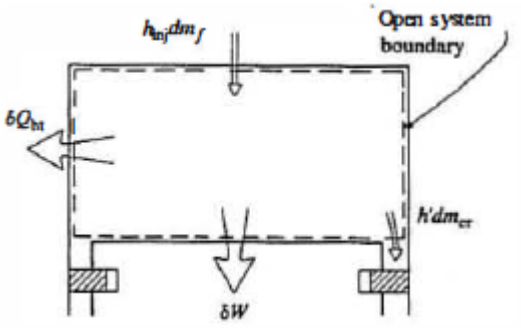

Figure 4. *Open system boundary for combustion chamber [11 p. 386]*

The system of Figure 4 can be described with the first law of thermodynamics $dQ = dU + W$. The equation can be extended by including heat transfer, crevice effects and liquid fuel evaporation yielding equation 2.20 that expresses among which components heat release from combustion is divided

$$dQ = dU + dW + dQ_{ht} + dQ_{cr} + dQ_{m_i}, \tag{2.20}$$

where dQ denotes the rate of heat released by the main fuel, dU equals to the change in internal energy of gases, dW is the power of work transfer, dQ_{ht} denotes rate of heat transfer to cylinder walls, dQ_{cr} means the rate of lost energy due to crevices and dQ_{m_i} equals to rate of heat loss due to vaporization. Internal energy can be expressed by equation 2.21

$$dU = mc_v dT, \tag{2.21}$$

where m is gas mass in combustion chamber, c_v denotes specific heat at constant volume and dT temperature change inside the chamber.

The rate of work done on the piston is determined by equation 2.22

$$dW = pdV, \tag{2.22}$$

where p is the pressure acting on piston and dV is the change in cylinder volume.

Finding T from the ideal gas law $pV = mR_sT$ and then differentiating the equation using partial derivative yields the change in temperature $dT = \frac{V}{mR_s}dp + \frac{p}{mR_s}dV$. This is substituted into equation 2.21 after which equations 2.21 and 2.22 are substituted into the first law of thermodynamics. Simplifying the result equation yields

$dQ = \frac{c_v}{R_s} V dp + \left(\frac{c_v}{R_s} + 1\right) p dV$. The specific heat expressions $c_p - c_v = R_s$ and $\frac{c_p}{c_v} = \gamma$ can be combined into $\frac{c_v}{R} = \frac{1}{\gamma - 1}$. Thus, the first law of thermodynamics can be expressed with specific heat ratio as shown in equation 2.23 [5 p. 107]

$$dQ = dU + W = \frac{1}{\gamma - 1} V dp + \frac{\gamma}{\gamma - 1} p dV. \tag{2.23}$$

The heat transfer equation is based on Newton's law of cooling $dQ_{ht} = h_c A (T - T_{wall})$ which can be transformed from time domain into crank angle domain with equation 2.24 [2]

$$dQ_{ht} = \frac{h_c \cdot A \cdot (T - T_{wall}) \cdot 60}{2\pi \cdot n_{eng}}, \tag{2.24}$$

where h_c denotes heat transfer coefficient, A is exposed cylinder wall area, T means temperature inside combustion chamber, T_{wall} denotes cylinder wall temperature and n_{eng} is engine speed in RPM. The heat transfer coefficient is difficult to measure due to the nature of heat transfer phenomena, and that makes it difficult to model. Hohenberg model was chosen because the coefficients were known for required operating point. Hohenberg equation is presented in equation 2.25 [2]

$$h_c = \frac{C_1 \cdot V^{-0.06} \cdot p^{0.8} \cdot \left(u_p + C_2\right)^{0.8}}{T^{0.4}}, \tag{2.25}$$

where C_1 and C_2 are transfer coefficients and u_p is mean piston speed calculated by $u_p = 2Ln_{eng}/60$. The effect of heat transfer increases towards the end of the combustion when average gas temperature reaches its peak and the flame has propagated to the cylinder walls. [11 p. 387]

Crevice effects are usually small and can be modeled with a single crevice volume where the gas is at the same pressure as the combustion chamber, but at different temperature. Since crevice regions are narrow, crevice gas can be assumed to be at wall temperature. [11 p. 387] The equation for crevice effect is dependent on the direction of the gas flow, which in turn depends on the cylinder pressure. When the pressure is increasing, meaning that the maximum pressure has not been reached yet, some of the air-fuel mixture flows into the crevices. That is when T' stands for the temperature of the gas and γ' denotes specific heat ratio at the gas temperature. After the peak pressure has passed, the crevice gas flows back into the cylinder chamber. Then T' means the temperature of the cylinder wall and γ' describes the gamma calculated with cylinder wall temperature. This dependency is expressed in equation 2.26 [2]

$$dQ_{cr} = \left(\frac{1}{\gamma - 1} T + T' + \frac{1}{b} \ln\left(\frac{\gamma' - 1}{\gamma - 1}\right)\right) \frac{V_{cr}}{T_w} dp, \tag{2.26}$$

where V_{cr} is the crevice volume and b denotes the slope of γ using a linear model $\gamma = \gamma + b(T - T_{ref})$. The value of b is approximated with specific heat ratio at $T_{ref} = 500$ K temperature and is then assumed to be constant.

In dual-fuel engines the gaseous air-fuel mixture is ignited with liquid pilot fuel injection that increases fuel mass inside the combustion chamber. The diesel spray evaporates partly before ignition, which extracts heat from inside the combustion chamber and changes enthalpy of the system. As the rate of heat transfer is very fast due to fast vaporization, it is expressed as enthalpy flux [14]. The injected amount of pilot fuel is only a few percent of the total fuel energy but in diesel mode the energy loss substantial. [11 p. 536–538] The heat loss from enthalpy flux is presented in equation 2.27 [5 p. 105–106]

$$dQ_{m_i} = h_i dm_i = \left(\frac{R_s \cdot dT_i}{\gamma_i' - 1} - u\right) dm_i, \tag{2.27}$$

where R_s is the specific gas constant of evaporated fuel, $u = \frac{R_s}{b} \ln\left(\frac{\gamma - 1}{\gamma_i' - 1}\right)$, b is a constant, γ_i' is specific heat ratio of evaporated fuel and dm_i is the injected fuel mass. When equations 2.23, 2.24, 2.26 and 2.27 are substituted into equation 2.20 the net heat release can be written in the form of equation 2.28

$$dQ = \frac{1}{\gamma - 1} V dp + \frac{\gamma}{\gamma - 1} p dV + \frac{h_c \cdot A \cdot (T - T_{wall}) \cdot 60}{2\pi \cdot n_{eng}} + \left(\frac{1}{\gamma - 1} T + T' + \frac{1}{b} \ln\left(\frac{\gamma' - 1}{\gamma - 1}\right)\right) \frac{V_{cr}}{T_w} dp + \left(\frac{R_i dT_i}{\gamma_i' - 1} - u\right) dm_i. \tag{2.28}$$

The heat release provided by equation 2.28 should be very close to the heat release from complete combustion presented in equation 2.19. In practice, there is always a fraction of fuel's chemical energy that is not fully released, and therefore $Q_{actual} < Q_{complete}$. The magnitude of difference depends on the completeness of combustion. Under lean operation, the combustion efficiency is usually greater than 95 %. [11 p. 509, p. 82] If the actual heat release is known, equation 2.28 can be used to solve the rate of change of cylinder pressure, which is done in equation 2.29

$$dp = \frac{dQ - \frac{\gamma}{\gamma - 1} \cdot p \cdot dV - \frac{h_c \cdot A \cdot (T - T_{wall}) \cdot 60}{2\pi \cdot n_{eng}} - \left(\frac{R_i \cdot dT_i}{\gamma_i' - 1} - u\right) \cdot dm_i}{\frac{1}{\gamma - 1} V + \frac{V_{cr}}{T_w}\left(\frac{1}{\gamma - 1} T + T' + \frac{1}{b} \ln\left(\frac{\gamma' - 1}{\gamma - 1}\right)\right)}. \tag{2.29}$$

The rate of change of temperature derived from the ideal gas law becomes slightly more complicated after the amount of injected fuel dm/m and other above-mentioned effects are taken into account, and is presented in equation 2.30

$$dT = T\left(\frac{dV}{V} + \frac{dp}{p} - \frac{dm}{m}\right). \tag{2.30}$$

3. W6L34DF ENGINE MODEL

3.1 Engine model introduction and structure

This chapter reviews the engine model made for W6L34DF engine. The model under evaluation is a zero-dimensional (0-D) thermodynamic mean value engine model. The term zero-dimensional refers to absence of flow modeling in the sense that geometric features of fluid motion cannot be predicted. Due to lack of dimensional description, state equations are solved in differential form. [3] The word thermodynamic indicates that the used equations that govern engine performance are mostly based on the law of energy conservation. [11 p. 749] Since engine processes are extremely complex, it is not possible to construct models that predict engine operation from basic physical equations alone. Therefore, experimental data is used to describe relations where the governing equations of the process are not known or they are too complex for modeling purposes.

The engine model is also a mean value engine model (MVEM). The definition of a MVEM is that it only captures engine dynamics on the average and does not describe variations that are faster than an engine cycle. The signals, parameters and variables are averaged over one or several cycles. [5 p. 145] The model considers time-varying phenomena as spatially averaged over each engine region. Due to the 0-D nature it cannot describe spatial variation and lumps all spatial information into one point. [11 p. 755] The lumped parameters lead to ordinary differential equations (ODE) as a function of time. If space dependency was not omitted, the model would contain more dimensions with distributed parameters leading to partial differential equations. ODEs are used throughout the engine model to describe system states. In the engine cooling system model state parameters are also location-dependent but can be represented with lumped parameters by partitioning heat exchangers into small segments. [12 p. 32]

The mean value engine model simulates air propagation through different volumes inside the engine. The flow of matter is expressed by mass flow, since it allows the use of mass balance equation and has a more direct connection to heat and power than volumetric flow. [12 p. 38] MVEM dynamically captures pressure and temperature of engine components outside cylinder, and uses those values along with fuel injection parameters in a combustion model to resolve the pressure inside the cylinder. Engine speed is calculated based on generated torque and engine load. Turbocharger speed depends on compressor and turbine performance. The engine processes that directly influence each combustion event inside the cylinders are described by crank-angle-dependent calculation. The engine processes outside of cylinders are described by time-dependent models.

The engine model consists of a number of sub-models that try to mimic the behavior of actual components in a realistic manner. Theoretical modeling yields the basic structure of the components, but precise models often require parameter tuning. Therefore, many physical equations contain parameters that are based on measurements from the actual engine or tabulated experimental data. The goal of the plant model is to include all the systems essential for comprehensive control software testing. The modeling focus is only on internal systems of the engine. The laboratory test cell also contains external systems that are necessary for engine operation but are not connected to the engine control system. All devices on W6L34DF that are controlled by engine control system are modeled, and their impact on engine performance can be simulated by the engine model.

3.2 MVEM – Mean Value Engine Model

It is often required to model different regions of the engine as open thermodynamic systems. This kind of modeling is appropriate when the composition and state of the gas inside the open system boundary (Figure 4) can be assumed uniform or changing due to heat transfer, work transfer or mass flow across the boundary. The change can also result from boundary displacement which occurs for example during cylinder chamber volume variation. [11 p. 750] Therefore, the first law of thermodynamics describing conservation of energy that was introduced in Chapter 2.3 can be used for these systems. Other important equations are the ideal gas law, the conservation of mass and Newton's laws of motion. Conservation of mass means that the rate of change of the total mass of an open system is equal to the sum of the mass flows into and out of the system [11 p. 750]. These above-mentioned principles are relied upon when modeling different components of the engine.

The engine is divided into 5 systems: Engine Model, Gas System, Lube Oil System, Fuel System and Cooling Water Circuit. These systems are modeled to a varying degree of accuracy. The condition of charge air combined with the fueling strategy will largely determine the torque delivered by the engine. Therefore, the systems directly influencing air and fuel conditions and their variation are the key systems to be modeled. The systems will be introduced in the following chapters in the order presented above.

3.2.1 Engine Model

The Engine Model is divided into 7 critical components: air filter, compressor, intercooler, engine manifold, cylinder, turbine and exhaust gas system. These components make up the engine's air-path. The gas flow through the engine is presented in Figure 5.

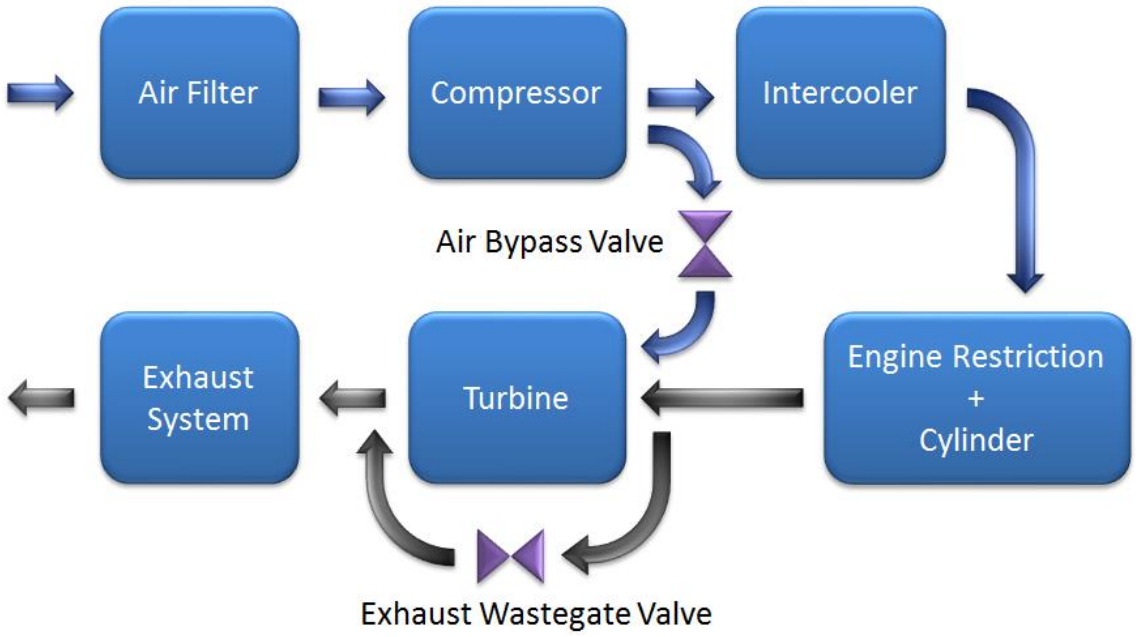

Figure 5. *Gas flow process through engine components.*

Each component of the Engine Model is an individual Simulink sub-model. Most of the components on the engine's air-path are represented with restriction and control volume. This modeling method is introduced as Filling and Emptying Method by Heywood [1. p 754]. The basic structure of these components is shown in Figure 6. Control volumes are treated as open systems of finite volume divided by restrictions. The pressure and temperature of the gas inside is determined according to entering and leaving mass flows as well as the temperature of ingoing fluid. The state of the gas inside a control volume varies periodically with time, but the composition remains uniform. [1. p 754] This kind of volume is called a well-stirred reactor since the incoming enthalpy is instantaneously spread out over the whole volume. [5 p. 163] The mass flow rate entering the control volume of each component $\dot{m}_{in}$ is used as the leaving mass flow rate in the control volume of the previous component $\dot{m}_{out}$. Therefore, the equations can be thought of being modeled in reverse order. The pressure of control volume is found by differentiating ideal gas law, and is introduced in equation 3.1

$$\frac{dp}{dt} = \frac{R_s T}{V}(\dot{m}_{in} - \dot{m}_{out}) + \frac{mR}{V}\frac{dT}{dt}, \tag{3.1}$$

where dp denotes pressure differential, R_s is the specific gas constant of air, T denotes temperature inside control volume, V is system volume, $\dot{m}_{in}$ means ingoing mass flow rate, $\dot{m}_{out}$ is outgoing mass flow rate, m denotes current air mass inside control volume and dT means change in temperature inside control volume. Temperature is found by differentiating the first law of thermodynamics and is shown in equation 3.2

$$\frac{dT}{dt} = \frac{1}{m}\left(\dot{m}_{in}(T_{in} - T)\right) + \frac{1}{mc_v}\left(R_s(T_{in}\dot{m}_{in} - T\dot{m}_{out}) + \dot{Q}\right), \tag{3.2}$$

where c_v is specific heat at constant volume and $\dot{Q}$ is possible heat transfer. When heat transfer equals zero the control volume can be called adiabatic volume. [5 p. 164–165]

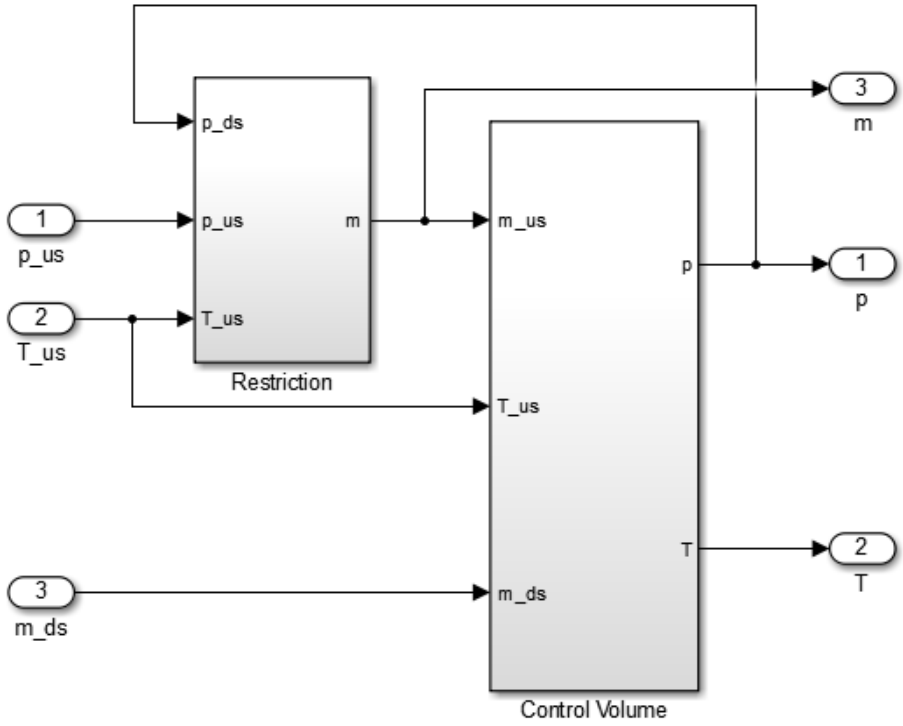

Figure 6. *Simulink model of engine component consisting of restriction and control volume. The subscript of pressure, temperature and mass flow is "us" before the component and "ds" after the component.*

Every control volume has a restriction for air flow. Mass flow through restriction between volumes is a core problem in fluid dynamics. Therefore, a large amount of theoretical and practical knowledge exists on the topic. There are two kinds of restrictions depending on the flow type: incompressible flow restrictions and compressible flow restrictions. However, there are numerous equations with varying degree of complexity tailored for different applications. The accuracy of the flow equations depends on made assumptions and considered effects. [10 p. 32] The equations describing incompressible and compressible flow restrictions used in this model are based on equations developed for turbocharged spark ignition engines. Mass flow rate through incompressible flow restrictions is defined by equation 3.3 [1]

$$\dot{m} = \sqrt{\frac{p_{bef}(p_{bef} - p_{aft})}{T_{bef} \cdot H}}, \tag{3.3}$$

where p_{bef} is gas pressure before restriction, p_{aft} is gas pressure after restriction, T_{bef} means temperature of entering gas and H denotes restriction flow properties. The parameter H is based on measurements from actual engine and has been tuned for each

restriction separately. Mass flow rate for compressible flow restrictions is introduced in equation 3.4 [1]

$$\dot{m} = \frac{p_{bef}}{\sqrt{R_s \cdot T_{bef}}} \Psi(\Pi) A_{eff}, \tag{3.4}$$

where A_{eff} is the effective flow area of restriction, $\Psi(\Pi) = \sqrt{\frac{2\gamma}{\gamma-1}(\Pi^{\frac{2}{\gamma}} - \Pi^{\frac{\gamma+1}{\gamma}})}$, $\Pi = \max\left(\frac{p_{aft}}{p_{bef}}, \left(\frac{2}{\gamma+1}\right)^{\frac{\gamma}{\gamma-1}}\right)$ and γ denotes the ratio of specific heats. The value of gamma used for air is 1.4. Psi function $\Psi(\Pi)$ relates the pressure ratio of compressible flow restriction and specific heat ratio of gas to flow characteristics. Figure 7 shows how different gamma values affect the psi function $\Psi(\Pi)$.

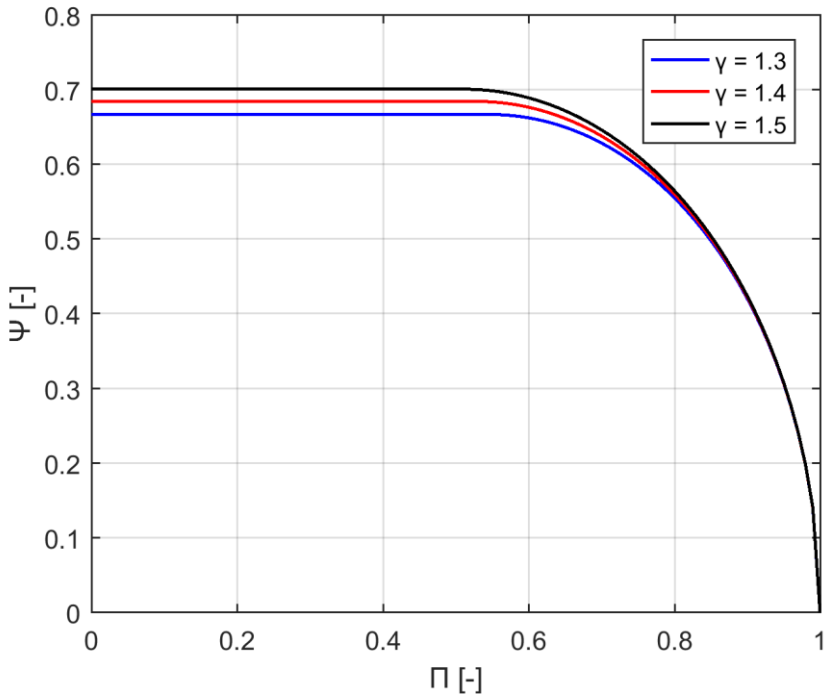

Figure 7. *Compressible flow psi function with different specific heat ratios.*

The first component on the engine's air-path is air filter through which the air flowing into the engine enters. The function of the air filter is to remove solid particles such as dirt and dust from the air to prevent mechanical wear and oil contamination. In addition, filter funnels are often designed to damp intake noise. [15 p. 387] Air Filter model is simply an incompressible flow restriction with a control volume. Next component is the compressor. Compressor is necessary for turbocharged engines to raise the pressure of intake air. More air allows more fuel to be burned each cycle, which results in increased volumetric efficiency and power output of the engine [9]. Lean combustion process and shorter air induction time into cylinder further increase the pressure demand for charge air. The compressor is connected to turbine through a shaft. When exhaust gas flows

through the turbine, compressor will spin at the same speed. The spinning compressor draws in ambient air and compresses it between compressor blades. Together compressor, turbine and the connecting shaft form the turbocharger. Turbocharger is an extremely important engine component as it grants higher power output from a given engine displacement by increasing the intake air pressure.

The Compressor model consists of restriction and control volume. The restriction is different to the previously mentioned restriction types. The mass flow through compressor restriction is based on experimental data instead of physical equations. This data is provided by the manufacturer. Society of Automotive Engineers (SAE) has created a standardized format for turbine and compressor maps. The data points of SAE maps describe the dependency between speed, pressure ratio, mass flow rate and efficiency. [7] If the speed of compressor and pressure ratio over it are known, the corresponding mass flow rate and efficiency can be found from the map. The maps are implemented as lookup-tables in Simulink to give appropriate mass flow rates and efficiencies according to the input values. In addition to mass flow rate, the restriction model gives compressor temperature and torque as outputs. Those are based on physical models introduced in equations 3.5 and 3.6

$$T_{comp} = T_{bef}\left(1 + \frac{\left(\frac{p_{aft}}{p_{bef}}\right)^{\frac{\gamma-1}{\gamma}} - 1}{\eta_{comp}}\right) \tag{3.5}$$

and

$$M_{comp} = \frac{c_p \cdot \dot{m} \cdot T_{bef}\left(\left(\frac{p_{aft}}{p_{bef}}\right)^{\frac{\gamma-1}{\gamma}} - 1\right)}{\eta_{comp} \cdot \omega}, \tag{3.6}$$

where η_{comp} is compressor efficiency and ω means angular speed of turbocharger. The control volume model is the same as introduced before. The W6L34DF engine uses single-stage turbocharging meaning that it has one compressor and one turbine.

When the pressure of intake air increases during compression, its temperature rises as well. The temperature can increase to over 200 °C. Feeding air with that high temperature into combustion chamber will have negative consequences. Hotter air is less dense and takes more space than cooler air, which results in less available oxygen and less usable fuel during combustion. Therefore, excessive charge air temperature reduces volumetric efficiency and engine power output. In addition, hot intake air causes combustion temperature to rise too high leading to engine knock and possibly damage the components. Engine overheating will also result in higher nitrogen oxide (NO_x) emissions.

In order to avoid high combustion temperatures, the compressed air goes through intercooler before reaching engine manifold. The intercooler has two consecutive charge air coolers that the charge air passes through. Intercooler is part of the engine's cooling system that will be introduced later. As Figure 5 shows, some of the compressor flow can also be directed to the turbine inlet, thus bypassing the intercooler and engine manifold. This can be done by opening the air bypass (ABP) valve. There are many different use cases for the bypass valve. There are two primary uses of this valve: First is to increase air flow to the engine as the extra air received by the turbine boosts turbocharger speed. Second is to prevent compressor surge that happens if pressure ratio of compressor rises too high at certain speed. In both cases mass flow through compressor increases, thus increasing charge air pressure and lambda, which decreases exhaust gas temperature. In diesel mode emphasis is more on having big enough air-fuel ratio, and in gas mode preventing surge is very important. ABP is also used to counter load drops when exhaust gas energy alone is not enough to drive the turbocharger. Air bypass valve is a butterfly throttle valve, the mass flow of which is modeled with compressible flow equation 3.4. The flow area of the valve is expressed as $A_{eff} = a \cdot pos_{ABP} + b$, where pos_{ABP} is the position of the valve which is proportional to control signal, and a and b are constant parameters obtained from air flow measurements in different operating points by fitting a linear function via least-squares method to the data. The measurements were done on W6L34DF engine.

The next component after intercooler is engine manifold which consists of intake manifold, cylinder and exhaust manifold. Intake manifold is also called receiver as it receives the compressed air. From the receiver cooled charge air will enter the cylinder chamber. Right before cylinder inlet valve opens, main gas valve on the engine is opened and high pressure natural gas starts to mix with intake air. The air-fuel mixture is then formed in the intake manifold as the air and fuel gas flow together into the combustion chamber. The intake process as well as the approximate location of the main gas valve are visualized in Figure 3. The flow through main gas valve is considered compressible following equation 3.4 with the exception that the effective flow area is replaced with valve constant. The valve is a direct actuated on/off face-type poppet valve with multiple concentric grooves and a moving plate [18]. Therefore, gas flow is controlled by opening duration instead of position signal. The duration of main gas valve opening requires fast control as it directly affects engine performance by controlling the amount of fuel. In addition, the pressure of fuel gas needs to be higher than charge air pressure in order for the gas to flow into the intake manifold. Fuel gas pressure is controlled by the gas valve unit (GVU) that is located off the engine and will be discussed in the gas system section. This was the engine's intake process during gas operation. In diesel mode, only air flows into the cylinder through intake manifold. Diesel fuel is then injected directly into combustion chamber. The engine manifold is modeled as restriction only and thus the sub-model is called Engine Restriction. The volume that usually follows a restriction is the cylinder in this case.

As opposed to previous engine components, the Engine Restriction model does not follow earlier flow equations. The mass flow of air into cylinder depends on receiver pressure and temperature, engine speed, cylinder volume and intake valve opening time. Some of the cylinder volume will be occupied by fuel gas so its mass flow has to be taken into account as well. The intake system from air filter to intake valve is not ideal and restricts the amount of air that the engine can induct [12 p. 76]. The parameter used to measure the effectiveness of engine's induction process is the volumetric efficiency [11 p. 53]. The biggest factors affecting flow losses are intake and exhaust gas system design, engine speed and air pressure. For four-stroke engines it has to be remembered that air is inducted once per two crankshaft revolutions. At this point of intake process it is relevant to take the volumetric efficiency of the engine into account. The volumetric efficiency is implemented as a lookup-table in similar way as was done with the compressor model. The lookup-table inputs are receiver pressure and engine speed. The air mass flow rate into cylinder can be calculated with equation 3.7

$$\dot{m}_{air} = \eta_{vol} \frac{\frac{n_{eng}}{2 \cdot 60} \cdot p_{rec} \cdot V_d}{R_s \cdot T_{rec}} - \dot{m}_{gas}, \tag{3.7}$$

where η_{vol} is the volumetric efficiency of the engine, n_{eng} means engine speed, p_{rec} denotes pressure in receiver, V_d is volume displaced by one cylinder, T_{rec} denotes temperature in receiver and $\dot{m}_{gas}$ is natural gas mass flow rate into cylinder.

The intake and exhaust valves are not modeled so there are no more restrictions between intake manifold and cylinder. The engine model is simplified in the sense that valve dynamics are not taken into account. When intake valve is open, it is assumed that gas flows freely into the cylinder. As intake manifold pressure is higher than exhaust manifold pressure due to turbocharging, and thus higher than the pressure of empty cylinder, this assumption is fairly justified. Intake valve closes at certain crank angle and at that point the available volume of combustion chamber will be filled with fuel gas, charge air and residual gases. The residual gases can occupy up to about 5 % of the total charge mass. The cylinder model receives intake manifold, exhaust manifold and diesel fuel pressures as well as engine speed and mass of fuel gas. The diesel fuel has different pressure, injection timing and duration depending on whether main injector or pilot injector in used. The cylinder model does not contain much functionality itself besides the mechanical operation as it only provides the setting for combustion process and work transfer. Combustion is the key process of the engine so all cylinder model inputs are passed to a combustion model inside the cylinder. The operation principle of the combustion model will be explained in Chapter 3.3. The engine contains 6 cylinders that all have the same specifications. Still there is variability in combustion and consequently in performance between actual cylinders. However, the differences in pressures and temperatures are not sufficiently big for modeling each cylinder separately to be viable. Thus, a computationally more optimal solution is to model one cylinder and multiply its effect by 6.

The outputs of the combustion model and consequently also the cylinder model are injected fuel mass, gas consumption, maximum cylinder pressure, brake mean effective pressure (BMEP), friction losses and heat losses. BMEP is the usable work delivered to the crankshaft per engine cycle divided by the volume displaced per cycle [11 p. 50]. There is an affine relation between BMEP and engine torque which in turn is linked to power output. Engine Inertia sub-model uses this relation to calculate engine speed. Engine speed depends on the power generated by the engine and the load acting on the engine. Inside the sub-model BMEP is converted to engine torque with equation 3.8

$$M_{eng} = \frac{BMEP \cdot V_d \cdot N_{cyl}}{2\pi \cdot n_r}, \tag{3.8}$$

where, N_{cyl} is the number of cylinders and $n_r = 2$ for four-stroke engines. [5 p. 186] Engine speed can then be solved with Newton's second law for rotation $M = I\alpha$, where M denotes torque, I means the moment of inertia and α is angular acceleration. The engine is usually coupled to a generator which produces the load torque. Therefore, the inertia of engine and the inertia of generator have to be taken into account. When engine speed is solved from the Newton's law in revolutions per minute, it gets the form of equation 3.9

$$\frac{dn_{eng}}{dt} = \frac{60}{2\pi} \cdot \frac{M_{eng} - M_{load}}{I_{eng} + I_{gen}}, \tag{3.9}$$

where M_{eng} means engine torque, M_{load} is load torque, I_{eng} denotes engine inertia and I_{gen} means generator inertia.

After the air-fuel mixture is burned during combustion, exhaust gases will leave cylinder through exhaust manifold. According to conservation of mass, the mass flow of exhaust gases is all the mass flows going into the cylinder combined. Some of the exhaust gases will stay in combustion chamber but they do not need to be accounted for because at the same time the residual gases from previous cycle are released. The engine restriction contains a model for calculating the exhaust gas temperature in addition to previously mentioned volumetric efficiency and mass flow rate calculation. There is no physical model used for exhaust gas temperature calculation, but the flame and exhaust temperatures for natural gas and diesel stay relatively constant with constant charge air temperature, completeness of combustion and ratios of work and heat transfer. After those parameters are taken into account, the biggest effect on exhaust gas is the amount of air. With the same released energy, smaller amount of air will have higher temperature than larger amount of air. Therefore, the exhaust gas temperature can be scaled based on air-fuel equivalence ratio. Higher lambda will result in cooler exhaust gas than lower lambda as long as there is always enough air for complete combustion.

The next component after engine exhaust manifold is the turbine of the turbocharger. The Turbine follows the original restriction and control volume-based modeling style. It is possible to limit the exhaust gas flow entering the turbine by opening the exhaust wastegate valve inside the restriction model, which will direct some of the flow past the turbine. The rest of exhaust gases flow through the turbine. The air flow that was directed from compressor through the bypass valve is added to the turbine intake mass flow. The exhaust gas contains a lot of energy due to its high temperature and pressure. The same applies to the charge air bypassing the engine manifold. This energy is utilized by the turbine. The operating principle of turbine is the opposite of compressor. When compressor transforms rotational energy of the turbocharger into potential energy of high pressure air, turbine does the opposite as it converts the energy of exhaust gas into turbocharger rotation. The mass flow rate through the Turbine model comes from a map in the same way as in the Compressor. Turbine efficiency is set to a constant of 90 %. The equations for temperature and torque outputs deviate slightly from compressor side due to opposite operation principle, and are presented in equations 3.10 and 3.11

$$T_{turb} = T_{bef} + T_{bef}\left(1 - \left(\frac{p_{bef}}{p_{aft}}\right)^{\frac{\gamma-1}{\gamma}}\right)\eta_{turb} \tag{3.10}$$

and

$$M_{turb} = \eta_{turb}\frac{c_p \cdot \dot{m} \cdot T_{bef}\left(1-\left(\frac{p_{bef}}{p_{aft}}\right)^{-\left(\frac{\gamma-1}{\gamma}\right)}\right)}{\omega}, \tag{3.11}$$

where η_{turb} is turbine efficiency and ω means angular speed of turbocharger. The rotational speed of turbocharger is calculated as revolutions per minute in a separate sub-model from the torques of compressor, turbine and turbocharger friction using equation 3.12

$$\frac{dn_{TC}}{dt} = \frac{60}{2\pi} \cdot \frac{M_{turb} - M_{comp} - M_{friction}}{I_{TC}}, \tag{3.12}$$

where I_{TC} denotes the moment of inertia of the turbocharger and $M_{friction} = a_1 n_{turb} + a_2 {n_{turb}}^2 + a_3$. The torque generated by friction comes from simple regression model where a_1, a_2, and a_3 are adjustable coefficients. As the turbine and compressor share a common shaft, the turbine supplies the drive energy for the compressor. If charge air pressure rises too high, turbocharger speed can be decreased by limiting the exhaust gas flow through the turbine. This can be done by opening the exhaust wastegate (EWG) valve. The effect of EWG valve is somewhat opposite to ABP valve as the latter one increases turbine mass flow while the former one decreases it. Flow through exhaust wastegate is modeled with compressible flow equation 3.4.

The effective area is estimated from measurements in the same way as with the air bypass valve. Exhaust wastegate is also a butterfly throttle valve.

The last component regarding air flow through engine is Exhaust System. The exhaust gas system normally contains mufflers to damp noise and catalytic converters to purify exhaust gases. In some applications exhaust gas boilers are added for heat recovery. However, the function of the exhaust system on W6L34DF test engine is simply to discharge hot exhaust gases out. Low flow resistance is particularly important in exhaust systems to reduce back pressure. [15 p. 393] Therefore, exhaust system pressure is close to ambient air pressure. The Exhaust System model is simply an incompressible flow restriction with a control volume. The engine's air-path has thus been analyzed and flows from air intake to its exhaust are now covered. The next system to be discussed is the fuel gas system that supplies natural gas to the engine.

3.2.2 Gas System

The fuel gas used by the engine comes from the gas system. Gas system is an external system located outside the engine. In case of the modeled W6L34DF engine it is outside the test bed cell. Liquefied natural gas (LNG) is used as the fuel gas and it is stored in tanks. Before use LNG has to be evaporated by passing it through vaporizer that heats the fuel. Once the natural gas is in gaseous state, it can be fed to the engine. The component controlling gas delivery to the engine is the gas valve unit that is located near the engine test bed. GVU controls the gas pressure by maintaining a certain pressure difference between the fuel gas and charge air pressure. When the external gas system is functioning properly, it supplies gas with moderately constant pressure and temperature. Therefore, LNG storage and transformation from liquid to gas in the vaporizer is not modeled, and it is assumed that gas with constant pressure and temperature is delivered to the GVU. The modeled gas system includes the gas valve unit, gas piping on the engine and a degassing valve. The Gas System components are modeled with same restriction and volume blocks as were used in the Engine Model. The GVU is not actually a single valve but contains one or more shut-off valves in addition to the gas flow control valve. Shut-off valves are on/off valves that are closed during diesel operation but open in gas mode. Before engine starts, gas leak test is performed to check that gas system is okay and shut-off valves are functioning. The flow control valve of the GVU is a butterfly throttle valve which is modeled as a restriction using compressible flow equation 3.4. There are no flow measurements available from the GVU so the relative valve opening is approximated with a function that has a shape common to basic proportional valves. The relative opening as a function of valve control signal is shown in Figure 8. The diameter of the throttle valve is known so the relative opening is then multiplied by the maximum flow area of the valve to get the effective area A_{eff}. The GVU also has a control volume, the output of which gives gas pressure after GVU.

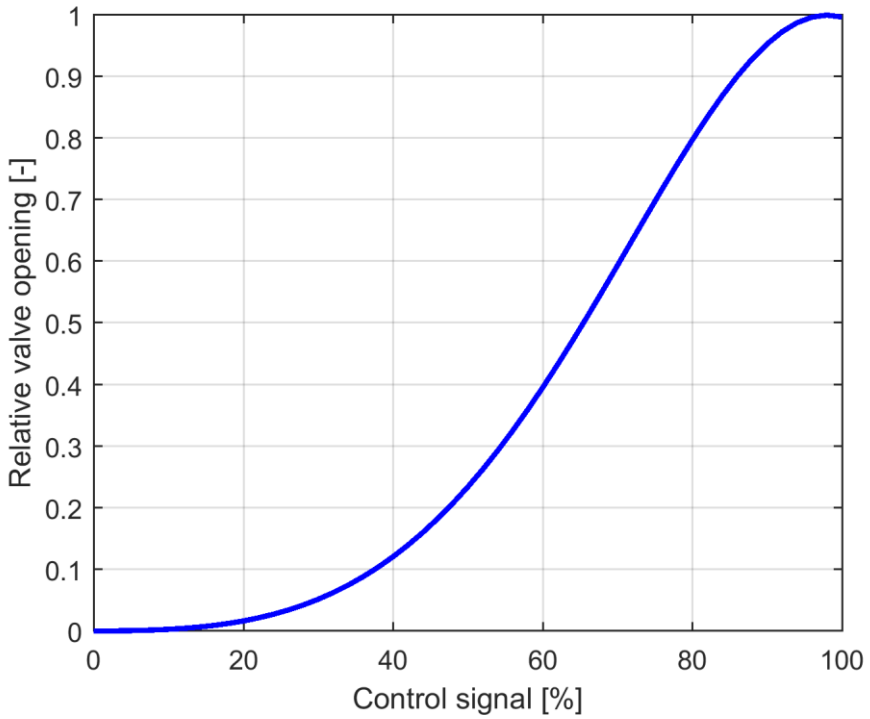

Figure 8. *Relative valve opening of butterfly throttle valve in GVU as a function of control signal.*

After gas valve unit the gas enters a pipe leading to the engine. The pipe is modeled with incompressible flow restriction of equation 3.3 and a control volume. The pipe runs along the engine and continues with individual feed pipes to main gas valves from where the fuel gas enters cylinder inlet channels. [19] Therefore, the output of Pipe Volume model gives the main gas pressure of the engine. The temperature of gas system is assumed to stay constant and thus 27 °C temperature after vaporizer is used in all components. That is also why GVU Volume and Pipe Volume blocks do not have temperature as output as opposed to Engine Model control volumes. The Gas System has another valve model with compressible flow restriction which is the Degassing Valve. Degassing valve is located at the end of the main gas pipe on the engine [19]. If gas pressure suddenly rises too high or if charge air pressure drops for example due to abrupt load decrease, the main gas valve will not be able to open due to too big pressure difference between gas pipe and intake manifold. In order to lower gas pressure, degassing valve at the end of the gas pipe can be opened.

3.2.3 Fuel System, Lube Oil System and air systems

Next Fuel System, Lube Oil System, Instrument Air System and Start Air System will be discussed. These systems are important parts of the engine but they are not actually modeled. What is meant by the Fuel System is the diesel fuel system as fuel gas delivery is covered by the Gas System. There are different system designs for diesel fuel delivery into the combustion chamber. The fuel system on W6L34DF engine consists of

injection pumps, delivery pipes, fuel injectors and injector nozzles. These components operate under extremely high pressures up to 1800 bar [12 p. 301]. The pilot fuel has a separate injection system. Large pressure differences across injector nozzle are required so that injected liquid fuel jet will reach high velocity when entering combustion chamber. High velocity is needed to ensure fuel atomization into small droplets to enable rapid evaporation. Another reason is to make sure that fuel penetrates the dense air charge in the cylinder to achieve good mixing between diesel fuel and air-gas mixture. [11 p. 517] Figure 3 shows the injector location in the middle of the cylinder head. Injection timing and duration require precise control for each cylinder in order to effectively use the fuel at any given engine speed and load. The main diesel fuel is drawn from a fuel tank by a supply pump, and goes through a filter reaching the injection pumps. The injection pumps then send the fuel under high pressure to main fuel injectors containing needle valves in their nozzles. When diesel pressure overcomes the force of injector spring, the needle valve opens and fuel is injected directly into cylinder chamber through injector nozzle. Excess fuel goes back to the fuel tank. Injection pumps on the W6L34DF engine are so called jerk pumps or in-line pumps that contain a plunger and barrel assembly for each cylinder. These pumps are operated by camshaft as each plunger is raised by a cam and is forced back by the plunger return spring. Therefore, the injection timing is fixed to the camshaft in the same way as the inlet and exhaust valve timings are. However, engine control system can change injection duration by varying the effective plunger stroke. [11 p. 518] A more advanced system is the common rail injection system that has a single rail feeding multiple solenoid actuated injectors allowing electronic control of both injection timing and duration. The pilot fuel injection system uses this kind of common rail system with its own high pressure pump and fuel filter. A common rail pipe delivers the pilot fuel to each pilot fuel injector and acts as a pressure regulator against pressure pulses. [19]

The actual above-mentioned fuel system components are not modeled. The pressure of both main diesel and pilot fuel is set to constant so it is assumed that injection pressure stays always the same. This assumption is valid for main fuel as jerk pumps mechanically produce the same pressure for every injection. The assumption is also justified for pilot fuel injection because even though pilot fuel pressure varies slightly at pump outlet, common rail pressure at the injectors stays very stable. In addition, slight fluctuation in pilot fuel pressure has no noticeable effect to engine operation due to small injection amounts. The pilot fuel pressure can be set to different levels by engine control system. There are however, some injection parameters that are taken into account by the Combustion Model inside Cylinder. The injectors have some latency after intended start and stop timings. These opening and closing latencies result from pressure increase and decrease delays before needle valve starts to react. There are also opening and closing times as the injector needle moves steadily between end positions. These parameters have been generated by investigating actual needle lift measurements. As a result, the dynamics of injectors are taken into account in the form of trapezoidal

position profile when calculating injected fuel masses. The fuel injection profile is shown in Figure 9, where SOI stands for start of injection and EOI denotes end of injection. Main and pilot fuel injectors have similar profiles but slightly differing parameters.

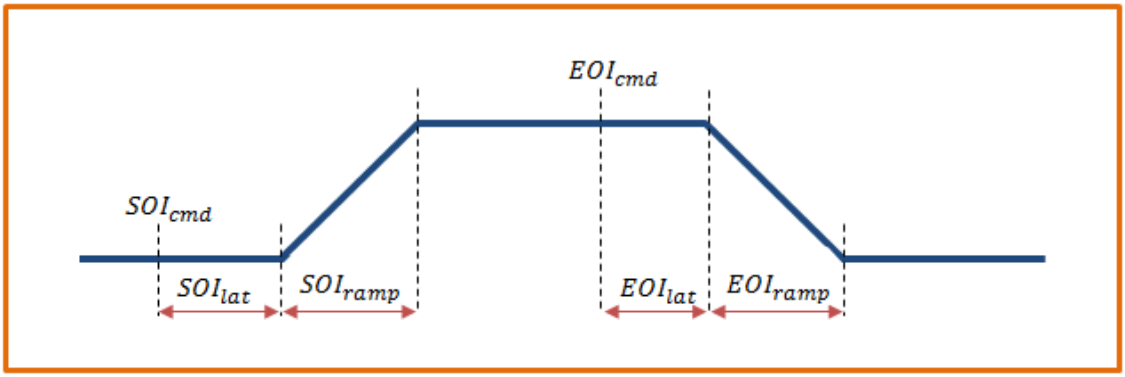

Figure 9. *Injector needle valve opening profile, where SOI_{cmd} and EOI_{cmd} mean start and end of injection commands, SOI_{lat} and EOI_{lat} are opening and closing latencies of injector and SOI_{ramp} and EOI_{ramp} denote injector opening and closing times.*

The lubricating oil system consists of the following components: main oil pump, prelubricating oil pump, oil cooler, thermostat valve, automatic filter, centrifugal filter, and pressure control valve [19]. Prelubricating pump is used to circulate oil around the engine prior to engine start. When engine is on, main pump is used to draw oil from the tank. The oil is then cooled, filtered with the automatic filter and supplied to the engine. The pressure control valve maintains oil pressure at desired level. All moving engine components require lubrication. Those include crankshaft bearings, camshaft bearings, pistons, injection pumps and the turbocharger. In the end of lubrication cycle the oil drains back into the tank or into a sump under the engine. Oil in the tank is constantly circulated through the centrifugal filter to remove any water or particles. However, in similar way to the Fuel System, Lube Oil System modeling is kept minimal and only the processes directly affecting engine power production are included.

Assuming that engine lubrication is properly taken care of, lube oil does not affect engine performance. Therefore, engine friction can be estimated with a simple model instead of modeling the whole lubrication system. However, in addition to lubricating the moving parts, circulating oil is also the main method of removing heat from the components. As lube oil plays an important role in engine cooling, heat transfer to the oil is included in the engine model. Therefore, a model of oil cooler is added into the engine cooling system. All of the friction losses and 25 % of the cylinder heat losses are assumed to be transferred to lubricating oil. These power losses will heat up the oil going into the cooler. The oil mass flow through the cooler is assumed to stay constant.

The Instrument Air System of the engine is not modeled at all. Instrument air is clean and dry compressed air free from particles and oil. The instrument air is used to provide

actuating energy for safety and control devices. For example many valves such as charge air bypass and exhaust wastegate are pneumatically actuated. The engine is started with the help of Start Air System. The start air system of the engine is not modeled either. Before actual engine start, air is fed directly into cylinders through a slow turning valve, which rotates the engine slowly for a few turns to get any condensed water out of the cylinder chambers. During engine start, compressed start air is injected into cylinders through starting air valves in the cylinder head. Fuel injection is enabled after initial speed is achieved. As long as instrument and start air systems are assumed to work properly and simulation does not focus on engine start, modeling these systems would bring little value.

3.2.4 Cooling Water Circuit

The purpose of cooling system is to remove waste heat from the engine. The internal system consists of two water circuits: high temperature (HT) side and low temperature (LT) side. High temperature water is about 80 °C and low temperature water varies around 50 °C. Both sides have their own engine driven pumps and flow control valves to regulate water temperature. HT- and LT-side pumps are assumed to work at constant rates so the mass flow of both circuits is set to constant. There is also an external circuit that supplies about 30 °C sea water to a central cooler for cooling the internal circuits. The external circuit has steady flow as well. The cooling water system can be different for each engine installation. In W6L34DF engine HT-water circulates through the cylinder jackets in engine manifold and then goes through the first charge air cooler. LT-water is used in the second charge air cooler and lubricating oil cooler. When water temperature rises over a set point, flow control valve is opened directing water through the central cooler with sea water as coolant. The Cooling Water Circuit of W6L34DF is depicted in Figure 10. As can be seen from the figure, the engine has two-stage charge air cooling. However, both heat exchangers are physically inside one engine component which is the intercooler. When charge air of the Engine Model goes into the Intercooler, it passes through both charge air coolers before continuing to Engine Restriction. The charge air loses some of its energy during cooling process but it is necessary for engine operation. Charge air temperature control is especially important in gas mode as hot air can ignite the fuel gas before pilot fuel injection. Sometimes the terms intercooler and charge air cooler are used interchangeably.

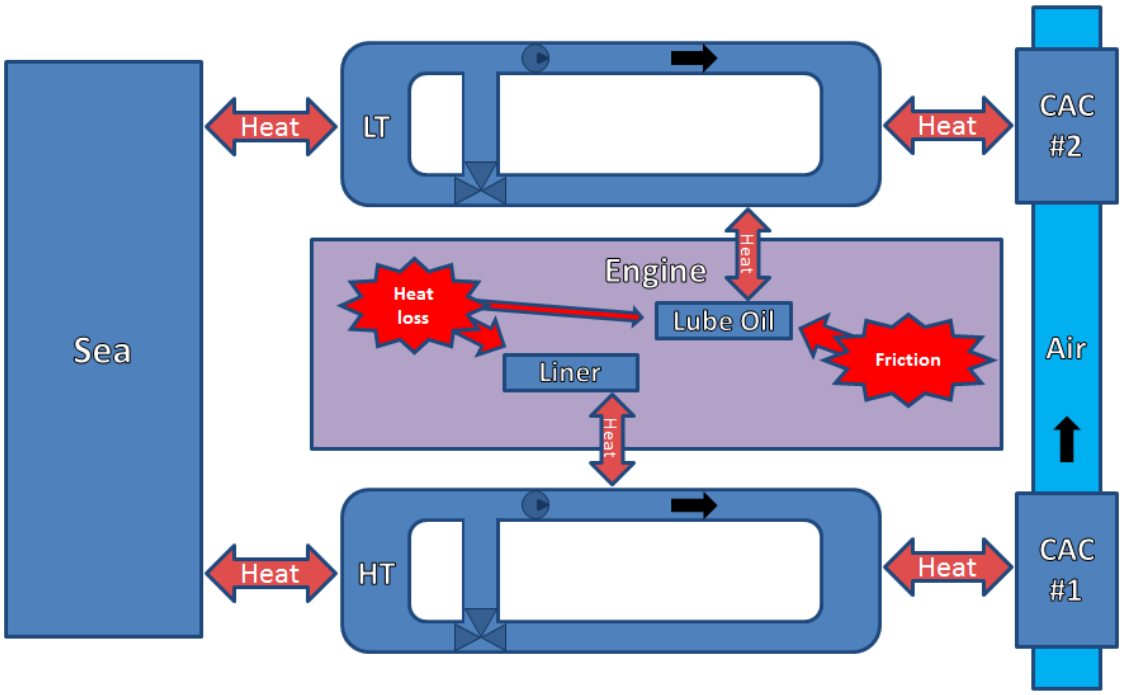

Figure 10. *Cooling water circuit of the engine.*

The Cooling Water Circuit of the engine has 6 modeled heat exchange processes marked with double sided arrows in Figure 10. All heat exchangers are modeled as counter-flow double-pipes. Their operating principle is shown in Figure 11. The hot fluid flows through the inner pipe that will be called the tube and transfers its heat to the cooling water flowing to the opposite direction in the outer pipe called the shell. The convective heat transfer can be approximated with Newton's law of cooling $\dot{Q}_{transfer} = h_c A(T_{tube} - T_{shell})$, where h_c denotes convective heat transfer coefficient from one fluid to another, A means heat transfer surface area of the pipe, T_{tube} is the tube temperature and T_{shell} is the shell temperature. Heat transfer coefficient is set to constant. It is also assumed that tube and shell pipes have the same temperatures as the fluids inside them. The heat exchange process in double-pipes is divided into segments. The rate of thermal energy accumulation at the end of a heat exchanger tube segment can be written as equation 3.13

$$dQ_{out} = \dot{Q}_{in} - \dot{Q}_{out} - \dot{Q}_{transfer}, \tag{3.13}$$

where $\dot{Q}_{in}$ means the rate of incoming energy at the beginning of a tube segment, $\dot{Q}_{out}$ means the rate of outgoing energy at the end of the tube segment and $\dot{Q}_{transfer}$ is the heat transfer of the tube segment. When the change in thermal energy due to temperature $dQ = mC_p \frac{dT}{dt}$ and mass flow $\dot{Q} = \dot{m}C_p T$ as well as heat transfer are substituted into equation 3.11, the temperature at the end of a tube segment can be solved from equation 3.14

$$\frac{dT_{out}}{dt} = \frac{1}{m}\left(\dot{m}(T_{in} - T_{out}) - \frac{h_c A}{C_p}(T_{tube} - T_{shell})\right), \tag{3.14}$$

where m is the fluid mass inside the pipe, $\dot{m}$ denotes mass flow rate through the pipe, T_{in} is temperature of incoming fluid, T_{out} is temperature of outgoing fluid and C_p is specific heat capacity of the fluid in the pipe. The same equations can also be used for shell with the difference that heat transfer will be positive. Every heat exchanger has a model for the double-pipe that takes lengths, pipe radiuses, pipe thicknesses and fluid properties into account to calculate heat transfer area and fluid masses.

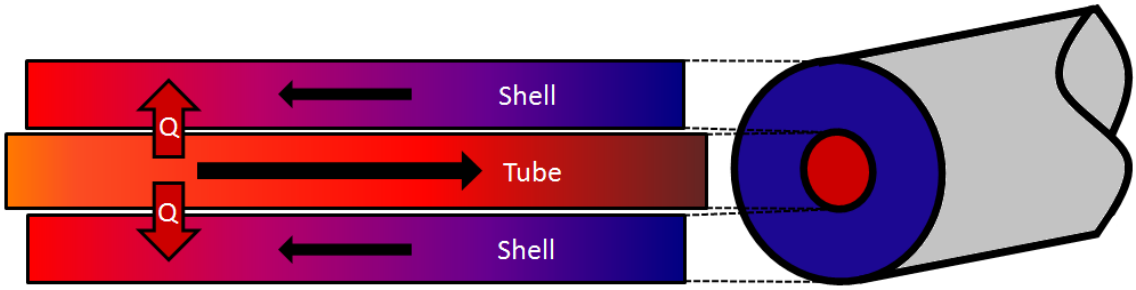

Figure 11. *Double-pipe heat exchanger.*

The waste heat comes from engine friction and in-cylinder heat-losses. A small part of the heat losses is assumed to radiate out of the engine into surrounding air through engine manifold instead of being transferred into cooling water. According to Stefan-Boltzmann law the radiation loss is $P_{rad} = \sigma \cdot A_{rad} \cdot ({T_{HT}}^4 - {T_{amb}}^4)$, where σ denotes Stefan-Boltzmann constant, A_{rad} means radiating surface area, T_{HT} is temperature of HT-water at the end of the circuit and T_{amb} is ambient air temperature. In this case the radiating part of the engine manifold is assumed to have the same temperature as heated HT-water, which is a good estimate between hot cylinder liners and cool HT-water.

Engine friction losses are transferred to lube oil as well as 25 % of the remaining heat losses. The rest 75 % of heat losses are delivered to cylinder liners. On HT-side the water goes first through the engine manifold to cool cylinder walls. Because cylinder liners are stationary, and HT-water moves around them inside the jackets, it is not very accurate to describe the heat exchanger as double-pipe. As this kind of direct cooling is possible only with solid parts of the engine, exception was made with the liners, and heat transfer area is adjusted with length parameter for better fit. The tube side of the heat exchanger has a fixed mass and specific heat capacity of iron. The HT-water will next flow into the first charge air cooler to receive heat from the high pressure air. During this cooling process the temperature stabilizes and the difference between charge air and HT-water output temperatures stays within a few degrees Celsius. At the end of the HT-circuit there is a thermostatic self-regulating three-way valve with a reference temperature. The valve has a wax element inside the thermostat that expands

and contracts according to the temperature. If the outgoing HT-water is colder than the set point, the valve stays closed and directs the flow back into engine circulation. When water temperature increases over the reference, the HT-valve starts to open and lets some of the flow into the external circuit that leads through the central cooler. In the central cooler HT-water undergoes the last heat exchange process before returning back to internal system and mixing with the hot HT-water. Even though HT-valve does not have feedback control, the dynamics of the valve are modeled with a slow controller and low sampling frequency.

LT-side undergoes similar cooling process. After LT-pump water goes through the second charge air cooler where temperatures of air and water stabilize. After that water continues to the lube oil cooler before reaching the LT-side three-way valve. Some of the water is then directed through the central cooler outside the engine if water temperature is too high. Unlike the HT-valve, LT-valve position is controlled by the engine control system. This is because the second charge air cooler sets the final temperature of engine intake air before it is drawn into the cylinders. Therefore, LT-valve must have faster reaction to temperature changes. However, the process itself is quite slow and charge air temperature usually requires minutes to settle to any reference value.

3.3 Combustion Model

The combustion model is a thermodynamic model based on the physics of gas exchange, fuel injection and combustion [12 p. 156]. These processes control engine power but are very complicated. Even today the exact chemical reactions undergoing inside the combustion chamber are not known except for few basic fuels. [11 p. 72] Therefore, some idealized cycle processes are usually defined. The following simplifications have been applied to the combustion model: gases are ideal, there are no flow losses during cylinder gas exchange, intake and exhaust processes are adiabatic and pressure differences between cylinder and engine manifold drop to zero during intake and exhaust. [12 p. 158] However, there are many real-world phenomena that the model does take into account, even though they are often idealized. The change of specific heats of gases as a function of temperature is modeled. Heat transfer to cylinder walls is included during compression and expansion phases. Friction losses are estimated with a simple model for FMEP. In addition, some functionality such as intake and exhaust valve openings as well as injector openings have been defined inside Combustion Model even though the components itself are not modeled.

The Combustion Model is written as an embedded Matlab function block which is located inside the Cylinder model. Embedded Matlab function is the only suitable option to incorporate Matlab algorithms into a Simulink model when it is needed to generate stand-alone code that will run on real-time target PC. The inputs of the main function are: engine speed, intake manifold pressure, exhaust manifold pressure, charge

air temperature, intake valve closing time, start and end times of main and pilot fuel injections and the mass of fuel gas. The combustion model will simulate cylinder chamber conditions of the whole 720 degree engine cycle based on these input parameters. Cylinder pressure is the main variable to be solved by the model as it can be directly related to engine power.

The Combustion Model has a main function that initializes the model, calls a solver function, and calculates the output values of the model in the end of the cycle. Initialization of the function involves defining the combustion chamber conditions at the time of intake valve closing. This means calculating cylinder volume based on cylinder geometry presented in Figure 2 and the crank angle at which the intake valve closes. Ideal gas law is then used to determine the amount of charge air this volume can fit. After that main function calls the solver function passing parameters from initialization as well as all combustion model inputs to it. The solver function is an iterative routine that uses fourth order Runge-Kutta method to find solutions for ordinary differential equations. It uses the initial cylinder conditions and integrates a set of equations over a specified interval. The integration period is divided into fixed steps, and the solution of each step is the weighted average of four increments. This means that four iterations are made to approximate the solution in order to minimize error. The integration period and step size are inputs of the solver function as well. The interval is set from intake valve closing to exhaust valve opening with the step size of one crank angle degree. The separate ODE-solver enables solving differential equations in crank angle domain while the rest of the engine model operates in time domain. The flowchart of Combustion Model execution order including all the functions is presented in Figure 12. When solver function is done, it will produce solutions from IVC to EVO including the compression and combustion phases, which is when cylinder pressure undergoes the biggest changes.

The rest of the engine cycle is not covered by integration, meaning that intake, end of combustion and exhaust phases still have to be solved. However, cylinder pressure does not change severely during those processes. Therefore, simpler approach such as interpolation can be chosen as a solving method. As a matter of fact, intake pressure does not require any computation. Since there is no modeled pressure drop over the intake valve, pressure inside cylinder chamber during intake is the same as intake manifold pressure, which is practically the pressure of charge air. The same applies to the latter part of exhaust stroke when cylinder pressure decreases to exhaust manifold pressure level which is also known. The only remaining gap in engine cycle is from exhaust valve opening to when cylinder pressure reaches exhaust manifold pressure. Cylinder pressure will be decreasing steadily after EVO for about the next 60 °ca so this gap interval can be interpolated. As cubic interpolation is not supported in embedded Matlab, linear interpolation is used instead. The ODE-solver is used in the Combustion Model to speed up simulation. However, integration of multiple equations is still heavy

especially for real-time purposes. Estimates for constant and linear cylinder pressure allow avoiding integration over the full 720 degree engine cycle, which somewhat simplifies the Combustion Model.

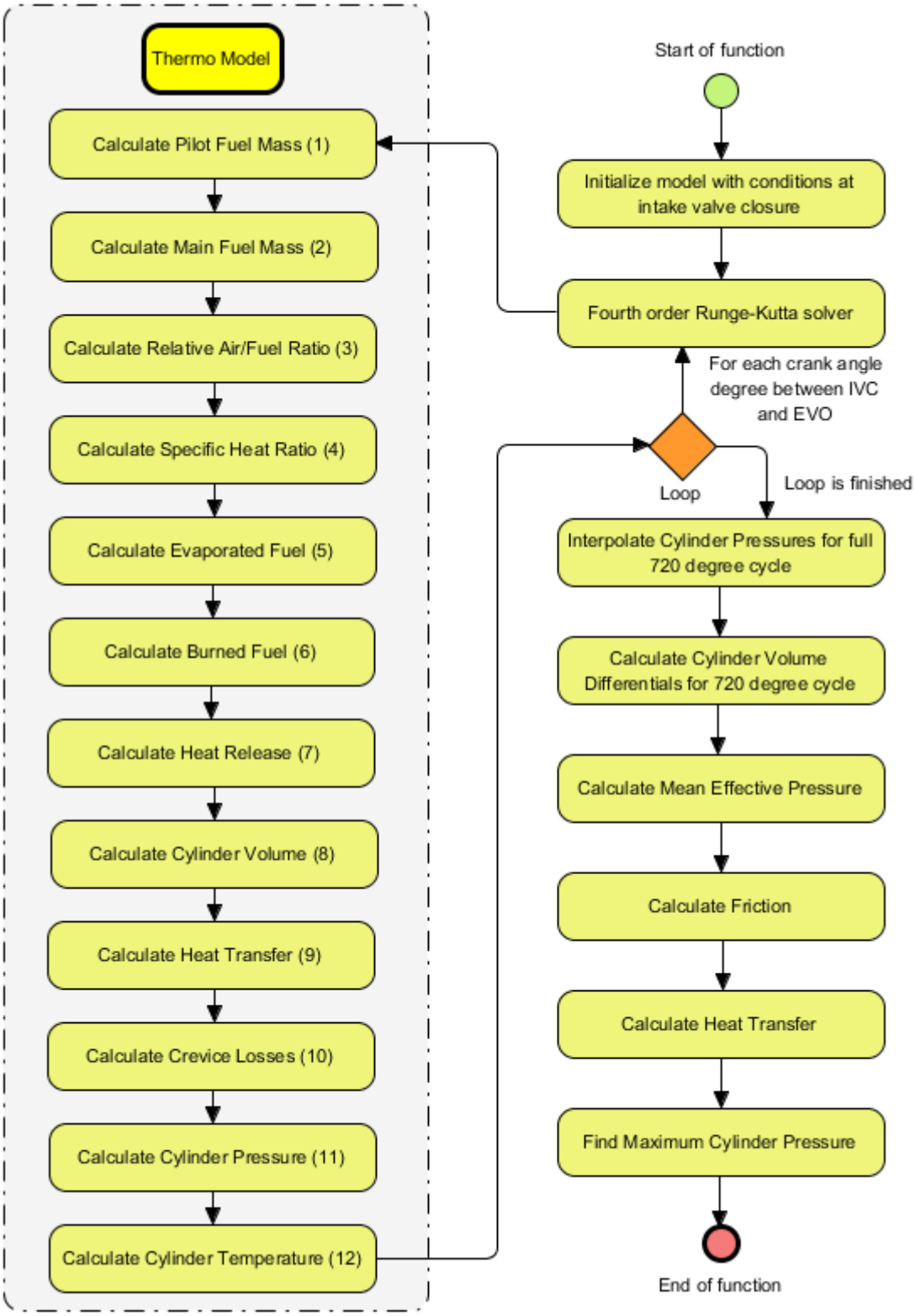

Figure 12. *Combustion model flowchart.*

Figure 12 presents the pseudocode of the Combustion Model. On the left side is a Thermo Model function that is called by the ODE-solver and is responsible for the thermodynamic calculation of the Combustion Model. The execution order is marked with numbers 1–12, and each number represents another function. The solver calls the Thermo Model function four times every integration step. It means that four iterations are made during each crank angle degree from IVC to EVO in order to solve the equations of every function marked with a number from 1–12. Every round the functions use the outputs from previous iteration to calculate new values. First two functions calculate the masses of injected pilot and main diesel fuel. As was explained in Chapter 3.2, injector opening follows a trapezoidal profile. Injected fuel mass can be calculated with equation 3.15

$$dm_{inj} = x_{inj} C_{inj} \sqrt{p_{fuel} - p_{cyl}}, \tag{3.15}$$

where x_{inj} is injector opening, C_{inj} denotes injector valve constant, p_{fuel} means fuel pressure and p_{cyl} is cylinder pressure. The injector opening value 0 means completely closed and 1 is fully open. The same equation is used for main and pilot injectors. Both fuel masses are then added together because pilot injector is used also during diesel operation. When the total amount of diesel fuel is known, the relative air-fuel ratio can be calculated with equation 3.16

$$\lambda = \frac{m_{air}}{m_{fuel}} \cdot \frac{1}{AFR_s}, \tag{3.16}$$

where m_{air} is the air mass in cylinder, m_{fuel} is the combined mass of diesel and gas fuels and AFR_s is the stoichiometric air-fuel ratio. Stoichiometric air-fuel ratio depends on the used fuel. If there is more natural gas than diesel, AFR_s of methane is chosen. Otherwise, the respective value for diesel is used. In case of gas operation, the mass of injected pilot fuel is added to the fuel mass. Therefore, the used stoichiometric air-fuel ratio 16.7 is slightly lower than the AFR_s of natural gas which is about 17.2. The fourth Thermo Model function is for calculating the ratio of specific heats. Gamma is modeled throughout the combustion process according to the theory presented in Chapter 2.3, and calculation is done by following equations 2.1 to 2.18. The NIST-JANAF tables for specific heats of different gas species are incorporated into the model as presented in Tables 3 and 4. Chemical composition and equilibrium computation greatly increases Combustion Model complexity so a simplified function was developed as an alternative option to determine the ratio of specific heats. This second gamma function is a regression model obtained by using chemical equilibrium equations. The regression model predicts specific heat ratio from pressure, temperature and lambda, and it is introduced in equation 3.17

$$\gamma = g_1 + g_2 T + g_3 T^2 + g_4 T^3 + \frac{g_5}{\lambda} + \frac{g_6 T}{\lambda} + \frac{g_7 T^2}{\lambda} + g_8 p + g_9 pT + \frac{g_{10} p}{\lambda}, \tag{3.17}$$

where g_i are coefficients, T means cylinder temperature, λ denotes relative air-fuel ratio and p is cylinder pressure. If temperature is under 1600 K, coefficients g_1 to g_7 are used and rest are set to zero. When temperature is above that, all coefficients are used. Whether the Combustion Model will use the original gamma model or the regression model can be decided by changing the value of one parameter.

The next three functions aim for heat release calculation. The first one calculates the evaporation rate of diesel fuel, and the used equation is presented in equation 3.18

$$dm_{evap} = C_1 \cdot {m_{inj}}^{1-x} \cdot {p_{O_2}}^{0.4} \cdot \left(m_{inj} - m_{evap}\right)^x, \tag{3.18}$$

where C_1 is evaporation coefficient that has different values for diesel and gas modes, m_{inj} denotes thus far injected fuel mass, p_{O_2} means partial pressure of oxygen, m_{evap} is evaporated diesel mass and x is a factor between [0… 1]. A value of 1 is used for x. The amount of burned diesel and fuel gas is calculated next. Diesel fuel burn rate is presented in equation 3.19

$$dm_{burn} = \frac{C_2 \cdot p_{O_2}}{\frac{n_{eng}}{60} \cdot \sqrt{T}} e^{(T_C/T)} (m_{evap} - m_{burn}), \tag{3.19}$$

where C_2 denotes burn coefficient, T_C is a constant, T means cylinder temperature and m_{burn} is the mass of burned diesel. Modeling ignition and combustion processes for direct-injection engines is complex because of unsteady liquid-fuel droplet motion, atomization and evaporation as well as fuel-air mixing and ignition chemistry. However, models at various levels of detail have been developed and proven useful in engine analysis. [11 p. 778] Equations 3.18 and 3.19 are modified from research publications regarding simulation and modeling of combustion in diesel engines. Pilot ignited gas combustion modeling principle is a compromise between diesel and gas operation. It is assumed that gas ignites when about 5 % of the pilot fuel has burned. This is used as a way to simulate ignition delay which is the time from start of injection to start of combustion. [5 p. 126] After the ignition flame starts to propagate inside the cylinder chamber. The leading edge of the flame can be approximated by the surface of a sphere. As a result, burned gas volume and thus the mass is proportional to the cube of flame radius. [11 p. 766] The mass increase rate should be the derivative of mass and thus proportional to square of the radius. Fuel gas burn rate is based on both diesel equations and spherical burning of gas, and can be estimated with equation 3.20

$$dm_{burngas} = C_3 p\left(\dot{m}_{burn} + C_4 {m_{burngas}}^2\right)\left(m_{gas} - m_{burngas}\right), \tag{3.20}$$

where C_3 and C_4 are coefficients that describe the quadratic rate of burning gas, m_{gas} means fuel gas mass inside combustion chamber and $m_{burngas}$ denotes so far burned gas mass. With known burn rates for diesel and gas fuels, it is now possible to calculate their heat release rates with equation 2.19. The used lower heating values are

42.87 MJ/kg for diesel and 49.60 MJ/kg for natural gas. When the heat releases are summed together, the result is the energy released by combustion. After this is integrated by the ODE-solver, the outcome becomes the cumulative heat release.

The function to calculate combustion chamber volume comes next. The Combustion Model keeps track of the current cylinder volume, the rate of change of volume and cylinder area. The equations are based on cylinder geometry shown in Figure 2 and are presented as equations 3.21, 3.22 and 3.23

$$V = V_C + \frac{1}{4}\pi B^2\left(\sqrt{(l+a)^2 - {x_{off}}^2} - s\right), \tag{3.21}$$

$$\frac{dV}{d\theta} = \frac{1}{4}\pi B^2 a(\sin\theta + \frac{(x_{off}+a\cdot\sin\theta)\cdot\cos\theta}{\sqrt{l^2-\left(x_{off}+a\cdot\sin\theta\right)^2}}) \tag{3.22}$$

and

$$A = \frac{2\pi B^2}{4} + \pi B\left(\sqrt{(l+a)^2 - {x_{off}}^2} - s\right), \tag{3.23}$$

where all parameters are same as used in Chapter 2.1.

Heat and crevice losses are solved next. These losses were described in Chapter 2.3 and same principle is used in the Combustion Model. Heat transfer to cylinder walls is calculated with equation 2.24. Equation 2.26 is used to solve crevice losses, and heat losses from diesel fuel evaporation are calculated with equation 2.27. When heat release from combustion as well as all in-cylinder losses are known, it is possible to substitute the values into equation 2.29 to solve cylinder pressure differential. Temperature differential can then be computed from with equation 2.30.

After solver function has integrated the results given by Thermo Model for each crank angle degree from intake valve closing to exhaust valve opening, cylinder pressure is interpolated for the rest of the engine cycle as was explained in the beginning of this chapter. The cylinder pressure is used in mean effective pressure calculation. There are four different MEPs that are solved: indicated mean effective pressure (IMEP), pumping mean effective pressure (PMEP), friction mean effective pressure (FMEP) and brake mean effective pressure (BMEP). IMEP is calculated from cylinder pressure over compression and expansion portions of engine cycle and PMEP over intake and exhaust portions. IMEP and PMEP are solved with equations 3.24 and 3.25 when combustion takes place around 0 °ca

$$IMEP = \int_{-180}^{180} pdV \tag{3.24}$$

and

$$PMEP = \int_{-360}^{-180} pdV + \int_{180}^{360} pdV. \quad (3.25)$$

IMEP and PMEP correspond to the work produced inside the cylinder by combustion and moving gases. Some of this work is consumed by the friction between piston and cylinder wall as well as friction in connecting rod and crankshaft bearings. This friction can be modeled with FMEP which is the theoretical mean effective pressure required to overcome engine friction. [5 p. 87] One example of a friction model is the ETH model that takes into account mean piston speed, the effect of turbocharging on bearing dimensions, load from auxiliary devices and the effect that engine load has on rubbing friction. [5 p. 190] However, this model requires BMEP to be known before FMEP can be calculated, so a simpler model was chosen that only varies with speed. This kind of polynomial regression model was introduced by Heywood [11 p. 719] and it is presented in equation 3.26

$$FMEP = C_5 + C_6 n_{eng} + C_7 {n_{eng}}^2, \quad (3.26)$$

where C_5, C_6 and C_7 are coefficients tuned for the modeled engine. When all other mean effective pressures are known, BMEP can be solved from equation 3.27

$$BMEP = IMEP + PMEP - FMEP. \quad (3.27)$$

BMEP is one of the outputs of the Combustion Model. Other output values are friction and heat transfer after being converted to power losses. FMEP is first recalculated to corresponding torque with same principle as equation 3.8 and then to power using $P_{fric} = M_{fric} 2\pi n_{eng}$. Heat transfer is converted to power through $P_{ht} = \frac{Q_{ht}}{t}$ taking into account the total number of combustions per second. Maximum pressure of each cycle is also chosen as an output.

Compared to other simulated systems of the engine model, the combustion model is computationally the heaviest. Modeling 6 cylinders separately each with their own combustion models would be an overly complex approach. Instead, the functionality of all cylinders can be modeled with sufficient accuracy with one cylinder and one combustion model. A pulse generator block is used to implement a combustion trigger in order to control Combustion Model execution. With 6 cylinders there are 6 combustion events during each engine cycle. When engine is operating at its nominal speed of 750 rpm, there are 37.5 combustions per second. Therefore, in order to simulate combustion at full accuracy, the Combustion Model would have to be triggered 37.5 times each second. That would leave a maximum time of 26 ms to execute the model if run in real-time. In order to manage real-time simulation requirements and improve simulation speed without decreasing combustion accuracy too much, Combustion Model is triggered every 6th combustion. That leaves 6.25 combustion events per second, which is a reasonable compromise. Combustion trigger can be changed according to simulation needs.

4. SIMULATION AND PARAMETERIZATION

4.1 First modifications and model set up

In order to run an engine, a control system is needed. Control software development in turn requires testing. Especially in the earlier phases of the development process as well as during later modifications, it is preferable to use an engine model to test the control system before running actual engine tests. According to control theory the engine can be called the plant as it contains the controllable process and actuators. The plant receives control signals as inputs and returns measurement signals as outputs. In order to simulate an engine, the plant model needs to have actuators that respond to control signals and influence engine processes. The processes have to be modeled as well to generate output values that correspond to sensor measurements of the real engine. In closed-loop control these measurement signals are used as feedback to the control system. Therefore, all units have to be correct. In order to compare engine model response to the actual engine performance, the operating principle of both systems must be identical.

The original W6L34DF engine model described in Chapter 3 contained a simplified control system to run the model. In order to run the engine model with a new control system, it is essential that the model accepts the control signals and interprets them in the correct way. To establish an appropriate testing environment, the parameterization work was started by replacing the old controllers with the actual control system that would be tested. Both the engine model and the control system have been made with Simulink so integration of the two systems does not cause software compatibility issues. However, the new control system is more complicated than the old one as it contains multiple controller applications that pass information between one another before sending control signals to the engine. In addition, the engine model uses a continuous solver but control system is discrete with sample-time rates that vary by controller. In order to keep the engine model functional, old controllers were changed one by one and the model was adjusted accordingly. This way data compatibility could be verified between every step by simulation. Input and output blocks were added to the plant model for signal data type and unit conversions as well as signal rate transitions. The original controllers to be replaced were fuel controller responsible for diesel fuel injection, exhaust wastegate valve controller, air bypass valve controller, gas controller for main gas valve opening duration and GVU flow control, and cooling system controller for LT-valve control. Proportional-Integral-Derivative (PID) controllers were used as the control method for these actuators in both old and new control systems.

The conversion work was somewhat complicated by the architecture of the new control system as many controller applications had strong dependency on each other. The control system also required some new feedback signals from the engine model such as completion of gas leak test and engine revolution count. Models for these processes had to be added to provide the measurement. Gas leak test is carried out every time before switching the engine into gas mode. However, gas leaks do not occur in the GVU of the engine model. Therefore, there is no reason to model the actual process of testing shut-off valves, so gas leak test can be simulated with a simple time delay instead. As a result, a couple of seconds after the gas leak test request, the engine model assumes that test is successful and returns the completion result. Otherwise gas transfer will not begin. Some minor modifications had to be done on the control software side as well. As explained in Chapter 3.2, the engine is started with compressed air. Fuel injection is enabled only after a number of crankshaft revolutions when air has given adequate speed to the engine. However, due to the fact that instrument air system is not modeled, this cannot be achieved. Therefore, the required number of revolutions was set to zero. In order for compression ignition to take effect, engine has to be spinning close to 100 rpm. This initial value is set into the integrator that gives the speed according to equation 3.9. This way engine can be started without modeling the start air system.

The Simulink control system was made for common rail engines with one injector per cylinder, while the W6L34DF has a jerk pump system connected to main injectors and common rail system for pilot injectors. Therefore, SOI and EOI control signals had to be divided. Main injection with fixed SOI was set to activate in diesel mode and pilot injection with variable SOI was used in gas mode. There were also other parameters in the control software that were set to zero to disable the control functions that are not supported by the W6L34DF engine.

The original engine model was integrated with Wärtsilä Simulink Design Environment (WSDE). WSDE linked inputs and outputs of the model so that hardware-in-the-loop (HIL) simulation of the engine would be possible on a test rig. However, due to the new control system being fully implemented in Simulink, control modules of the test rig were not needed anymore. Thus, WSDE-dependency was removed. Also, the original user interface made with Simulink S-function was replaced with a more comprehensive one supporting the use of the new control system.

After the old controllers were replaced and the engine model was made compatible with the new control system, they were integrated into the same Simulink model. As a result, the system became an independent Simulink model that can be used for model-in-the-loop (MIL) simulation of the engine. The engine model serves as the plant model and the controllers are in charge of making the plant reach the reference values set for each operating point. The main reference values are engine speed and power decided by the operator. However, there are hundreds of parameters and set points that the control system follows. Most of the reference values are tabled into arrays with

engine speed measurement on one axis and load on the other. Controllers of different engine systems then choose appropriate set points from these lookup tables. To be able to compare engine model response to the real engine, the reference values of both control systems must match. Therefore, control system parameterization was the next step in model setup. The test run of the actual W6L34DF engine is described in the next chapter. The used parameter set was saved for this purpose.

Marine engines are often connected to a generator when used. So is done with the W6L34DF laboratory engine too. The actual load measurement of the engine is done from the generator shaft. However, there is no generator model connected to the engine model. Thus, the engine model power output is not directly comparable to the measurement from the actual engine. Generator efficiency is around 95 %. Therefore, the usable engine power decreases by a few percent. A generator efficiency map is taken into account in engine model power measurement to estimate generator losses but the generator itself is not modeled. The magnetic phenomena or the electrical behavior of the generator are not considered.

As both the plant model and the controllers are in the same Simulink model, it is important to separate engine outputs and control system inputs during each simulation cycle. Using the measurement directly during the same simulation time step would mean instant signal propagation. In practice there is always some delay before feedback signal reaches controller. Therefore, engine model outputs are written to Simulink data store memory blocks that are read by the control system during the next simulation cycle. This eliminates algebraic loops by delaying the signal by one major integration step. At the same time it imitates signal propagation delay before measurement value reaches control system. In addition, real sensors have some dynamics of their own but those are not modeled. After the process described in this chapter, the environment for MIL simulation on development PC was set up allowing engine model performance comparison to the real engine.

4.2 Engine test run and data collection

Engine tests were carried out to collect reference data for model parameterization. The test run was done on the same W6L34DF engine that was used to parameterize the original model. Since then, engine had undergone some changes mostly regarding turbocharging. The engine was run on laboratory test bed coupled to a generator, and measurement signals were recorded. The tests were done in gas operation and load control mode. In load control mode engine speed is kept at nominal speed of 750 rpm and generator load is varied. The generator was connected to the electricity grid. Engine load was first increased 0–100 % as a ramp with 30 kW/s load ramp rate. The load was then decreased 100–0 % with the same ramp rate. Same rising and falling load ramp tests were done with 60 kW/s ramp rates. After that steady-state measurements were done with 9 different engine loads chosen between 0 and 100 %. The measurements

were taken after all process values had settled. Cooling water temperature and consequently charge air temperature were the slowest to stabilize. These steady-state and ramp measurements were done with a commonly used engine control system parameter set that was saved for reference.

The test plan also included instant load steps. The electricity grid has too much capacitance for instant load changes. Therefore, the generator was taken off the grid and connected to a resistor pack. However, due to reasons beyond our control the tests could not be completed. The aim of load steps was to measure the transient response of the engine. Due to this setback, only the accuracy of engine model steady-states could be evaluated. Nevertheless, the captured ramp measurements provide some reference of the dynamic behavior of the engine.

4.3 Development PC simulation and model parameterization

At this point the control system and engine model were ready for simulation on the development PC. The control applications have fixed-step solvers with sample rates from 1 to 100 ms depending on controlled process. The plant model was set to run in continuous-time with ode23tb solver due to the stiff nature of mean value engine model. First simulation tests showed that with the inclusion of new controllers the system model required 3–4 seconds for every second of simulation. The development PC used was a windows system with quad-core 2.70 GHz processor and 16 GB RAM. The system model was running without simulation errors but there were multiple discrepancies between simulation results and measured data. A clear difference between model and real engine operation could be seen in the values of charge air pressure. The simulated pressure was nearly 1 bar higher than measured values throughout the engine operating range. At the same time, the turbocharger speed of the model was continuously 3000–6000 rpm lower than on the real engine. It is practically impossible to produce so much higher air pressure with so much lower compressor speed. Even though it was known that the turbocharger of the W6L34DF engine had been changed, the charge air pressure could not have been as high before as the model suggests. An explanation was found in pressure measurement. On the real engine pressure is measured in relation to ambient air pressure. This is called gauge pressure. In the engine model however, absolute pressure is used for all physical calculation and so the output of the plant was also referenced against vacuum. The same applied to gas pressure measurement. After fixing the problem by subtracting atmospheric pressure from every pressure measurement, charge air pressure dropped to below values measured on the actual engine.

Especially in the beginning of simulation work engine’s safety system activated often causing engine shutdown. This was mostly caused by too hot exhaust gases or engine overspeed. Safety limits had to be modified in order to carry out testing without interruptions before problems with the model would be fixed. Simulation was mainly

done in gas mode and load control as the parameterization of the model focused on gas operation. A problem was noticed to occur during gas transfer when engine switches its main fuel from diesel to natural gas while running. During gas transfer, the control system gradually decreases the amount of diesel by shortening injection duration and simultaneously increases the amount of natural gas. However, after a short period of gas introduction into the cylinders, the demand for fuel gas was cut to zero by the control system and engine kept running with only pilot fuel injection. The engine's pilot fuel system is based on common rail and has electronic control over injection timing and duration. The problem was that even though injection controller followed the reference value of pilot fuel duration, the burning diesel produced too much power leaving no need to use any gas. The fault was discovered to be caused by the use of wrong injector. During engine input signal management it was defined that diesel fuel injection is switched from main to pilot injectors when engine mode changes to gas operation. However, gas mode is activated only after gas transfer is complete. Therefore, injector swap was not made. When the switch from main to pilot injectors was fixed to take place during gas transfer, engine model was able to make the change from diesel to gas operation smoothly.

There was also another problem with gas admission into the cylinders, which often occurred in gas mode when engine load was increased. This time there was not enough natural gas going into the cylinder chambers for the combustion to produce enough power after increased load requirement. The control system demanded more fuel by fully opening the main gas valves to no avail. As a result the engine could not maintain its nominal speed and came to a stop. The reason for this was too low gas pressure due to slow GVU control. The dynamic properties of the engine model clearly did not match to the actual engine. Therefore, the control system parameters of the Simulink model had to be modified. The gas pressure PID controller was tuned so that it would keep up with the increasing load and maintain a proper pressure difference over the main gas valves.

Earlier pressure measurement correction had also affected exhaust wastegate operation. The purpose of EWG is to regulate charge air pressure by directing some of the exhaust gas flow past the turbine. Before the fix, charge air pressure measurement was constantly over the set point. However, in reality absolute pressure was too low, and engine model had difficulties with power increments. Yet, EWG was opening because the control system thought that charge air pressure was too high. When pressure measurement was done correctly, exhaust wastegate stayed shut most of the time as the pressure was below reference. During high engine load oscillation when charge air pressure experienced fluctuation as well, the valve would suddenly fully open if air pressure momentarily crossed over the set point. Sometimes the opening would occur late after charge air pressure had already decreased. This could not be influenced by controller tuning, but was fixed during later parameterization. However, the reasons

behind EWG model malfunctions remained unclear. The presumption is that flow area estimation is not entirely accurate.

The analysis of engine load oscillation led to combustion efficiency study. It was discovered that at times, only 75 % of the fuel gas actually burned during combustion. When the values of relative air-fuel ratio were checked, it turned out that lambda was constantly over 3 and there would often be as much as 7 times more air than required to burn the fuel. Thus, there was a clear contradiction between low charge air pressure and high lambda. While inspecting the combustion model, the timing of IVC was found to be set to the end of intake stroke, meaning that the valve closes at 180 °ca when piston reaches BDC. The inlet valve closing on the W6L34DF engine at the time of test run was 55 °ca before BDC. That was clearly one reason why there was too much air inside the cylinder resulting in too lean air-fuel mixture. Adding 55 °ca Miller timing required similar extension of the integration period in Combustion Model. IVC directly affects the volumetric efficiency of the engine. As the efficiency is not modeled physically, modifying the closing time obligated to updating the volumetric efficiency map as well. The efficiency map for the latest engine configuration was provided by the test laboratory. The previous volumetric efficiency was a 2-D lookup-table but the new efficiency was measured only as a function of engine speed. According to the performance engineer of W6L34DF engine the accuracy was sufficient so new volumetric efficiency was implemented as 1-D lookup-table. After these changes were made, lambda dropped to values between 1–2 and combustion efficiency increased to 90–99 %.

By this time simulation began to produce more realistic results. The known issue of new turbocharger was tackled next. Before making any changes, the real turbocharger speed measurements were applied to the engine model in order to test its behavior. When the turbocharger speed in different steady-states was manually set to the corresponding measurements, charge air pressure settled to reference values with idle operation and 10 % load. However, with higher loads difference increased proportionally and at 85 % load the pressure was about 1.5 bar over the set point. The test proved that turbocharger parameters had to be corrected. The characteristics of the turbocharger model are defined by the mass flow and efficiency maps of compressor and turbine. The laboratory provided SAE maps for both compressor and turbine. The problem with SAE maps is that the data only includes a limited number of data points. However, when simulation of the engine model is run, there is no guarantee that the operating points will remain within the range of SAE map. Therefore, laboratory produced extended compressor and turbine maps by extrapolation. These extended maps could still not be used directly in Simulink lookup-tables because each speed line contained mass flow and efficiency data on irregular pressure ratio intervals. To make the speed lines and pressure ratio lines constant over the whole map, each map was interpolated with Gridfit Matlab function. The resulting compressor and turbine maps are presented in

Figures 13–16. The original SAE data points are marked with red asterisk. The interpolation result of efficiency maps presented in Figures 14 and 16 was not as smooth as in case of mass flows, which is indicated by the sharp edges at the top of both surfaces. In addition, it can be seen that there is some deviation especially between extended and interpolated efficiencies compared to the SAE data points. Otherwise the maps show good fit and they should model turbocharger characteristics with adequate accuracy.

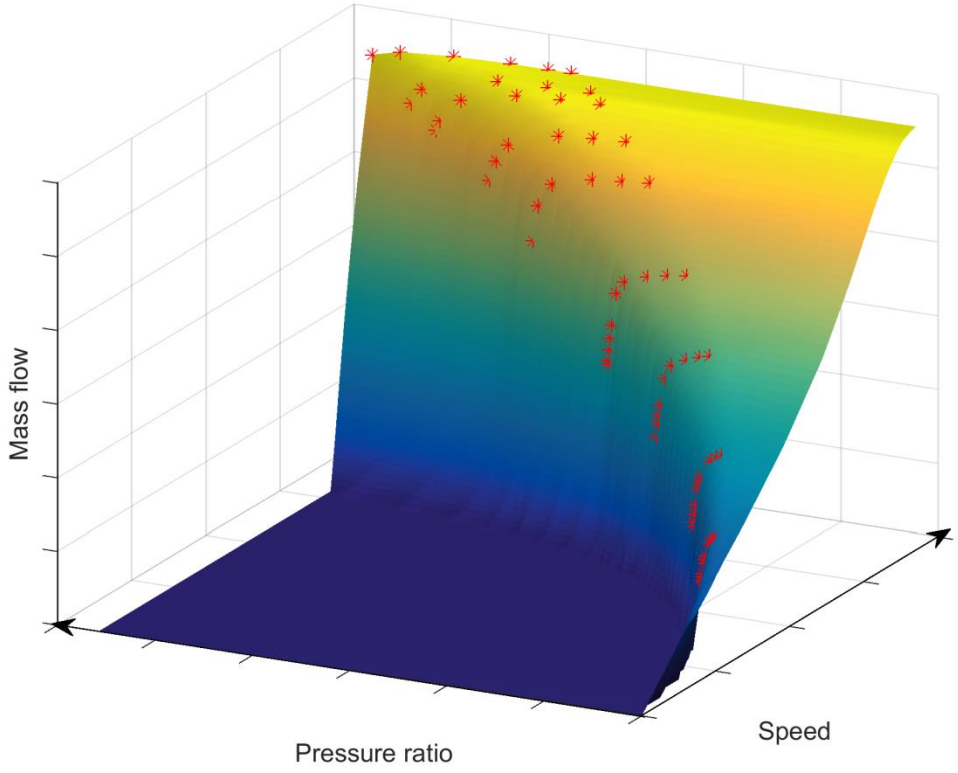

Figure 13. *Compressor mass flow map as a function of speed and pressure ratio.*

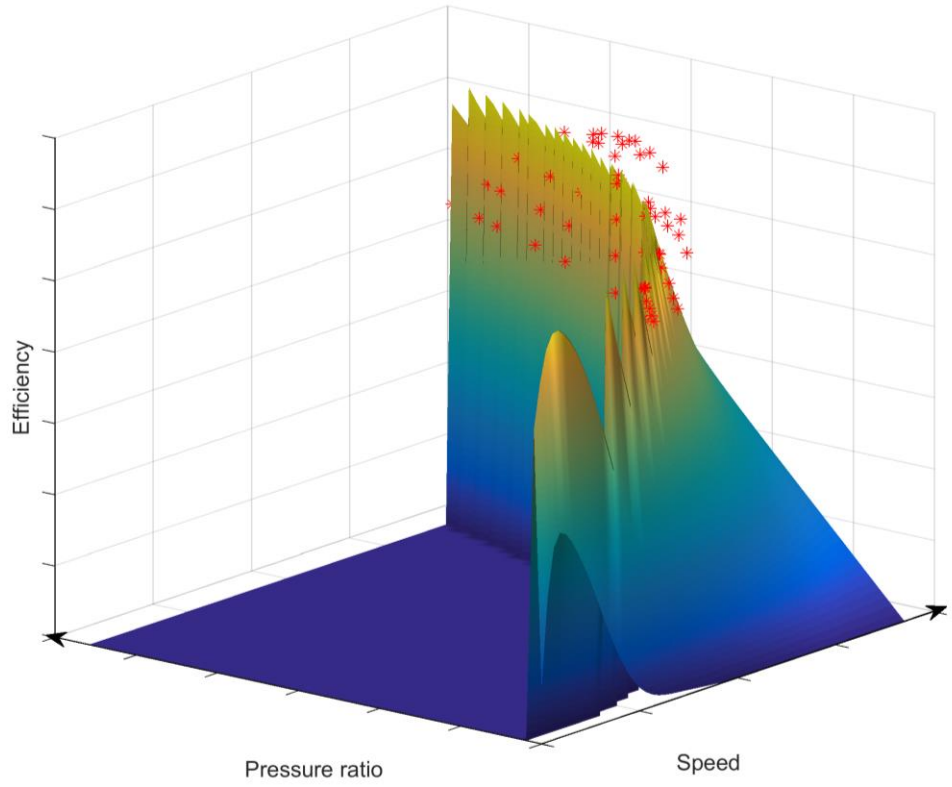

Figure 14. *Compressor efficiency map as a function of speed and pressure ratio.*

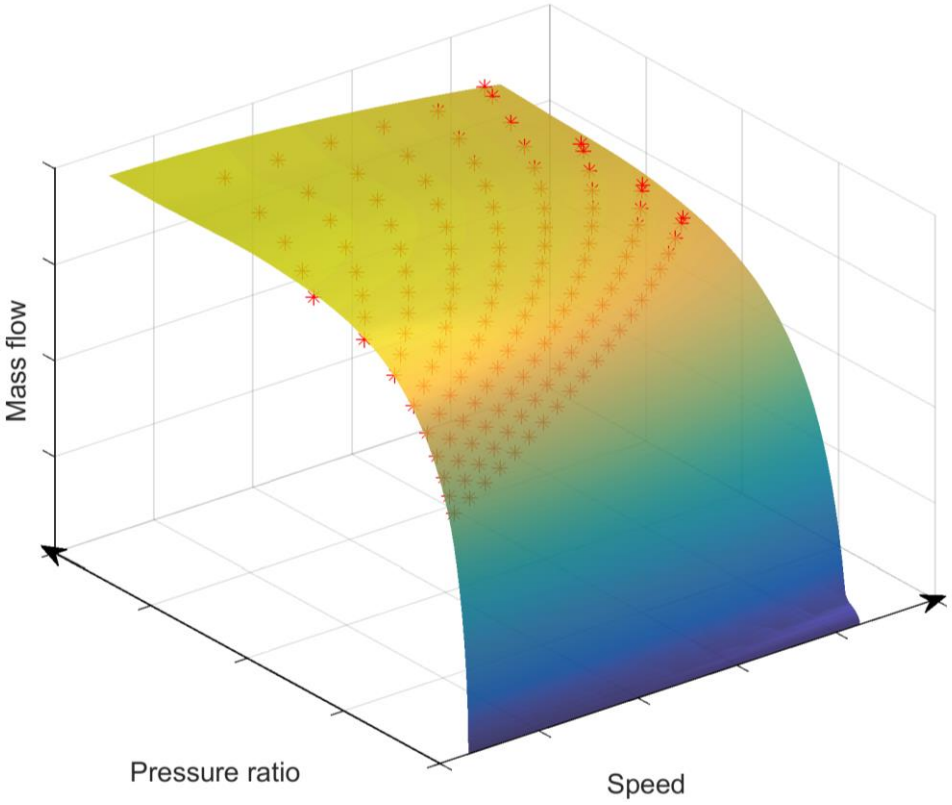

Figure 15. *Turbine mass flow map as a function of speed and pressure ratio.*

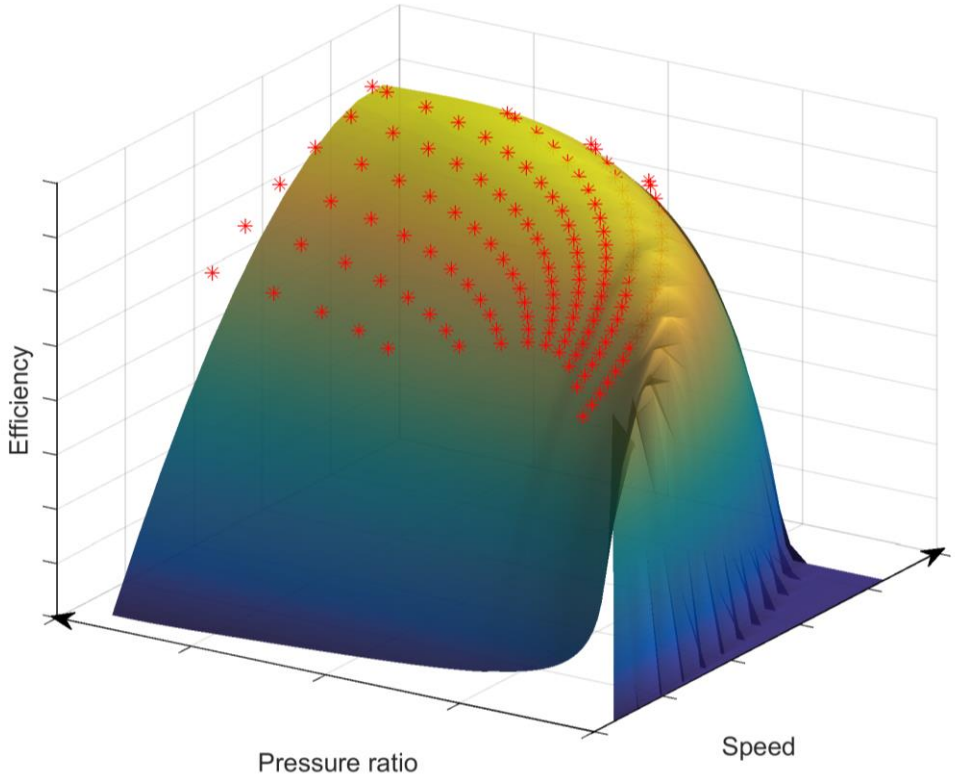

Figure 16. *Turbine efficiency map as a function of speed and pressure ratio.*

Because the compressor and turbine measurements were done in a controlled environment by the manufacturer, the mass flow maps presented in Figures 13 and 15 must be adjusted to account for changes in temperatures and absolute pressures. In the compressor model, the mass flow is corrected to a reference temperature of 25 °C and pressure of 1.013 bar. In case of turbocharger, the data given by manufacturer is already reduced and mass flow is expressed as $kg/s \cdot \sqrt{K}/kPa$. In the turbocharger model the mass flow has to be converted to have the unit of kg/s.

Engine model simulation with new compressor and turbine maps showed that both turbocharger speed and charge air pressure were increased. The speed was still slightly lower than what the engine measurements showed. Therefore, the turbocharger friction model presented in Chapter 3.2 was removed. With no friction the accuracy of simulation results was improved. The only problem was encountered with loads of 85 % and over due to insufficient turbine speed. One reason could be that after the inclusion of turbine efficiency map the turbine could not produce enough torque for faster rotation. As a consequence charge air pressure was also lower with high loads. The turbocharger efficiency was a constant of 0.9 in the original engine model. However, it is too high for any turbine especially if set for the whole operating range. Even though the efficiency values of turbine map were increased at higher loads, the right speed could not be achieved during normal operation. Some experiments were also done with

turbocharger inertia, but lower inertia made the turbocharger more susceptible to oscillation. The actual inertia was quadrupled in the model to make the turbocharger more stable.

The energy of exhaust gases is used to spin the turbocharger. The hotter the exhaust gases are, the more energy they contain. The exhaust gas temperature model inside Engine Restriction calculates the temperature based on the amount of air inside cylinders. The more air there is, the more energy it takes to heat it up [5 p. 101]. Therefore, air-fuel equivalence ratio is used together with coefficients for natural gas and diesel to approximate the exhaust gas temperature. In the original engine model the value of lambda had been estimated with air flow going into the intake manifold and the amount of fuel used. In order to get more accurate results, the actual value of relative air-fuel ratio calculated in the Combustion Model was used instead. However, the actual lambda was about 40 % higher, which lowered exhaust gas temperature. The gas mode coefficients for lambda multiplication were then modified to raise exhaust gas temperature and boost turbocharger speed. However, this increased turbocharger speed on the whole operating range of the engine and caused the charge air pressure to rise too high. As the effects were mostly negative, the idea of increasing exhaust gas temperature was discarded.

During simulation it was noticed that the temperature of charge air was constantly too low. It meant that the cooling system of the engine was not functioning correctly. The fault was found in cooling water temperature control. The position of HT/LT-valves is regulated with reverse-acting control meaning that the control signal should increase valve opening when water temperature rises over the set point. With the change of controllers the direction of action of LT-valve control had been reversed. The valve opening was corrected by inverting the control-signal. As a result LT-water temperature started following the reference and cooling system had the right effect on charge air. In the original model the sea water temperature of the cooling system had been set slightly too low so it was increased by 5 °C. As charge air temperature increased to proper values, cylinder chamber received warmer air and exhaust gases produced by combustion became 20–30 °C hotter. There was no clear effect on turbocharger speed and slight charge air pressure changes were balanced out by the exhaust wastegate.

The last parameterization step with development PC simulation was setting the sizes of Engine Model control volumes. The approximate volumes for W6L34DF engine sections were received from the test laboratory and were fitted to the Engine Model structure. This had no influence on steady-state results but updated the dynamic characteristics of the model. In the next chapter simulation will be carried on in real-time environment.

4.4 Real-time simulation and transient performance

For control software development purposes it is important to be able to run engine simulation in real-time. Real-time simulation is preferred as it describes how control system influences the behavior of the plant within same period of time as it would on the real engine. It gives a more realistic idea about controller performance and engine model response. Therefore, real-time testing enables the evaluation of whether basic control system design specifications are met. Real-time simulation is carried out in discrete time so every simulation step has to be executed within a specified time frame. In order to do that, the engine model had to be discretized and Simulink solver changed from continuous ode23tb to fixed-step one. As a result Simulink blocks with continuous states were not supported anymore and had to be replaced with discrete blocks. This concerned operations such as integration and signal delay. The sample time of the engine model was set to 1 ms to match the fastest control applications. It means that all state equations introduced in Chapters 2 and 3 among other mechanisms that represent engine model characteristics must be solved within this time step. In addition, the simulation hardware must have enough computational power to be able to execute the code and produce the output values within the same time as real engine would. Therefore, the system architecture had to be upgraded for real-time simulation.

A real-time target PC with quad-core 3.6 GHz processor and 32 GB RAM was acquired to run the simulation model. The target computer did not have any operating system or software installed so executable stand-alone code had to be generated to run the model. First the model had to be built. In other words source code was generated by Simulink and compiled into an executable program. The program was then copied onto DOS bootable USB drive to be run on the target PC. During real-time simulation the model was running on the target computer. With 1 ms sample time the average task execution time varied between 7.5–7.8 µs. At the same time the development PC ran a calibration and diagnostic tool that served as user interface for engine operation and obtained measurement data from the model. The target computer communicated with the development PC via TCP/IP Ethernet connection.

When simulation was run on the development PC, it was noticed that the transient response of the engine model was extremely slow. That could lead to similar problems as the ones caused by slow gas pressure control. However, parameterizing PID controllers on the development computer was a tedious process due to slow simulation speed. Therefore, only crucial changes were made before and majority of PID tuning was left to be done on the real-time PC. After discretization and code generation simulation was possible in real-time environment, which nearly quadrupled simulation speed. As the controller gain parameters were being tuned, engine power started to oscillate before acceptable response could be achieved. The load fluctuation was caused by BMEP which is one of the Combustion Model outputs. The problem was not caused by the control software as all controller outputs including fuel demand remained

relatively stable. Other Combustion Model inputs did not have abrupt changes either. The BMEP induced load oscillation had high frequency and the amplitude reached 30 % of the engine's maximum power. However, a steady trend could be seen between the pulsating spikes of engine power output. Thus, it was assumed that fluctuation resulted from the reciprocating behavior of the cylinder. These effects should be damped in multi-cylinder engines but the model of W6L34DF engine had only 1 cylinder, the behavior of which was multiplied by 6. To remove this working stroke induced oscillation a low-pass filter was added after engine load calculation. Due to filtration engine model started to produce stable power output and allowed proper controller tuning. However, in order to achieve realistic engine response, the coefficients of PID controllers had to be increased up to 25 times bigger than the values that real engine had during test run. Therefore, the dynamic properties of the engine model were clearly different compared to the actual engine. Engine behaviour during transient manoeuvres is a result of both engine design and control system properties. However, even though the operating principles of W6L34DF engine model and its Simulink control system closely followed real system design, completely identical performance could not have been expected. Nevertheless, some deviation is acceptable for the purpose of control software functionality testing. The results of parameterization work discussed in this chapter will be presented in the next one.

5. SIMULATION RESULTS

5.1 Simulation results and model accuracy

In this chapter the results of parameterized engine model simulation will be presented and compared to measurements from actual W6L34DF engine. Engine model steady-states are evaluated first, after which the dynamic behavior is analyzed. All simulation tests were done in gas operation with nominal engine speed and load control mode. Steady-states of the model and real engine are presented in Figures 17–21. Figures 22–27 contain load ramp test results and can be found in Appendix 1. The numerical scale of engine state parameters was removed for company discretion. To visualize model accuracy, relative error was calculated for each steady-state. As the model was made to describe actual engine performance, the error of simulation results is expressed relative to W6L34DF engine measurements instead of control system reference values included in some figures. The simulated steady-state at 100 % load cannot be considered completely reliable because it could not be reached in most simulation cases. However, with just the right circumstances the engine model would obtain stability at full load. That is when the measurements presented in this chapter were captured. Instead of 100 % power output the engine model would more often settle to 110 %, which is mainly used as a reference point for marine diesel engines, and therefore has no measurement value.

Figure 17 presents simulated and measured charge air temperatures in different steady-states. The air temperature is directly proportional to the LT-side cooling water temperature as LT-water is used in the second charge air cooler. As can be seen from the figure, the simulated charge air temperature and thus, also the water temperature follow the reference value very well. This is a result of the corrected LT-valve control signal. During real-time simulation the time that charge air temperature took to reach steady-state was a few minutes. As Figure 17 shows, actual measurement values are mostly further away from the set point. During W6L34DF test run the average time given for engine to reach complete steady-state was 5–10 minutes. Due to lack of time the measurements were then taken even if charge air temperature had not completely stabilized. This proves that the modeled cooling process is faster than the real heat exchange due to better efficiency or smaller size of the cooling system. Therefore, the relative errors are also fairly big as absolute differences are compared to measured values.

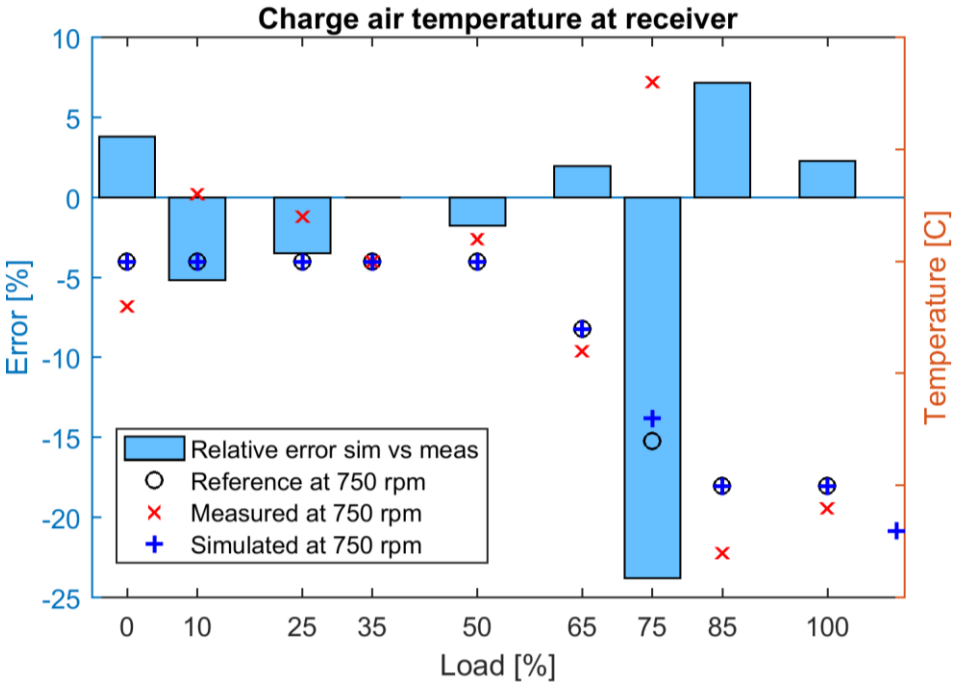

Figure 17. *Steady-state charge air temperature comparison between model and engine.*

According to Figure 18 the exhaust gas of engine model is in most test points hotter than on the real engine. However, there doesn't seem to be strong correlation between exhaust gas and charge air temperature. Instead, the exhaust gas temperature is directly proportional to relative air-fuel ratio shown in Figure 19. This was expected as exhaust gas temperature model is based on the amount of air inside the cylinder. Lowest lambda values can be found at 35, 50, 85 and 100 % loads, which is where exhaust gas reaches the highest temperatures. On the other hand high lambda reduces the temperature at loads under 25 %.

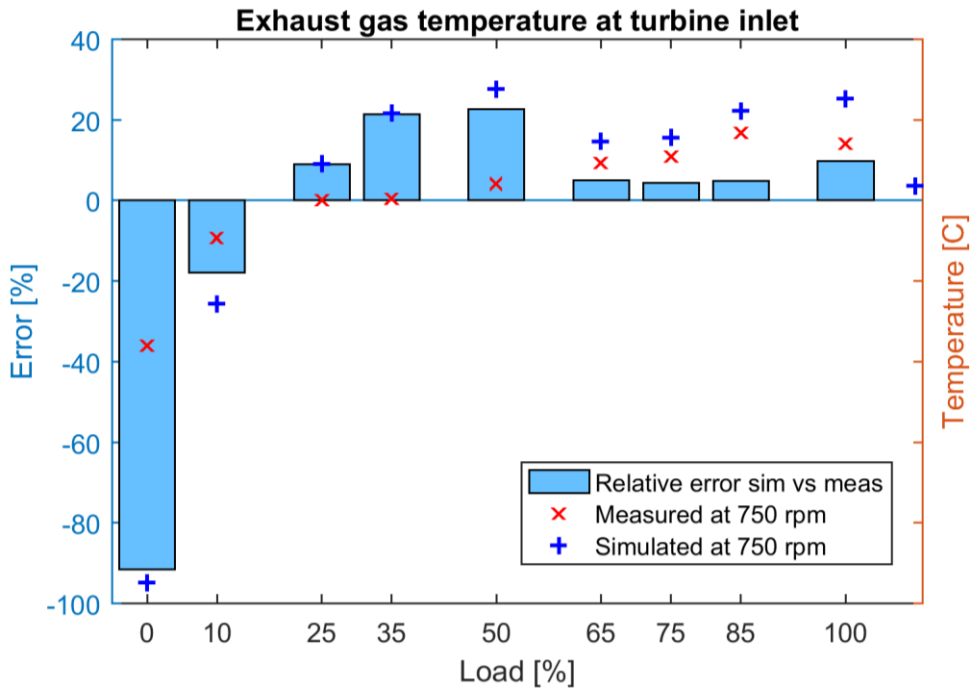

Figure 18. *Steady-state exhaust gas temperature comparison between model and engine*

The air-fuel equivalence ratio cannot be directly measured on the real engine. Therefore, the model's ability to show lambda values is an advantage. However, the values are constantly over 2.2. The most abnormal results given by Figure 19 are extremely high ratios at 0 and 10 % loads. This does not correspond to turbocharger speed presented in Figure 20 or charge air pressure in Figure 21. Therefore, the volumetric efficiency model must be providing the cylinder with too much air. The original volumetric efficiency map was based on engine speed and receiver pressure. However, the new 1-D lookup-table provides efficiency only as a function of engine speed. With very low charge air pressures volumetric efficiency should approach zero regardless of engine speed [5 p. 95]. Also, there is too much air inside the combustion chamber in general throughout the whole operating range of the engine. The air-fuel equivalence ratio could be fixed by taking intake manifold pressure into account and implementing a specific 2-D map for the used inlet valve closing time. Another option would be to model the physical processes behind air induction [5 p. 160].

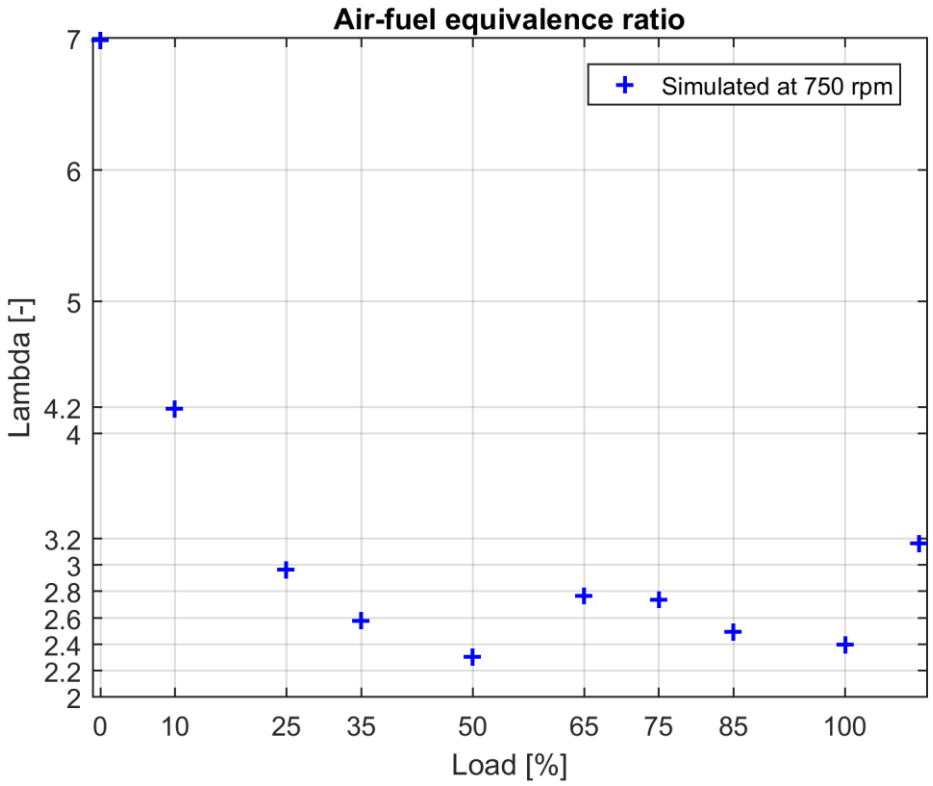

Figure 19. *Modeled air-fuel equivalence ratio in steady-states.*

Figure 20 displays turbocharger speeds during gas operation. Excluding the first measurement, simulation of loads under 40 % yield positive speed error, and loads over 40 % give negative error. By comparing Figures 18 and 20, unambiguous correlation cannot be shown between exhaust gas temperature and turbocharger speed even though exhaust manifold temperature is taken into account in turbine torque calculation. It seems that the turbocharger characteristics are mainly governed by the compressor and turbine maps. Therefore, turbine efficiency map was tuned by slightly increasing efficiency at higher speeds and decreasing it at lower speeds. In general, the mass flow and efficiency maps of compressor and turbine produce relatively good results in steady-states as simulated turbocharger speed deviation from the measured values does not exceed 3000 rpm. However, the problem with achieving 100 % load is related to turbocharger performance. In diesel mode it is not an issue as full load is reached before turbocharger arrives at problematic speed region.

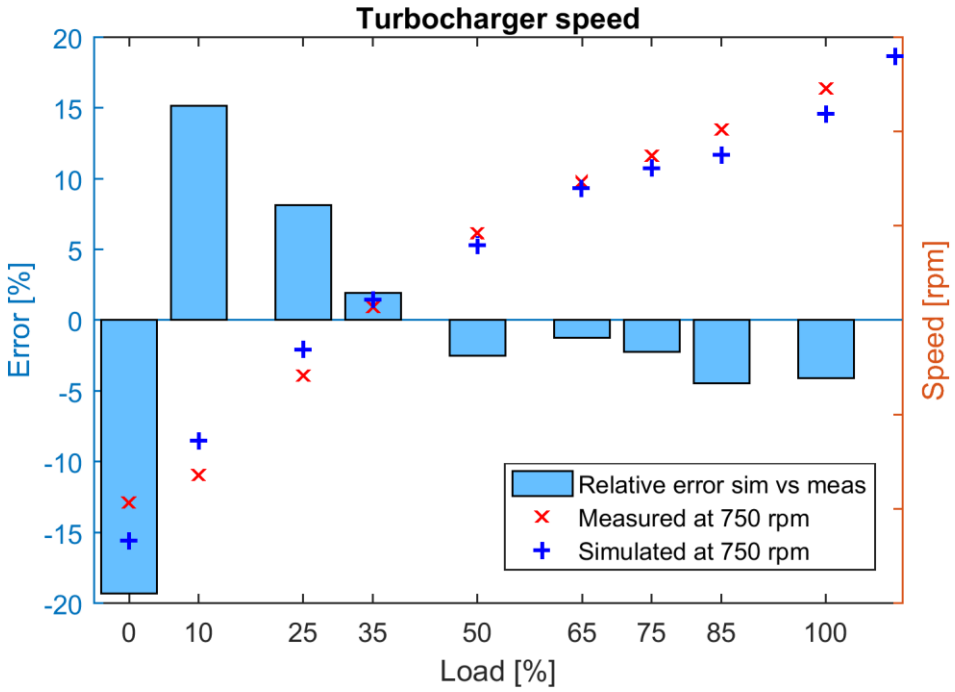

Figure 20. *Steady-state turbocharger speed comparison between model and engine.*

The charge air pressure presented in Figure 21 proportionally follows turbocharger speed. The steady-state accuracy is rather good as modeled pressure stays within 200 mbar from the actual measurements. The relative accuracy at loads under 40 % is poor due to very small values of charge air pressure used for comparison.

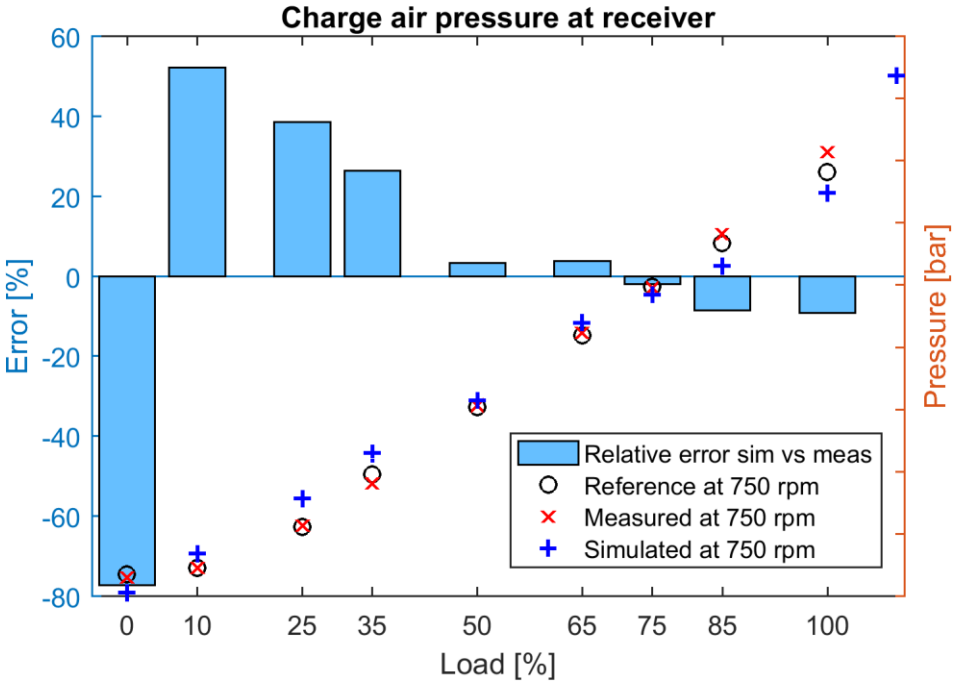

Figure 21. *Steady-state charge air pressure comparison between model and real engine*

The dynamic behavior of the engine model is assessed next. Due to problems with instant load steps during real engine test run, transient measurements are limited to load ramps. Figures 22–25 (found in Appendix 1) show simulation results and actual measurements from tests with two different ramp rates: 30 and 60 kW/s. In addition, a 120 kW/s load ramp is simulated to test the model response. The results are shown in Figures 26 and 27 (found in Appendix 1), but cannot be compared to real engine. Two tests are made with each ramp rate: First, load is increased 0–100 % and then decreased 100–0 %. The biggest shortcoming of the engine model is its difficulty to achieve loads above 85 % during gas operation, which can be seen in the ramp tests. This is caused by the turbocharger's inability to increase its speed after a certain point despite still rising load reference. However, occasionally the turbocharger speed will jump a few thousand rpm leading to possible steady-states of 100 or 110 % load, but that occurred only after longer simulation periods. It is also possible to inflict this jump on the engine model by opening the air bypass valve which is normally closed at full loads. Other phenomena common to the tests are the engine model's generally lower charge air temperature and higher exhaust gas temperature. These effects were also seen when comparing the engine model steady-states to the actual engine. Another thing to be noted is that the load measurement of the real engine is slightly noisy. During falling load ramps the signal oscillates more than during rising ramps. Simulated engine power on the other hand, has a stable signal. It is possible to add disturbance to the load measurement of the engine model to simulate this oscillation. Low amplitude white noise can be used as a theoretical approximation even though physical systems are never disturbed by white noise in practice. Otherwise real engine measurements remain steady.

Figures 22 and 23 show that the engine model can accurately follow 30 kW/s load ramps except near the full load. The rising load ramp has a short deviation around 65 % power. Figure 22 shows that the turbocharger gains speed faster than on the real engine, which increases charge air pressure over the measured value too. However, at the time of 43 s pressure difference grows too big and turbocharger speed settles until charge air pressure becomes too low again. That is when turbocharger speed jumps reaching its maximum speed, which causes the slight deflection in the engine power. After turbocharger speed and charge air pressure have reached their maximum, engine power can still be increased up to a certain point by feeding more fuel into the cylinder. After 2700 kW load is reached, engine model cannot increase the power output anymore without turbocharger spinning faster. Therefore, turbocharger model limits the engine performance. The simulated gas pressure stays well above charge air pressure but the difference decreases momentarily around 62 s when pressure rises abruptly. This shows the importance of having fast controller reaction. The falling load ramp in Figure 23 exceptionally has higher simulated charge air pressure values during the whole maneuver compared to actual measurements. Otherwise the response of the engine model is very similar to the real W6L34DF engine.

Figures 24 and 25 show the results of 60 kW/s load ramps tests. In the case of rising ramp, turbocharger speed increases steadily at the same rate as the actual measurement until maximum speed is reached. However, the speed is constantly too low except between 35–40 s when it gains similar values as on the real engine. That is also when engine model's power exceeds the reference. Again, this is caused by high values of charge air pressure. As can be seen from Figure 24, the engine model cannot produce steadily increasing power output that would be in phase with the 60 kW/s reference. Instead, the load increases with slightly lower rate until 20 s and after that with slightly higher rate until maximum power around 40 s. However, simulated values of engine load, turbocharger speed and charge air pressure are not far from the actual measurements. Figure 25 presents test results for the falling ramp. Again, model performance is better with decreasing load. Not taking high loads into account, engine model follows real measurements very closely regarding engine load, turbocharger speed and charge air pressure. Simulated exhaust gas temperature decreases much faster compared to the real engine.

Additional simulation tests were performed with 120 kW/s load ramps, and the results are presented in Figures 26 and 27. The shapes of simulated charge air temperature, exhaust gas temperature, turbocharger speed and charge air pressure precisely follow the shapes of 60 kW/s test results with both rising and falling load ramps. However, in case of increasing load, the power of the engine model cannot keep up with 120 kW/s rate anymore. With decreasing load ramp, engine power behaves in the same way as with the slower ramp rate. The results of these tests can also be used to estimate model behavior during instant load steps. The response of the engine model would very probably be as slow as during the 120 kW/s load ramp especially in case of increasing load steps. Turbocharger lag is the most notable cause for this. Turbocharger lag occurs because, although the fuel pump responds rapidly to the increased fueling demand after load or speed increase, the engine air-supply cannot match this higher fuel flow instantly due to the inertia of the whole system. As a result of this slow reaction, the relative air-fuel ratio during the early cycles of the transient event assumes low values, undermining combustion and leading to slow engine response. This is supported by the simulated lambda which was included into Figures 26 and 27. In steady-states the air-fuel equivalence ratio of the engine model was above 2 throughout the whole operating range. However, this time lambda mostly remained under 2 especially during the increasing load ramp in Figure 26.

5.2 Alternative solutions and models

When it comes to combustion modeling, the physical way to model it is through chemical energy heat release rate that gives the round S-shape cumulative heat release curve as a function of crank angle degrees. [11 p. 388] Instead of calculating heat release from thermodynamic properties of reactant and product mixture compositions, artificial functions can be used to approximate its shape. Heat release rate law is one possible approach to simulate single injection compression ignition. Combustion models following this approach usually employ first an ignition delay approximation, and after that a fuel burning law. Ignition delay model is typically made of Arrhenius type expression that provides delay time in milliseconds. [17 p. 328] Heywood summarizes the empirical constants of the model and provides alternative ignition delay correlations [11 p. 542–554].

There are three empirical burning law models briefly introduced here to simulate fuel burning in combustion chamber. First and widely used approach is Wiebe (Vibe) function. It models combustion with a parameterized function that gives the burned fraction of the total injected fuel-mass per cycle. [10 p. 337] In other words, the Wiebe function describes the gross cumulative heat release. Differentiating the function yields fuel mass burning rate which is also the heat release rate. Multiplying this with lower heating value minus the losses gives the net released energy. There are 4 parameters to adjust the shape of the curve. The Wiebe function is useful for investigating the influence of varying combustion parameters. A frequently used approach is also to use a sum of two Wiebe functions to model the combustion of single injection engine in two phases, a premixed burning and main burning. [5 p. 111]

Second option is a Watson model which is a two-part expression derived after extended calculation and curve fitting of experimental fuel burning diagrams for swirl-type diesel engines. It is very popular in engine models focusing on transient simulation. Watson model consists of premixed and diffusion burning fractions in similar way to double-Wiebe but has 7 parameters and takes also the fuel-air equivalence ratio into account. [17 p. 329]

The third option is Whitehouse-Way model which is an expression that has two parts likewise to Watson model. However, the Whitehouse-Way model includes more parameters related to thermochemistry as it takes into account the cumulative mass of injected fuel and surface area of fuel droplets. The first part of the expression indicates that at the beginning of burning period the temperature is low and chemical kinetics of premixed combustion prevail. As the temperature rises, the burning rate increases and diffusion mechanism takes over, which is described by the second part of the expression. [17 p. 330]

The three models presented above can be used to simplify the complexity of the combustion process if combustion details are not of concern. The thermodynamic model used for the combustion process of the engine model under inspection is much more comprehensive as it is based on actual fuel composition calculation. However, if simulation speed becomes an issue or if new nonstandard fuels will be used, one of the three above-mentioned models could be chosen to replace the calculation of fuel burning rate.

Regarding the engine model itself, an alternative option would be to switch from 0-D to 1-D modeling of the MVEM. 1-D models simulate the distribution of gas properties in the axis of primary flow. This means that the air-path of the engine would be continuous instead of separate linked volumes such as the 0-D model has. Modeling the actual air flow and fluid motions enables the evaluation of air-path modification effects on engine performance and gives more accurate results for engine behavior during transient maneuvers. For that purpose, a 1-D MVEM requires more parameters than a 0-D engine model on account of detailed description of volume and pipework dimensions. This also increases computational complexity. In addition, nonlinearity of the engine air-path system may limit stability and robustness of the model. [4]

The MVEM evaluated in this thesis is mainly based on the laws of thermodynamics. Another modeling strategy is fluid dynamic approach which results in multi-dimensional models due to the fact that it provides detailed geometric information about the flow. [11 p. 749] GT-Power is widely used engine simulation software that utilizes fluid centered 1-D simulation. It is specifically designed for engine performance simulation, and provides a comprehensive set of tools and features for engine modeling. The GT-Power solver is based on 1-D solution of the fully unsteady, nonlinear Navier-Stokes equations. It can be capable of real-time execution but the models are heavier to run than equivalent Matlab/Simulink solutions. For example, a vehicle model with 4-cylinder turbocharged engine executes at 0.7–0.8 times real-time. On the other hand, the accuracy of GT-Power models is higher due to more detailed 1-D approach. As a compromise, it is possible to integrate a GT-Power engine model into Simulink providing an alternative plant model for the Simulink control software testing. [6] This was done in reference [13] by integrating a GT-Power model of 6-cylinder diesel engine into Simulink. The model's accuracy was sufficient for control system testing but the best achieved execution time was 8 times slower than real-time. In reference [23] a GT-Power engine model was developed but it was used only for the calibration of Simulink real-time engine model.

5.3 Current potential and future development

After engine model and real W6L34DF engine comparison done in Chapter 5.1, the thesis objectives presented in Chapter 1.3 can be evaluated. The objective of making the engine model run in real-time was met. The overall relative error of simulated steady-states almost invariably stays under 25 %, but is usually nearer to 5 %. The dynamic performance of the engine model could not be completely assessed, but moderate load ramps can be simulated with good response. However, the accuracy of transient response is not good enough for control system parameterization. Therefore, controller tuning has to be done on the actual engine. The fact that the engine model cannot reach full load somewhat restricts its utilization. Otherwise, while the accuracy of the model is not acceptable considering engine control system calibration, it serves the purpose of control system functionality testing. This is due to the fact that the engine model detects associations between different engine systems, which allows the cause and effect relationships between different parts of the engine to be taken into consideration when running control system simulation tests. Therefore, overall performance is adequate for the model to be used in rapid prototyping-based control software development. In addition, MIL simulation with the parameterized model can be successfully applied to test the functionality and capabilities of control systems directly in office environment. That gives the model the potential to shorten development cycles and thus bring added value to control software development.

When constructing an engine plant model, the required accuracy and time to make the model have to be balanced. Therefore, model flexibility is an important aspect to consider. The engine model in question is fairly flexible due to its component-based structure, which makes adding and removing components relatively easy. The model's zero-dimensional nature and physical operating principle result in fewer parameters that need to be changed when updating the model or converting it for a different engine. However, measurements are always needed for reference when parameterizing the model. In addition, new components have to be created if no equivalent models are available.

In order to improve the accuracy of the engine model, the turbocharger model has to be looked into. It is difficult to extend SAE maps given by turbocharger manufacturers so that they would precisely describe the compressor and turbine characteristics over the whole operating range of the engine. Therefore, completely physical compressor and turbocharger models might take better account of the engine's operating conditions and provide more accurate turbocharger response. A turbocharger model based completely on physical equations would also be applicable to other engine models with less required conversion work. A formulation of completely physical turbocharger model fitting into component-based MVEM framework is introduced in [5 p. 211–261].

The model's current start process and idle operation at 0 % load have to be excluded from detailed control system performance tests due to unrealistic amount of air going through the engine. However, this could be fixed by improving the accuracy of the volumetric efficiency model. Inlet and exhaust valve operation testing cannot be performed either, as their dynamics are not included. This would require a detailed model of the gas exchange system. However, modeling the actual valves with the intake and exhaust system would demand very high geometric detail which cannot be provided by the 0-D model. A fluid dynamic modeling approach would have to be applied to create a 1-D model of the process. This would also allow the study of variable valve timing and valve overlap effects, which is currently not possible.

It is possible to simulate the effects of signal disturbances with the current engine model by adding artificial noise to the outputs. However, HIL testing will produce better results as it will provide genuine hardware originated effects. If the required sensor and actuator interfaces are implemented, the engine control system can cooperate with real signals. Then, real components can be included to operate together with the real-time engine model in HIL simulation. The benefit of MIL and HIL simulation compared to real engine test runs is that extreme operating conditions can also be tested without risking actual components or causing danger to people or environment. These are the fastest and cheapest forms of rapid prototyping that are applicable to control system development for optimizing design and control.

One of the future engine model development areas could be including a model for the start air system in order to properly simulate engine start. In addition, a more accurate friction model could be added for better power loss estimation. That might also require a detailed model of the lubricating oil system to be created. If computing power is not an issue, the Combustion Model integration period could be extended over the full 720 °ca for increased cylinder pressure accuracy. The diesel and gas fuel systems are also possible targets for improvement, so that fuel pressure fluctuation effects on engine performance could be analyzed.

An emerging control area is cylinder-wise control that utilizes different cylinder specific compensation parameters. To include every cylinder separately into the engine model would allow the simulation of these functions. However, this could be better done with 1-D simulation software such as GT-Power because it provides ready cylinder models that are coupled to a model of the crankshaft. It also allows taking possible cylinder geometry variation into account. To make an even more comprehensive engine model, slight component deformation and crank angle displacements could be simulated with a torsional vibration model of the crankshaft. Again, this kind of modeling is more convenient with software such as GT-Power. However, if such high detail is not needed, Simulink provides a more agile simulation platform for 0-D models.

6. CONCLUSIONS

The purpose of this work was to parameterize the W6L34DF engine model. The goal was to reproduce real medium-speed dual-fuel engine characteristics as closely as possible. Another objective was to evaluate the model and find out if it is suitable for rapid prototyping-based control software development. The parameterization was divided into 4 phases. Firstly, old controllers were replaced with a new control system. Secondly, the plant model was modified to accept the necessary control signals as inputs and give the required feedback signals as outputs. Thirdly, engine model was parameterized via development PC simulation. Fourthly, engine model was discretized and controllers were tuned during real-time simulation on target PC. All processes that are directly controlled by the control system were included in the parameterized engine model.

The model is a 0-D thermodynamic mean value engine model. For the most parts it is based on physical equations, which made the parameterization work easier by reducing the number of variables. Experimental data can provide better fit for the measurement points and allow faster implementation in case of complicated dependencies, but if the data has to be interpolated or extrapolated, the accuracy of the model may decrease. This was shown by the turbocharger model behavior as it restricted engine operation to 85 % load in gas mode. The models for compressor, turbine and volumetric efficiency of the engine are the only components to contain mapped parameters. However, these models proved to be crucial for accurate engine model operation as they greatly influence air induction into the cylinder. The updated volumetric efficiency map was used to compensate for added Miller timing. However, the new volumetric efficiency map was simplified due to omission of intake manifold pressure dependency. This greatly affected lambda and exhaust gas temperature. Therefore, the first actions to be taken in order to improve the engine model performance should be making corrections to compressor and turbine maps as well as volumetric efficiency.

Fuel and air together control engine power, which is why their systems are the most important ones to model. There is a clear difference in complexity between air induction and fuel delivery into the combustion chamber. The MVEM requires 6 different components with volumes and restrictions as well as 2 flow control valves excluding the inlet and exhaust valves to model the air flow through the engine. However, the diesel fuel system can be covered by including injector models with constant fuel pressure. The gas system model is also simpler as it has 2 valves and a pipe between natural gas supply and cylinder. Therefore, MVEM has many more parameters influencing air flow than fuel admission. It would be possible to reduce the number of these variables by

making completely physical turbocharger and volumetric efficiency models. As the functionality of both units stays the same regardless of the engine, physical modeling can reduce future parameterization. Despite the complexity of air flow modeling, steady-state simulation results of charge air pressure and temperature were very good. The inertia of the long air-path and turbocharger lag did not cause problems for the dynamic behavior of charge air pressure when simulating load ramps up to rates of 60 kW/s. The engine air-supply is also influenced by the cooling system. The cooling water circuit of the engine model is too effective in controlling water temperature. However, even though the process model is too fast, the cause and effect relationships are realistic.

Based on the analysis of simulation results, engine model performance and the accuracy to which the engine systems are modeled were found to be sufficient for rapid prototyping-based control software development. The factors that contributed to this decision are briefly summarized here. The overall relative error of simulated steady-states generally stayed under 25 %. That is the maximum error after excluding clearly incorrect simulation points near idle operation of the engine. More often, the relative error was approximately 5 %, which can be considered good. The transient response of the engine is satisfactory when performance problems are ignored at high loads. This can be claimed as all the simulated curves except charge air temperature have very similar shapes to the measured engine response. In addition, the model can handle 1 ms sample time during real-time simulation, which coincides with control system requirements. Lastly, the engine model detects associations between all the critical engine systems leading to realistic behavior. For these reasons, engine model can be used for control system functionality testing, but the accuracy is not good enough for control system calibration.

In order to extend the engine model's controllability and add support for cylinder-wise control, embedding a GT-Power model with crankshaft, engine manifold and 6 cylinders into the Simulink model could be a viable solution. [13] The current combustion model is already heavy, so replacing it with a 1-D model might not make a big difference in computational requirements. In addition, the GT-Power model would support crank-angle-degree-based calculation by default. This way the 0-D Simulink model could be upgraded to a hybrid multi-cylinder engine model. The coupled 1-D engine manifold model would allow inlet and exhaust valve dynamics to be incorporated and different fuel quantities to be injected into each cylinder. However, the effects on real-time simulation capabilities would need to be investigated. The modeling of engine processes continues to develop as our basic understanding of the physics and chemistry of the process phenomena expands and the capability of computers to solve complex mathematical problems continues to increase. Therefore, engine modeling and predicting engine behavior will evidently play an increasingly bigger role in future control software development.

7. REFERENCES

[1] P. Andersson, Air Charge Estimation in Turbocharged Spark Ignition Engines, Linköping University, 2005, 226 p.

[2] R. Backman, Combustion Model for Rapid Prototyping, SAE International, 2011, 15 p.

[3] F. Baldi, G. Theotokatos, K. Andersson, Development of a combined mean value-zero dimensional model and application for a large marine four-stroke Diesel engine simulation, Applied Energy, Vol. 154, 2015, pp. 402–415

[4] D. Cieslar, P. Dickinson, A. Darlington, K. Glover, N. Collings, Model based approach to closed loop control of 1-D engine simulation models, Control Engineering Practice, Vol. 29, 2014, pp. 212–224

[5] L. Eriksson, L. Nielsen, Modeling and Control of Engines and Drivelines, John Wiley & Sons, 2014, 567 p.

[6] Gamma Technologies, GT-POWER Engine Simulation Software, Available (accessed on 8.3.2017): https://www.gtisoft.com/gt-suite-applications/propulsion-systems/gt-power-engine-simulation-software/

[7] Gamma Technologies, GT-Suite Flow Theory Manual, 2017

[8] G. Gassner, P. Cenini, K.O. Ulstein, C. Contessi, World's first ethane-powered marine vessels, Wärstilä Technical Journal, Iss. 2, 2016, pp. 38–43

[9] A.C. George, A. Chiru, Internal combustion engine supercharging: turbocharger vs. pressure wave compressor. Performance comparison, Central European Journal of Engineering, Vol. 4, Iss. 2, 2014, pp. 110–118

[10] L. Guzzella, C.H. Onder, Introduction to Modeling and Control of Internal Combustion Engine Systems, Springer Berlin Heidelberg, 2010, 354 p.

[11] J.B. Heywood, Internal Combustion Engine Fundamentals, McGraw-Hill Book Company, 1988, 930 p.

[12] R. Isermann, Engine Modeling and Control - Modeling and Electronic Management of Internal Combustion Engines, Springer Berlin Heidelberg, 2014, 637 p.

[13] T. Isolahti, Use of detailed diesel engine simulation models in development of engine control system, Tampere University of Technology, 2016, 54 p. Available: http://URN.fi/URN:NBN:fi:tty-201611244782

[14] M. Klein, Single-Zone Cylinder Pressure Modeling and Estimation for Heat Release Analysis of SI Engines, Linköping University, 2007, 295 p.

[15] K. Mollenhauer, H. Tschöke, Handbook of Diesel Engines, Springer-Verlag Berlin Heidelberg, 2010, 636 p.

[16] NASA Glenn Research Center, Chemical Equilibrium with Applications, Available (accessed on 10.11.2016): https://www.grc.nasa.gov/WWW/CEAWeb/

[17] C.D. Rakopoulos, E.G. Giakoumis, Diesel Engine Transient Operation - Principles of Operation and Simulation Analysis, Springer-Verlag London, 2009, 390 p.

[18] Woodward, Gas Admission Valve Product Manual, Available (accessed on 20.2.2017): http://www.woodward.com/EngineAdmissionValves.aspx?terms=sogav

[19] Wärtsilä Corporation, W34DF Engine Presentation, Limited availability (accessed on 22.2.2017): https://wartsila.sharepoint.com/sites/compass/productsandsolutions/Engine_Products/4stroke/Wartsila_34DF/Pages/Default.aspx

[20] Wärtsilä Corporation, W34DF Product Review, Limited availability (accessed on 22.11.2016): https://wartsila.sharepoint.com/sites/compass/productsandsolutions/Engine_Products/4stroke/Wartsila_34DF/Pages/Default.aspx

[21] Wärtsilä Corporation, website. Available (accessed on 30.11.2016): http://www.wartsila.com/products/marine-oil-gas/engines-generating-sets/dual-fuel-engines/wartsila-34df

[22] Wärtsilä Corporation, Wärtsilä Encyclopedia of Marine Technology, website. Available (accessed on 20.3.2017): http://www.wartsila.com/encyclopedia/term/miller-timing

[23] X. Yang, G.G. Zhu, A Mixed Mean-Value and Crank-Based Model of a Dual-Stage Turbocharged SI Engine for Hardware-In-the-Loop Simulation, Proceedings of the American Control Conference, Baltimore, Maryland, USA, June 30–July 2, 2010, 6 p.

APPENDIX 1: SIMULATION RESULTS - LOAD RAMP TESTS

The figures showing load ramp test results are presented here.

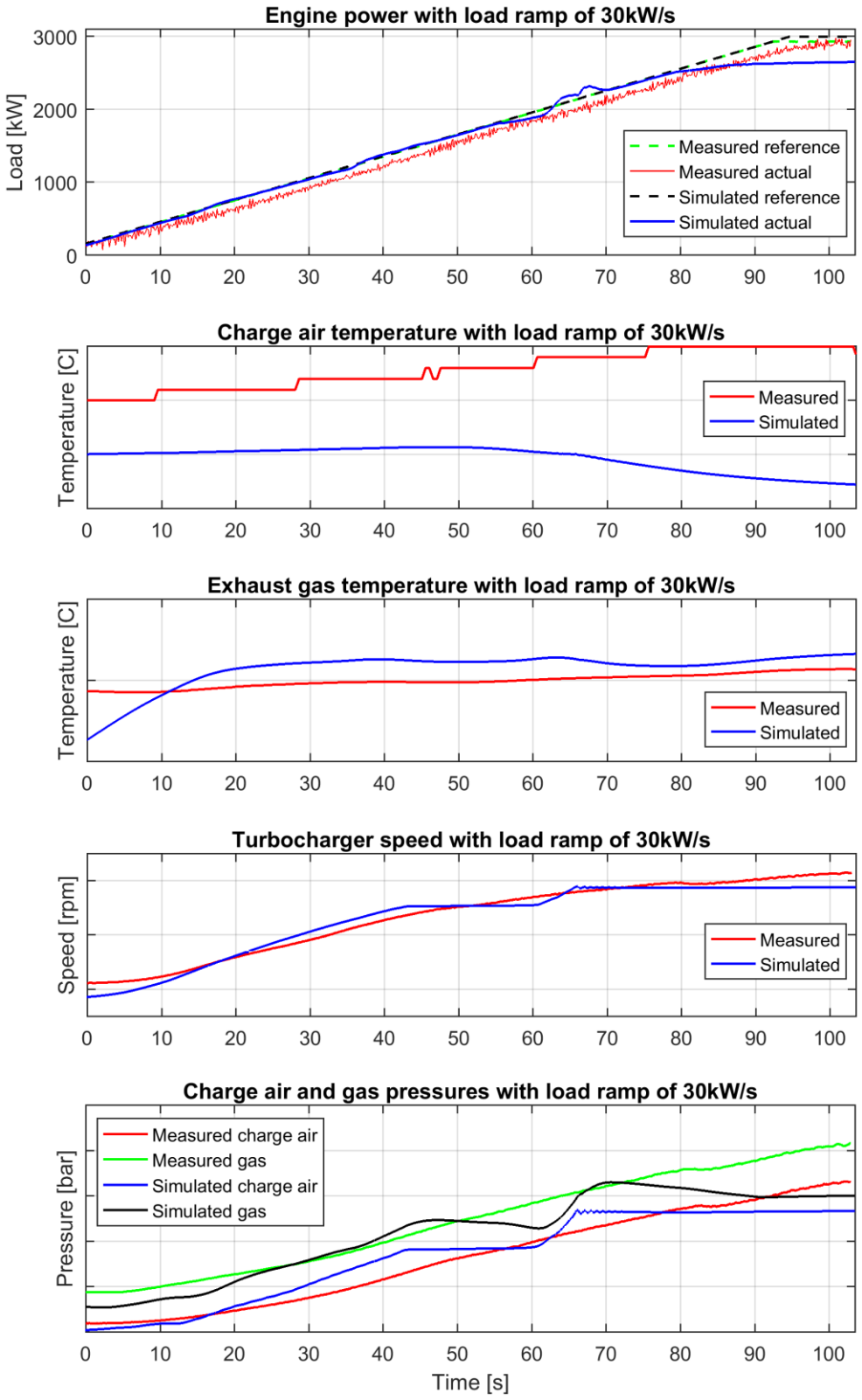

Figure 22. *30kW/s increasing load ramp response.*

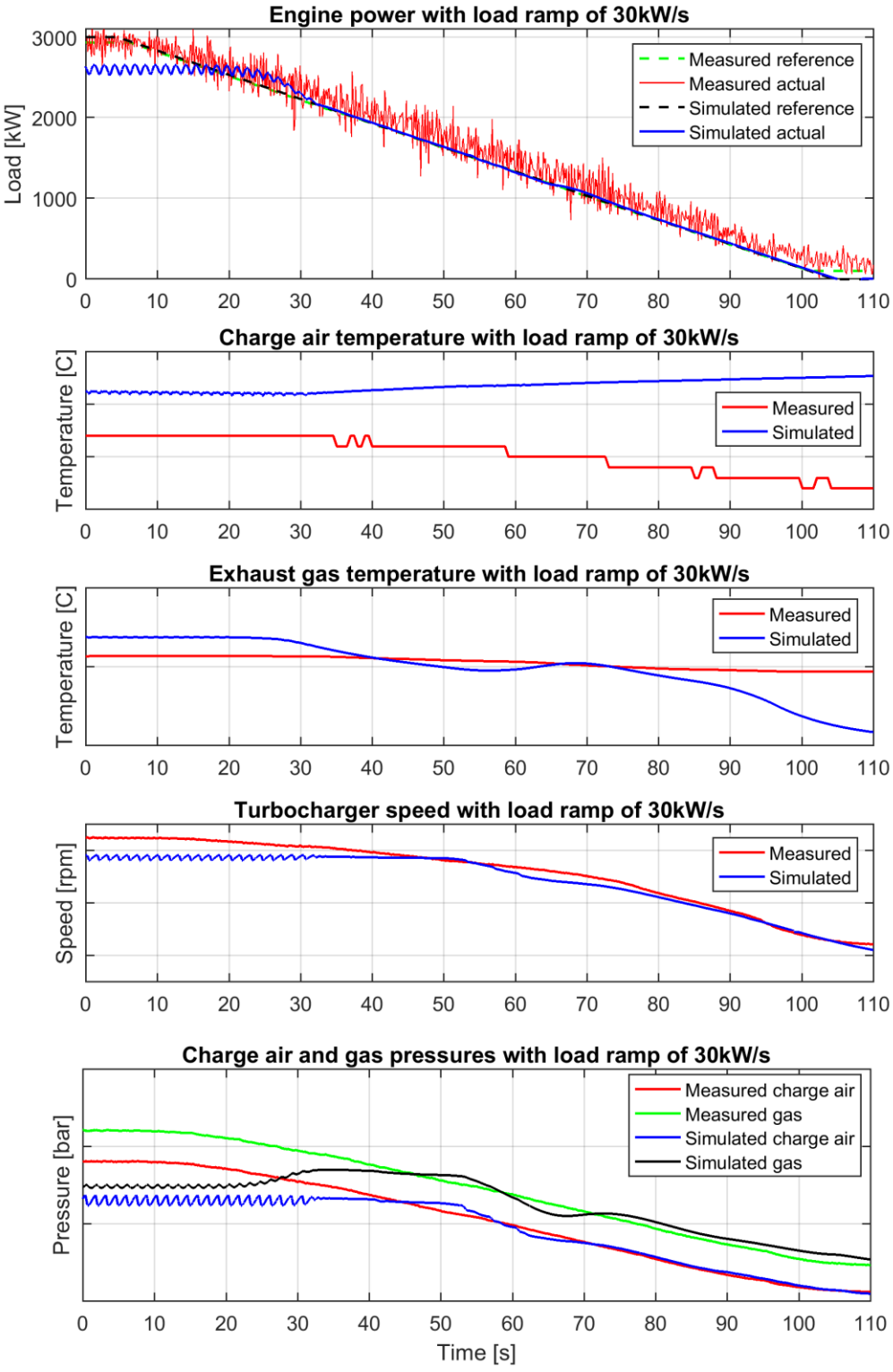

Figure 23. *30kW/s decreasing load ramp response.*

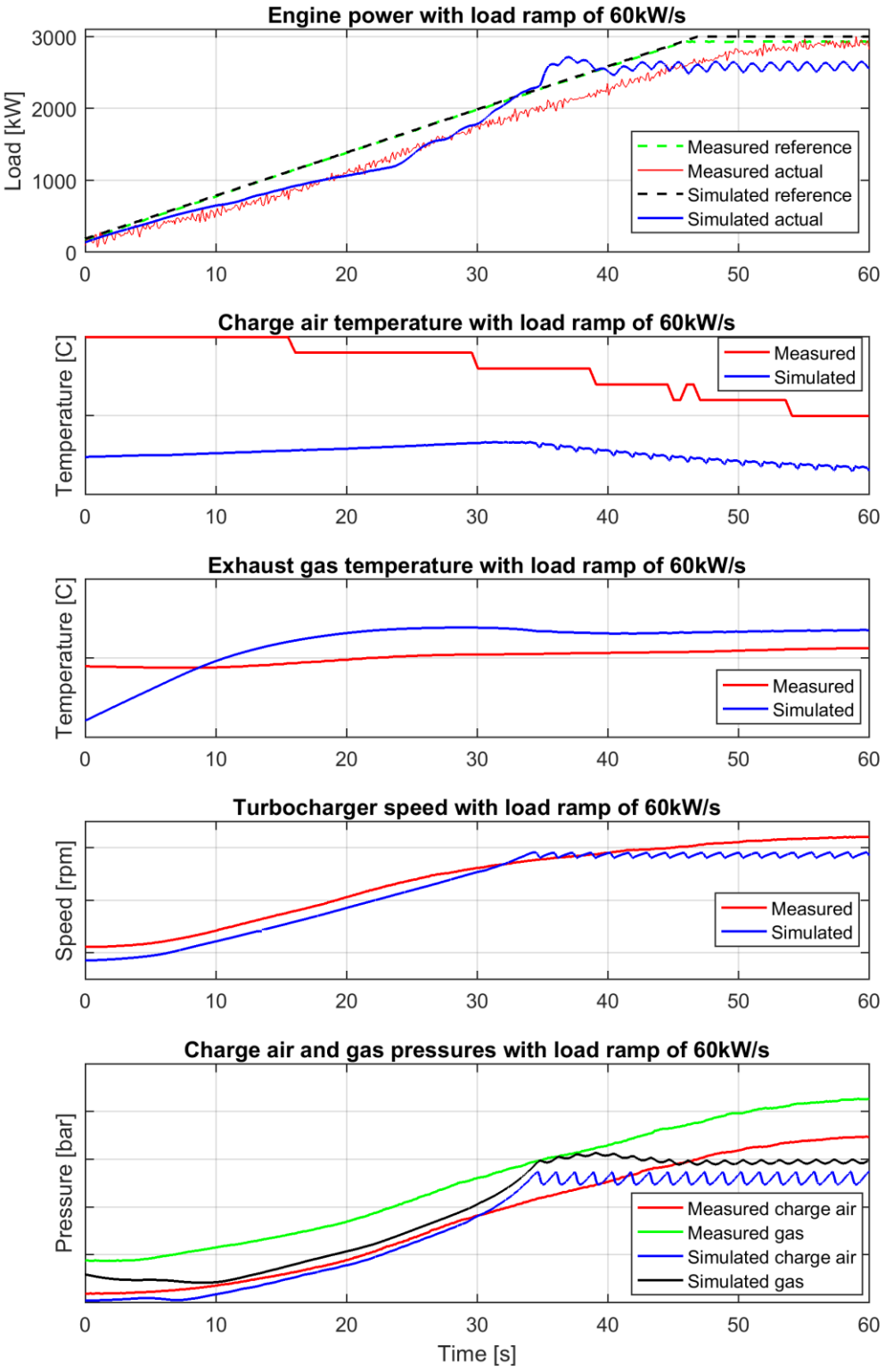

Figure 24. *60kW/s increasing load ramp response.*

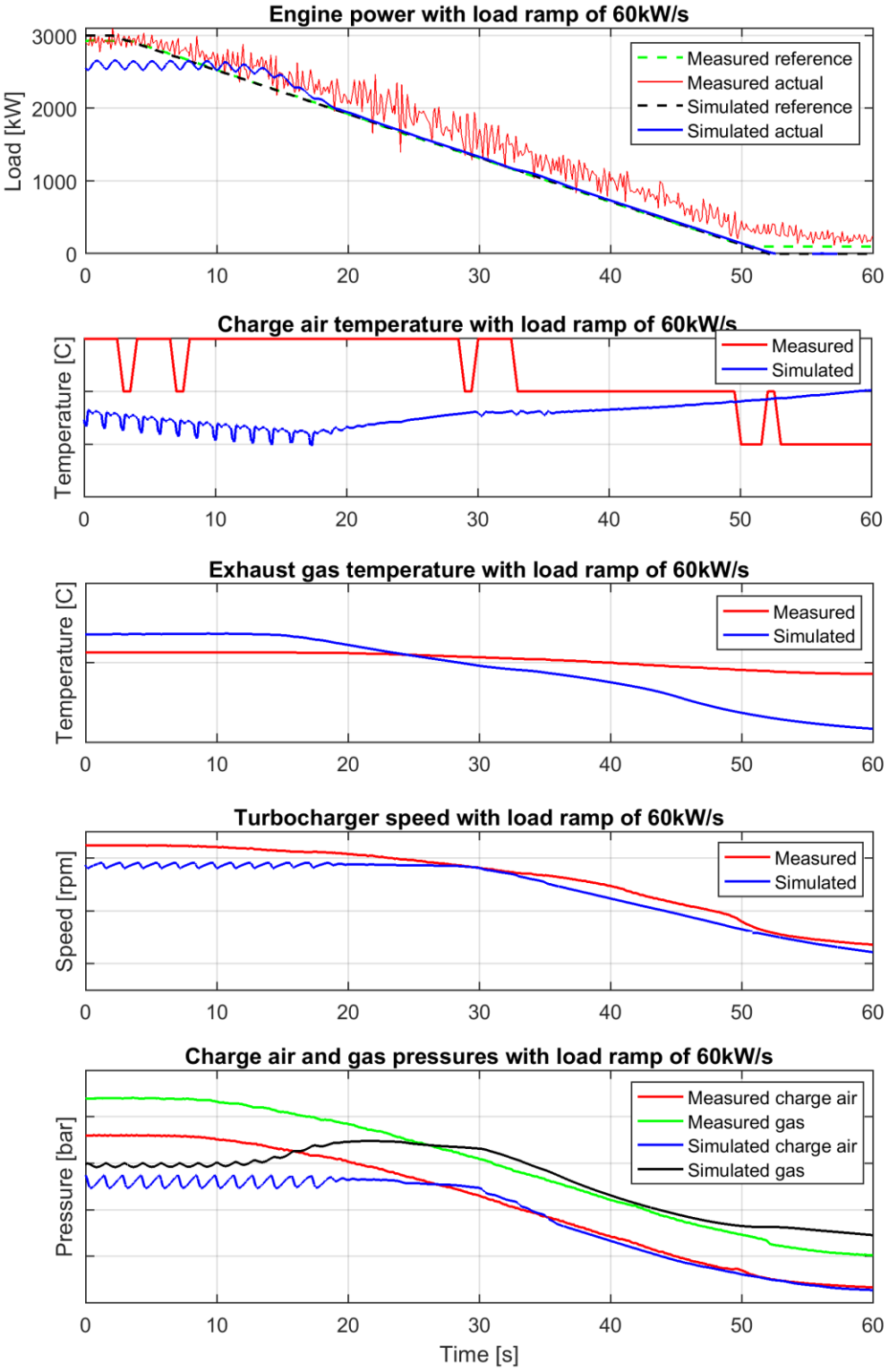

Figure 25. *60kW/s decreasing load ramp response.*

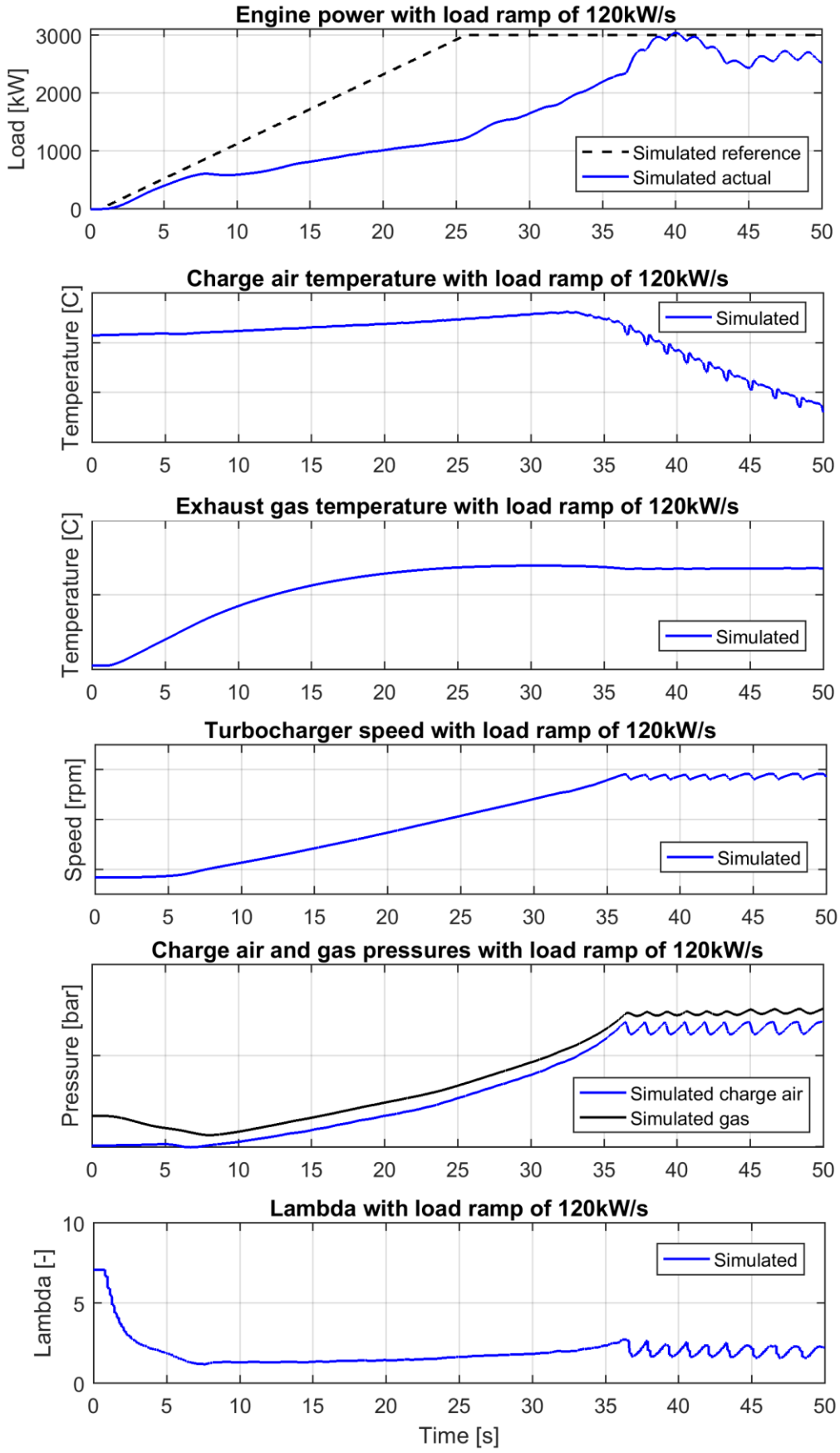

Figure 26. *120kW/s increasing load ramp response.*

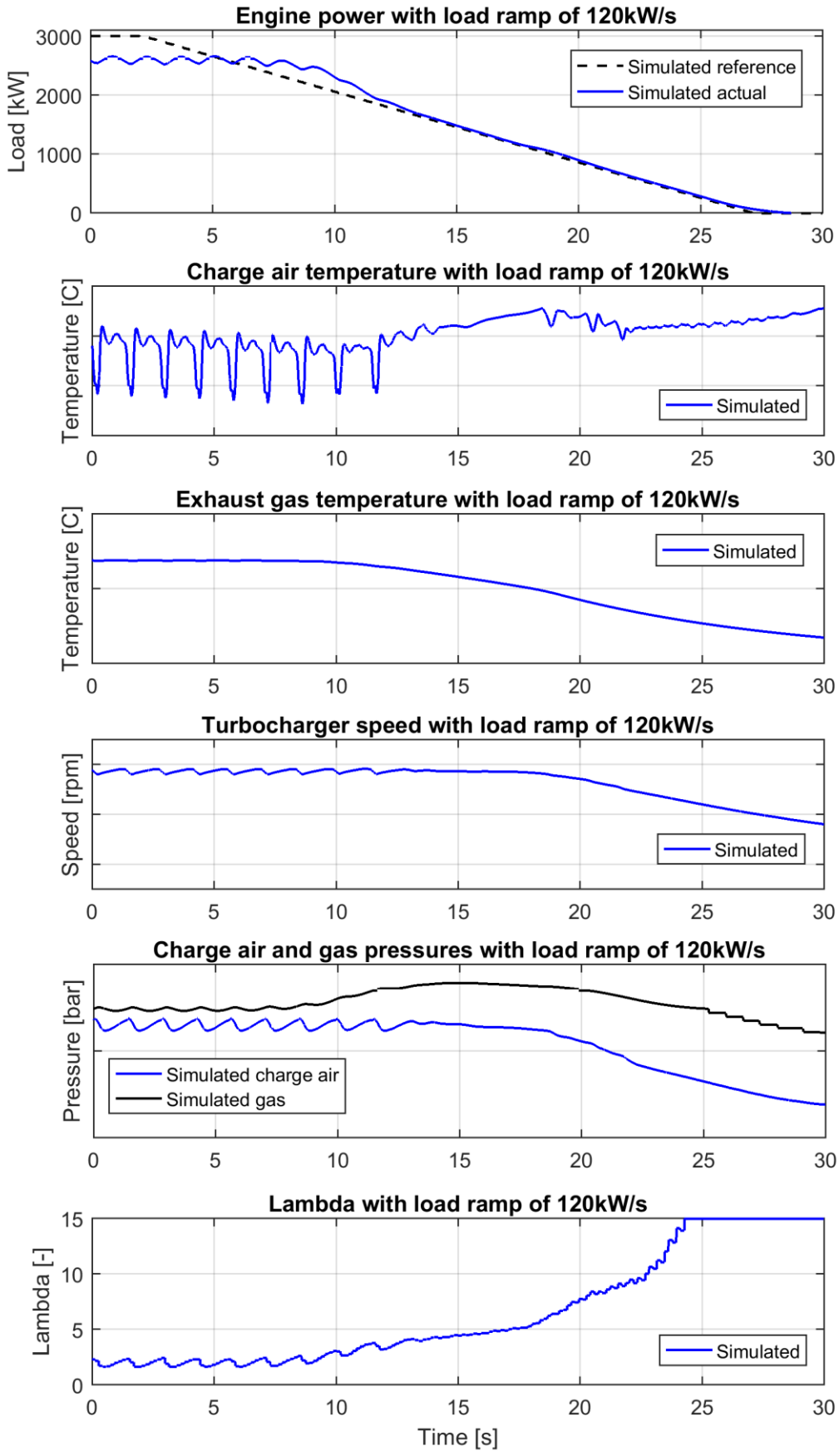

Figure 27. *120kW/s decreasing load ramp response.*